Norwegian University
of Life Sciences

Master's Thesis 2021 30 ECTS
Faculty of Chemistry, Biotechnology and Food Science

The role of TGF-β in collective cell migration

Jenny Nguyen
Master of Science, Chemistry and Biotechnology

The role of TGF-β in collective cell migration

Jenny Nguyen

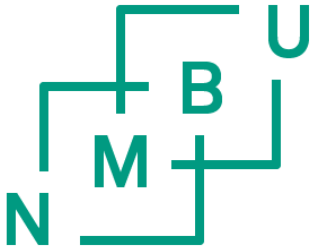

Supervisors:

Emma Lång
Stig Ove Bøe
Siv Kjølsrud Bøhn

Master thesis
Faculty of Chemistry, Biotechnology and Food Science

Norwegian University of Life Sciences
June 2021

2021
The role of TGF-β in collective cell migration
https://nmbu.brage.unit.no

Acknowledgments

This master thesis was conducted within the research group “Experimental Cancer Therapy” led by Stig Ove Bøe at the Department of Microbiology at Oslo University Hospital. This study is a part of a master's degree in Chemistry and Biotechnology at the Norwegian University of Life Sciences, the main affiliation being the Faculty of Chemistry, Biotechnology and Food Science.

Firstly, I would like to thank my main supervisor Emma Lång for the opportunity to be a part of Stig Ove Bøe’s research group, and the opportunity to explore an important field of science. I have learned so much during these past months, and I am grateful for all supervision, support, and encouragement throughout this master's process. Thank you for always being available for guidance in the laboratory and in the process of writing this thesis. I would also like to thank Stig Ove Bøe for valuable discussions and knowledge that have given me a better understanding of the cellular processes that regulate cell migration. Further, I would like to thank Anna Lång for helping me with the ImageXpress Micro Confocal Microscope and being available when I needed extra guidance during image acquisition and data processing. I would also express my gratitude to my internal supervisor at NMBU, Siv Kjølsrud Bøhn, for valuable feedback and guidance.

A big thanks to my fellow students in the student’s office. I have enjoyed the company, discussions, and friendship throughout these months. Thank you for the encouragement and motivation, as well as valuable knowledge.

Lastly, I would like to thank my friends and family, who have supported me throughout this entire process. Thank you for always being there for me, and for all the love, support and encouragement you have given me.

Oslo, June 2021

Jenny Nguyen

Abstract

Background: TGF-β is an important growth factor associated with cell growth, cell proliferation, cell differentiation, and apoptosis. TGF-β is also related to the regulation of wound healing and spreading of cancer cells through metastasis, possibly through the transactivation of the EGF/EGFR signaling pathway. The spreading of cancer cells is associated with collective cell migration. Therefore, this master thesis aimed to study the role of TGF-β in collective cell migration, and the intracellular crosstalk between the TGF-β and EGF/EGFR signaling pathways.

Methods: Quiescent confluent monolayers of HaCaT cells were treated with FBS, TGF-β, EGF, and inhibitors of their receptors, SB431542 and Gefitinib, respectively. The magnitude and directionality of collective cell motions were monitored using a high-content ImageXpress Micro Confocal Microscope. The acquired data were further processed by the use of particle image velocimetry (PIV) analysis to generate information on the cell coordination and cell migration velocities.

Results: TGF-β activates cell sheet migration after 15 hours of stimulation, and a lower concentration of TGF-β (5 ng/mL) was more efficient in stimulating cell sheet migration than higher TGF-β concentrations (20-40 ng/mL). Inhibition of the TGF-β signaling pathway in FBS stimulated cell sheets resulted in a slight inhibition of the cell migration response compared to FBS stimulation alone. In contrast, stimulation with FBS combined with TGF-β led to sustained and amplified cell migration response over time. Stimulation with TGF-β produced a lower level of cell coordination (φ) between the migrating cells compared to FBS stimulation, φ = 0.6-0.7 and φ = 0.9, respectively. Notably, TGF-β stimulation alone was not able to transactivate the EGFR cell signaling pathway in this study. However, the results indicate that both signaling pathways are closely connected and produce a different migration response than observed with the two growth factors alone. A combination of TGF-β and EGF stimulation produced a reduction in cell sheet velocities at the earlier time points and enhancement at the later time points.

Conclusion: Our results showed that TGF-β stimulation of quiescent cell sheets does not activate a coordinated collective cell migration response. However, TGF-β does affect the cell

sheet migration velocities produced after stimulation together with FBS or EGF. The cell sheet migration response observed was first inhibited and later enhanced during the 30 hours of live cell imaging, indicating intracellular crosstalk between TGF-β and EGF. The crosstalk between these growth factors leads to enhanced p-AKT and cell motility. Therefore, further studies are required in order to acquire a better understanding of how TGF-β regulates collective cell movements. Notably, more insight into the dynamics between the inhibitory and subsequent stimulatory effect of TGF-β on epithelial cell migration is important in the development of improved wound healing and anticancer drug therapies.

Sammendrag

Bakgrunn: TGF-β er en viktig vekstfaktor som er assosiert med cellevekst, celleproliferasjon, celledifferensiering og celledød. TGF-β er også relatert til regulering av sårheling og spredning av kreftceller gjennom metastasering, antakelig gjennom transaktivering av EGF/EGFR-signaleringsveien. Spredning av kreftceller er assosiert med kollektiv cellemigrering. Målet med denne masteroppgaven var å studere hvordan TGF-β regulerer cellemigrering, og det intracellulære samarbeidet mellom TGF-β og EGF/EGFR signaleringsveiene.

Metode: Inaktive konfluente monolag av HaCaT-celler ble behandlet med henholdsvis FBS, TGF-β, EGF og inhibitorene SB431542 og Gefitinib. Magnituden og retningen av kollektive bevegelser i cellelaget ble studert ved bruk av et automatisert konfokalt mikroskop, ImageXpress Micro Confocal Microscope. Dataene fra mikroskopet ble prosessert med PIV-analyser for å generere informasjon om koordinasjonen og hastigheten til cellene under migrering.

Resultater: TGF-β aktiverte cellemigrering etter 15 timer med stimulering, og en lavere konsentrasjon av TGF-β (5 ng/mL) var mer effektiv i å stimulere cellemigrering enn høyere konsentrasjoner (20-40 ng/mL). Inhibering av TGF-β signaleringsveien i FBS-stimulerte celler resulterte i en svak inhibering av cellemigreringen sammenlignet med kun FBS stimulering. Stimulering med FBS kombinert med TGF-β derimot førte til at cellemigreringen ble opprettholdt og forbedret over tid. Stimulering med TGF-β produserte et lavt nivå av cellekoordinering (φ) mellom de migrerte cellene sammenlignet med FBS stimulering, henholdsvis $\varphi = 0{,}6\text{-}0{,}7$ og $\varphi = 0{,}9$. TGF-β aktiverte ikke EGFR signaleringsveien, men resultatene viste at begge signaleringsveiene samarbeidet, og resulterte i en ny migreringsfenotype. En kombinasjon av TGF-β og EGF stimulering førte til en reduksjon i migreringshastigheten på starten, og en forbedret migreringshastighet over tid.

Konklusjon: Resultatene fra forsøket viste at stimulering med TGF-β i inaktive celler ikke førte til aktivering av koordinering eller kollektiv cellemigrering. Migreringshastigheten ble derimot påvirket når cellene var behandlet med TGF-β kombinert med FBS eller EGF. Cellemigreringen ble først hemmet, og deretter stimulert i løpet av 30 timer med «live cell imaging», noe som indikerer intracellulært samarbeid mellom TGF-β og EGF signaleringsveiene. Samarbeidet mellom disse signaleringsveiene fører til økt p-AKT og bedre

cellemotilitet. Flere studier er derfor nødvendig for å få en bedre forståelse av hvordan TGF-β regulerer kollektive cellebevegelser. Det er spesielt viktig å få innsikt i dynamikken mellom den inhiberende og stimulerende effekten av TGF-β i epitel cellemigrering, som igjen er viktig for å utvikle legemidler for å behandle kroniske sår, eller medisiner mot kreft.

List of Contents

List of Figures

List of Tables

Abbreviations

AKT	Protein kinase B
BMPs	Bone morphogenetic proteins
BSA	Bovine serum albumin
CDK	Cyclin-dependent kinase
Co-Smads	Common mediator Smads
Da	Dalton
DMSO	Dimethyl sulfoxide
ECM	Extracellular matrix
EGF	Epidermal growth factor
EGFR	Epidermal growth factor receptor
ELISA	Enzyme-linked immunosorbent assay
EMT	Epithelial-mesenchymal transition
ERK	Extracellular signal-regulated kinase
FBS	Fetal bovine serum
GDFs	Growth and differentiation factors
HPLC	High-performance liquid chromatography
HRP	Horseradish peroxidase
IDE	Integrated development environment
IFN-γ	Interferon-γ
IMDM	Iscove's Modified Dulbecco's Medium
I-Smads	Inhibitory Smads
LC-MS	Liquid chromatography-mass spectrometry
LTBP	Latent TGF-β binding protein
Mad	Mothers against decapentaplegic

MAP	Mitogen-activated protein
MAPK	Mitogen-activated protein kinase
mTOR	Mammalian target of rapamycin
MQ-water	Milli-Q water
PAGE	Polyacrylamide gel electrophoresis
p-AKT	Phosphorylated AKT
PBS	Phosphate-buffered saline
PenStrep	Penicillin/Streptomycin
PIV	Particle image velocimetry
PI3K	Phosphatidylinositol-3 kinase
SDS	Sodium dodecyl sulfate
Sma	Genes related to *Caenorhabditis elegans,* "small" worm phenotype
Smads	A family of proteins that are structurally similar to the Sma and Mad family
S6K1	S6 kinase 1
TGF-β	Transforming growth factor-β
TβR1	TGF-β receptor type I
TβR2	TGF-β receptor type II
ROS	Reactive oxygen species
R-Smads	Receptor-activated Smads
βME	β-mercaptoethanol
4E-BP1	The eukaryotic initiation factor 4E–binding protein 1

1 Introduction

1.1 The transforming growth factor-β (TGF-β)

The transforming growth factor-β (TGF-β) is a multifunctional cytokine that regulates cell proliferation, and cell differentiation, and is involved in wound healing, the immune system (Morikawa et al., 2016), embryonic development, and stem cell functions (Massagué, Joan, 2012), among other things. Since TGF-β has a diversity of roles in cell regulation, malfunctions of TGF-β signaling are associated with several developmental disorders (Suriyamurthy et al., 2019) and diseases such as cancer (Wakefield & Hill, 2013), chronic wounds (Liarte et al., 2020), and fibrosis (Lafyatis, 2014). Therefore, it is of great interest to study TGF-β signaling to understand pathological processes *in vivo*, such as connective tissue disorders, cancer, fibrosis, and infectious diseases (Morikawa et al., 2016).

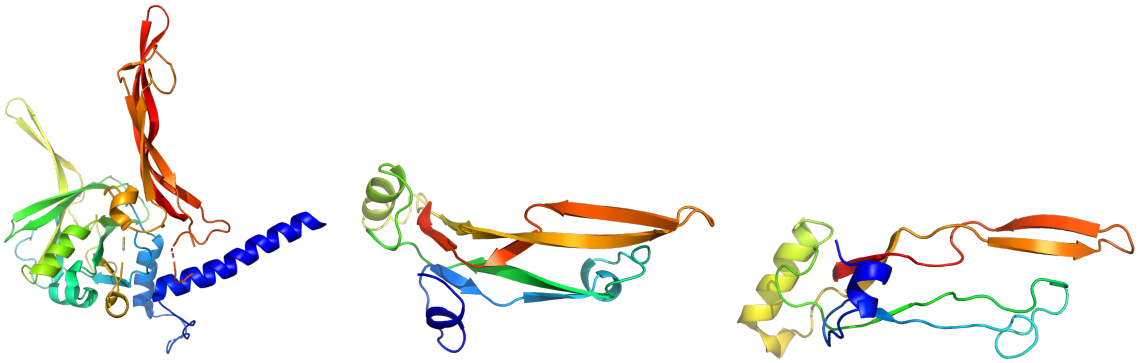

Figure 1.1. *Computational illustrations of the TGF-β protein structure. From left to right: Crystal structure of human pro-TGF-β1 (PDB ID: 5VQP), crystal structure of human TGF-β2 (PDB ID: 2TGI), and human TGF-β3 crystallized from PEG4000 (PDB ID: 1TGK). The figures were made with PyMol using the PDB IDs obtained from the RCSB PDB (rcsb.org) (H.M. Berman et al., 2000).*

The protein structure of TGF-β includes two identical peptide chains consisting of 112 amino acids each, and they are held together by cross-linking of nine disulfide-bonded cysteines. The three-dimensional structure of TGF-β consists of mostly short, two-stranded antiparallel β-sheets and three α-helices (figure 1.1) (Assoian et al., 1983; Daopin et al., 1992). Several approaches have been used to identify polypeptides that are structurally similar to TGF-β1. So far, 33 TGF-β related polypeptides have been identified in mammals, and these include three TGF-β isoforms (TGF-β1, TGF-β2, and TGF-β3; figure 1.1), activins, nodal growth differentiation factor, bone morphogenetic proteins (BMPs), and growth and differentiation

factors (GDFs). Together, these polypeptides form the TGF-β family, and they are all encoded by large precursor polypeptides (Morikawa et al., 2016).

1.1.1 The TGF-β signaling pathway

TGF-β can bind to the TGF-β receptors (TβR1/2) on the cell membrane with high affinity, leading to activation of intracellular responses. The TGF-β receptors are comprised of two related complexes that are ubiquitously expressed (Otten et al., 2010; Suriyamurthy et al., 2019). The kinase domain of these receptors is comprised of a transmembrane serine/threonine-specific protein kinase, suggesting that the TGF-β signaling pathway is mediated through the transmembrane serine/threonine kinases. When TGF-β binds to the TGF-β receptor type II (TβR2), a stable hetero-tetrameric complex with the TGF-β receptor type I (TβR1) are formed, and their signaling capacities become activated (Massagué, J., 2012; Morikawa et al., 2016).

The activation and formation of the receptor complex lead to activation of intracellular effector molecules (Suriyamurthy et al., 2019). The main intracellular effector molecules of the TGF-β signaling pathway are Smad proteins (Feng & Derynck, 2005). The name "Smad" was given to these proteins due to its structural similarity to the *Mad* and *sma* genes (Morikawa et al., 2016). The Smad proteins are categorized into three groups: (1) the receptor-activated Smads (R-Smads), which consist of Smad1, Smad2, Smad3, Smad5, and Smad8; (2) the common mediator Smads (Co-Smads), which consist of Smad4 (Feng & Derynck, 2005; Gu & Feng, 2018); and (3) the inhibitory Smads (I-Smads), consisting of Smad6 and Smad7 (Derynck & Zhang, 2003). The Smad proteins have both roles as substrates for TGF-β receptors and signal transducers for TGF-β signaling (Massagué, J., 2012).

The TGF-β signaling pathway is activated once the TGF-β ligand binds to TβR2, leading to activation and phosphorylation of TβR1, which in turn leads to phosphorylation of R-Smads (figure 1.2). Once R-Smads are activated, a hetero-oligomeric complex with the Co-Smad, Smad4, is formed and accumulates in the nucleus (Feng & Derynck, 2005; Morikawa et al., 2016). The last group of Smads, I-Smads are mainly induced by the TGF-β/BMP family signaling pathway, and act as a negative feedback loop by regulating the signaling pathways negatively (Yan et al., 2009). Besides, TGF-β can also signal through non-Smad pathways, for instance, by inducing the phosphatidylinositol-3 kinase (PI3K) – protein kinase B (AKT) signaling, and activation of the common mitogen-activated protein (MAP) kinase (MAPK) pathways (Morikawa et al., 2016). These pathways can also be mediated by the epidermal

growth factor (EGF) and are found downstream of the EGF/EGF receptor (EGFR) signaling pathway (Mendelsohn & Baselga, 2000; Vitiello et al., 2019).

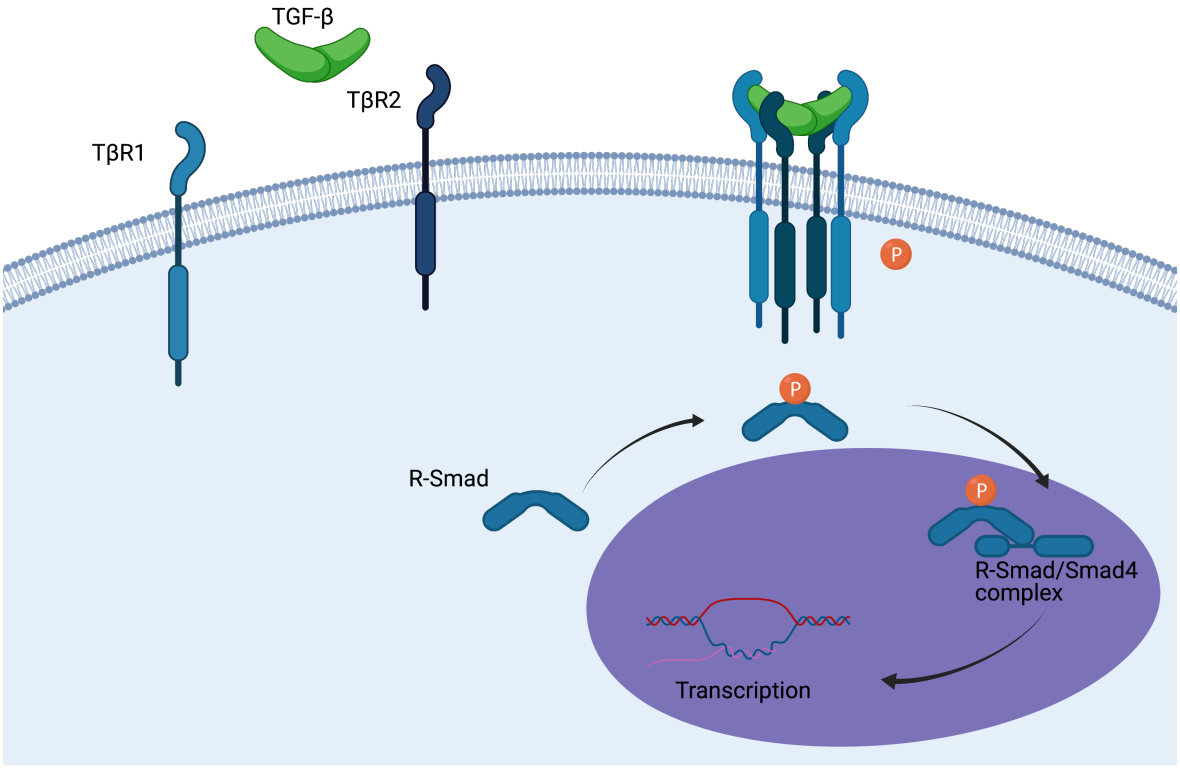

Figure 1.2. *The TGF-β signaling pathway. TGF-β binds to TβR2, leading to recruitment of TβR1 and formation of a hetero-tetrameric complex. Once the TβR1 is activated, R-Smad becomes phosphorylated and forms a hetero-oligomeric complex with Smad4. The R-Smad/Smad4 complex can then enter the nucleus and act as a transcription factor. This figure was created with BioRender.com and inspired by Suriyamurthy et al. (2019).*

1.1.2 TGF-β and its regulatory role on cell proliferation and cell differentiation

Activation of the TGF-β receptor by its ligands has a strong inhibitory effect on most cell types, but the inhibition is reversible once the ligands are detached from the receptor (Ohta et al., 1987). TGF-β inhibits cell proliferation mainly through two mechanisms: induction of cyclin-dependent kinase (CDK) inhibitors, and inhibition of mediators that contribute to cell proliferation (Morikawa et al., 2016). However, TGF-β can also promote cell proliferation in different types of cells, such as mesenchymal stem cells (Jian et al., 2006), endothelial cells (Goumans et al., 2002), and fibroblast cells (Roberts et al., 1981).

The outcome of TGF-β signaling depends on the current cell culture condition, resulting in either cell growth or growth inhibition (Roberts et al., 1985). Therefore, the same type of cells may display opposite responses under different experimental conditions (Morikawa et al., 2016). For instance, the study by Roberts et al. (1985) showed that TGF-β inhibited EGF-dependent cell proliferation in a monolayer culture of A549 cells, which is a human adenocarcinoma epithelial cell line. In the same study, TGF-β and EGF were shown to work together to enhance the anchorage-independent growth of the cells in the same cell culture. EGF is a mitogenic factor that stimulates cell proliferation of several cell types (Carpenter, 1987) by binding to the EGFR on the cell surface, leading to dimerization of the receptor (Dawson et al., 2005) and activation of its protein-tyrosine kinase activity (Chen et al., 1987).

Furthermore, the members of the TGF-β family also regulate cell differentiation (Morikawa et al., 2016). Previous studies have reported that TGF-β is associated with differentiation in a broad range of cell lineages, such as inhibited differentiation toward adipocytes (Ignotz & Massagué, 1985) and enhanced differentiation toward chondrocytes (Seyedin et al., 1985). The TGF-β/activin signaling pathway has also been suggested to have an important role in maintaining stem cell-like properties of certain cells that can promote cancer, for example, neoplastic human breast stem-like cells (Mani et al., 2008) and glioma-initiating cells (Ikushima et al., 2009). Recent studies have shown that pharmacological inhibitors can be used to reduce cancer progression by inhibition of TGF-β/activin type I receptor kinases (Ikushima et al., 2009; Lonardo et al., 2011). In contrast, other studies have reported that TGF-β signaling reduced the population of cancer-initiating cells in certain cancers (Ehata et al., 2011; Hoshino et al., 2015; Tang et al., 2007).

1.2 TGF-β signaling in disease

1.2.1 TGF-β in wound healing

Wound healing is a timely controlled and very complex process with specific phases. In order to repair the injured skin and close the wound, one phase has to be completed before the other begins. A wound can be either acute or chronic depending on how the healing process proceeds; An acute wound shows signs of healing within four weeks, whereas a chronic wound fails to follow the normal wound healing process, leading to formation of a non-healing wound. The wound healing process consists of a cascade of four phases: hemostasis, inflammation, proliferation, and remodeling (Guo & Dipietro, 2010; Spear, 2013). These four phases are

regulated by TGF-β signaling, leading to an accelerated wound healing response (Sporn et al., 1983). A previously published study has reported that TGF-β is one of many growth factors that are known to speed up the wound healing process, both in acute and chronic wounds (Penn et al., 2012).

When an injury occurs, platelets at the injury site become activated by forming a hemostatic plug that temporarily seals the open wound. The hemostatic plug contains a large amount of TGF-β1 protein (Assoian et al., 1983) that attracts monocytes (Wahl et al., 1987) and fibroblasts (Postlethwaite et al., 1987) to the inflammation site (Morikawa et al., 2016). The formation of the hemostatic plug leads to the inflammation phase, where TGF-β serves as a potent chemoattractant and inflammatory mediator for neutrophil cells (Reibman et al., 1991). The neutrophils are attracted to the inflammation site, where they can adhere to the injured vascular endothelial cell walls to defend the injured site against infection. Additionally, the neutrophils also produce inflammatory mediators to recruit and activate fibroblast and epithelial cells to the wounded area (Tarnuzzer & Schultz, 1996).

The proliferation phase is initiated once the number of neutrophils and inflammatory mediators are decreased and replaced with macrophages, which have a role in phagocytosis and production of collagenase and elastase (Spear, 2013; Tarnuzzer & Schultz, 1996). During the proliferation phase, the wounded skin is repaired and decreased, leading to a healed wound. The wound healing is mediated by TGF-β, resulting in the construction of new connective tissue and granulation, contractions, and epithelialization (Gurtner et al., 2008; Mahdavian Delavary et al., 2011). Once the macrophages have left the healing site, growth factors are secreted by fibroblast, endothelial, and keratinocyte cells to ensure a continuous proliferation, leading to a closed wound and scarless wound healing (Mast & Schultz, 1996). Finally, the remodeling phase is initiated by the scar formation, leading to reorganizing, remodeling, and maturation of collagen fibers that provide tensile strength to the new skin (Spear, 2013). The collagen fibers are deposited by fibroblast cells, which are promoted by TGF-β, and this is an important process to ensure a proper replacement of the extracellular matrix (ECM) during the remodeling phase (Liarte et al., 2020).

Occasionally, the amount of inflammatory mediators does not decrease during the inflammation phase. This could eventually lead to extensive tissue damage and an extended inflammatory phase of the wound healing process. Subsequently, the proliferation and remodeling phases of

the wound healing process will not be initiated due to the chronic inflammation in the wound (Tarnuzzer & Schultz, 1996), leading to pathological inflammation and development of a chronic wound. Wounds that are chronic and non-healing are frequently showing a loss of TGF-β1 signaling (Pastar et al., 2010). A recent study by Hanson et al. (2016) reported that stem cells, such as adipose-derived stem cells, may be applied to the injured skin as a potential wound healing agent as these cells secrete many useful growth factors, one of them being TGF-β (Park et al., 2008). An increase in TGF-β signaling can lead to an epithelial to mesenchymal transition (EMT), where the epithelial cells undergo several biochemical transformations to adopt a phenotype similar to mesenchymal cells. This transition gives rise to enhanced migration, invasiveness, enhanced resistance to apoptosis, and increased production of ECM components, which in turn leads to development and regeneration of epithelial tissue (Kalluri & Neilson, 2003; Kalluri & Weinberg, 2009).

1.2.2 TGF-β signaling in cancer

TGF-β can have both positive and negative effects on cancer development, depending on if it acts as a tumor suppressor or promoter (Derynck et al., 2001). As a tumor suppressor, TGF-β functions as an inhibitor of cell proliferation (Morikawa et al., 2016) by stimulating cell differentiation in normal and premalignant cells (Colak & Ten Dijke, 2017; Massagué, Joan, 2012). The cell proliferation is inhibited by TGF-β through induction of CDK inhibitors (Feng et al., 2000) and suppression of the proto-oncogene c-*myc* expression (Pardali et al., 2000).

However, as a tumor promoter, TGF-β can stimulate tumor progression and cancer metastasis (Derynck et al., 2001). This occurs during the advanced stages of cancer, where genes involved in the TGF-β signaling pathway are either deleted or mutated (Suriyamurthy et al., 2019), leading to a reduced sensitivity to TGF-β induced growth inhibition (Hahn et al., 1996). However, tumors that do not obtain mutations in the core components of TGF-β signaling, such as gliomas and breast cancers, may keep the ability to utilize TGF-β signaling to promote EMT, tumor invasion, metastatic dissemination, and evasion of the immune system (Morikawa et al., 2016). TGF-β can also activate and phosphorylate the PI3K-dependent AKT serine-threonine kinase (Shin et al., 2001), which leads to cancer progression and metastasis through EMT, cell migration, and invasion of cancer cells (Hanahan & Weinberg, 2011). At the same time, TGF-β and PI3K can activate the MAP proteins, ERK1 and ERK2, and downstream effectors, which lead to stimulation of cell survival and anti-apoptotic pathways in cancer (Parvani et al., 2011; Wang et al., 2020).

1.2.3 The relationship between wound healing and cancer

Several studies have shown that chronic inflammation can lead to tumorigenesis, which may suggest that the molecular mechanisms in wound healing and cancer are common (Dunham, 1972; Schäfer & Werner, 2008). A previous study reported that the tumor stroma and the granulation tissue of healing skin wounds resembled each other, suggesting that the formation of epithelial tumor stroma is promoted to activate the wound healing response (Dvorak, 1986). However, unlike wound healing, the active processes in cancer tissues are not controlled, which leads to excessive cell proliferation, invasion, and metastasis (Schäfer & Werner, 2008). Furthermore, the studies by Balkwill et al. (2005) and de Visser et al. (2006) showed that an abundance of inflammatory cells in chronic wounds may contribute to cancer development. Likewise, a recent study reported that inflammatory cells are probably involved in malignant transformation by releasing reactive oxygen species (ROS) and reactive nitrogen species. Reactive species can cause DNA damage and mutation of the proteins involved in DNA repair, cell-cycle checkpoint control, and apoptosis (Allavena et al., 2008). Therefore, an enhanced malignant transformation is often associated with inflammatory cells found in chronic wounds (Hussain et al., 2003).

1.3 Cell migration

The ability to migrate is important for the cells to perform physiological functions, for instance, during development, tissue remodeling, immune response, wound healing, as well as during cancer spreading (Scarpa & Mayor, 2016). The cells can either move individually as single cells or collectively as a group of cells, as shown in figure 1.3 (Loosdregt, 2020; te Boekhorst et al., 2016). Single cells migrate without cell-to-cell interactions to neighboring cells (Ridley et al., 2003), while cells moving in groups maintain their cell-to-cell interactions and migrate coordinately within the group (Friedl & Gilmour, 2009).

Cell migration is mediated through cytoskeletal activity, where the cells need to be polarized, form lamellipodium, and adhere to the ECM or other cells. Adhesion to the ECM is important to stabilize the lamellipodium, which further contributes to cell migration. These adhesions are mediated through integrin-based adhesion complexes expressed on the basal side of the migrating cells (Ridley et al., 2003; te Boekhorst et al., 2016). Cell migrations often occur in response to specific external stimuli, including chemical and mechanical signals (Mak et al., 2016; te Boekhorst et al., 2016). Cells can stimulate activation of cell motility when they are

exposed to a gradient of growth factors (chemotaxis) (Swaney et al., 2010), a gradient of ECM ligands (haptotaxis) (Smith et al., 2006), a stiffness gradient (durotaxis) (Vincent et al., 2013), or a gradient of electric fields (galvanotaxis) (Tai et al., 2018).

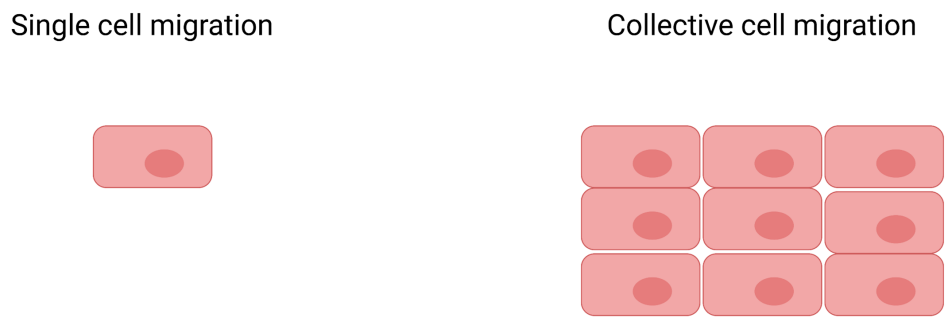

Figure 1.3. *Overview of different modes of cell migration. The cells can move individually as single cells (left), or collectively as a group with cell-to-cell contacts (right). Created with BioRender.com.*

1.3.1 Collective cell migration

Collective cell migration is a process where a group of cells moves together as a coordinated multicellular unit with the same speed and direction (Desai et al., 2013; Friedl, 2004). The cells are connected by cell-to-cell junctions and follow the migration direction by coordinating their response signals with the environment, leading to more effective cell migration (Lång et al., 2018; Mayor & Etienne-Manneville, 2016). In a cohesive cell group, there are leader cells and follower cells, depending on the position of the cells within the group. The leader cells are positioned at the front, whereas the following cells are positioned behind the leader cells. The leader cells can sense signals from the environment, and thereby determine the direction and speed of migration of the entire cohesive cell group (Friedl & Gilmour, 2009).

Collective cell migration is an important activity during development like for example gastrulation and organogenesis, where the cells are moving collectively to the necessary locations to perform specific functions (Weijer, 2009). However, collective cell migration also occurs during wound healing and cancer invasion (Friedl & Gilmour, 2009). Previously, studies have reported that the growth factor EGF is involved in dermal wound healing, where processes like cell stimulation, proliferation, and migration contribute to regeneration of new skin layers and wound closure (Bodnar, 2013; Shu et al., 2019; Singla et al., 2012). Recent studies have reported that TGF-β regulates cancer metastasis through the transactivation of other signaling

pathways such as the EGF/EGFR signaling pathway (Le Bras et al., 2015; Sundqvist et al., 2020; Zhao et al., 2018). EGF and other downstream signaling pathways associated with the EGF, such as the cell cycle regulator $p15^{INK4B}$ (Dunfield & Nachtigal, 2003), interferon-γ (IFN-γ)/STAT pathway (Ulloa et al., 1999), and oncogenic ras (Kretzschmar et al., 1999) can also regulate TGF-β signaling in several cell types.

1.3.2 Epithelial collective cell migration

Epithelial cells have an apical and a basal side, which give the cells the ability to form strong interactions during collective cell migration. These interactions are formed by the adhesion complexes expressed on the basal and apical sides of the cells. Subsequently, the specific cell sheet structure that epithelial cells form also mediates these strong interactions (Weijer, 2009). The epithelial cells maintain stable and strong cell-to-cell interactions during collective cell migration (Theveneau & Mayor, 2013), resulting in a restriction of the cell movements and cell rearrangements in the cell group (figure 1.4) (Zallen & Blankenship, 2008). Epithelial collective cell migration can be seen as branches, for instance, in the development of new blood vessels (Hamm et al., 2016). However, epithelial cells can also be seen as separated groups, for example as seen in border cells in *Drosophila* egg chambers (Lin et al., 2014). In addition to migrating as a group, the cells can also migrate as large epithelial cell sheets, where the cells are maintained in stronger and closer contact while moving forward (Lång et al., 2018; Rørth, 2009; Weijer, 2009).

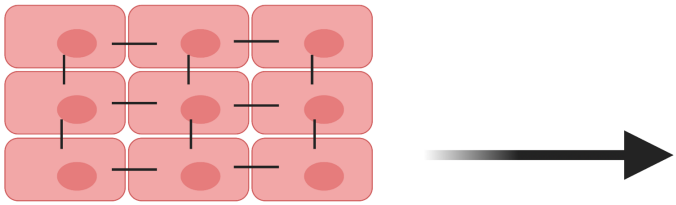

Figure 1.4. *Epithelial collective cell migration. The cells are interacting with each other through stable cell-to-cell adhesions. Cell-to-cell contacts are illustrated by black lines. The illustration is inspired by (Loosdregt, 2020), and created with BioRender.com.*

1.3.3 Mesenchymal collective cell migration

Epithelial cells need to partially transmit to mesenchymal cells to migrate over an extensive distance, but this transition requires a weakening of the tight cell-to-cell interactions, leading to

individual and polarized cells (figure 1.5) (Revenu & Gilmour, 2009). The polarized mesenchymal cells form cell-to-cell interactions when they collide, leading to loss of polarity and prevention of cell migration. Thus, the cells get repolarized and move in the opposite direction due to the contact-inhibition of locomotion (Loosdregt, 2020; Stramer & Mayor, 2017). However, the cells still move collectively due to secreted attractants (Theveneau & Mayor, 2013). The transient cell-to-cell adhesions lead to a reduced epithelial organization and more efficient motility (Revenu & Gilmour, 2009), allowing nearby cells to migrate to distinct locations (Weijer, 2009).

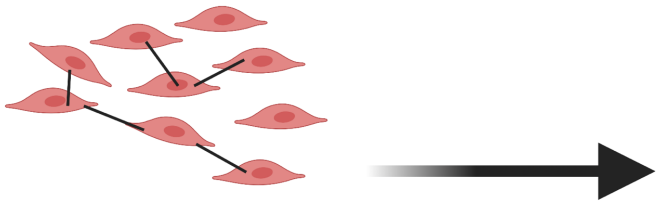

Figure 1.5. *Mesenchymal collective cell migration. The cells are interacting with each other through transient cell-to-cell adhesions. Cell-to-cell contacts are illustrated by black lines. The illustration is inspired by (Loosdregt, 2020), and created with BioRender.com.*

1.3.4 TGF-β induced cell migration

Studies have reported that TGF-β is upregulated in several tumors and can stimulate migration of tumor cells through EMT (Lee & Schiemann, 2014; Liu et al., 2019). TGF-β induced EMT leads to increased cell size, motility, and invasion due to rapid phosphorylation of AKT as the TGF-β signaling pathway is linked to PI3K, AKT, mammalian target of rapamycin (mTOR) complex 1, S6 kinase 1 (S6K1), and the eukaryotic initiation factor 4E–binding protein 1 (4E-BP1) (Lamouille & Derynck, 2007). A previous study reported that the PI3K inhibitor, LY294002, inhibited EMT induced by TGF-β, which supports the involvement of PI3K-AKT signaling in TGF-β induced EMT (Bakin et al., 2000). The activation of the PI3K-AKT pathway is also required for TGF-β induced cell migration (Hamidi et al., 2017), which may demonstrate the importance of the PI3K-AKT signaling pathway in cell migration. Furthermore, it has also been reported that the activation of the PI3K-AKT pathway can lead to down-regulation of TGF-β mediated apoptosis due to suppression of Smad3 (Chen et al., 1998; Song et al., 2003).

Activation of AKT leads to direct interaction with unphosphorylated Smad3, preventing Smad3 to become phosphorylated by TβR1. Further, this prevents the formation of a heteromeric complex with Smad4, leading to inhibition of the Smad-dependent pathway in the TGF-β signaling pathway (Remy et al., 2004). Suwanabol et al. (2012) demonstrated that overexpression of Smad3 led to accumulation of enhanced phosphorylated AKT (p-AKT) proteins, while inhibition of Smad3 led to a basal level of p-AKT in vascular smooth muscle cells, which further supports that TGF-β stimulated activation of AKT is mediated through Smad3. Further, the study reported that the intermediate between the TGF-β-Smad3 and PI3K-AKT signaling was p38 MAPK (Suwanabol et al., 2012), which may demonstrate that TGF-β stimulated cell migration could be mediated through Smad3, PI3K, AKT, and p38 MAPK.

1.4 Live cell imaging

Live cell imaging is a technique used to study living cells, for example, cellular responses after different stimuli by monitoring cell movements. The cells are usually tagged with a fluorescent dye and visualized with a fluorescence microscope to obtain images of living cells over time (Frigault et al., 2009; Haraguchi, 2002). Live cell imaging was performed with an ImageXpress Micro Confocal High-Content Imaging System Microscope from Molecular Devices. Further, the live cell imaging data were processed with automated data programs using particle image velocimetry (PIV) analysis.

1.4.1 The experimental system used to study collective cell migration

Live cell imaging experiments performed in this master thesis was based on a previously published *in vitro* experimental system (Lång et al., 2018). The main hallmarks of this assay are the use of confluent epithelial cell sheets and synchronization of the cells by serum deprivation. Serum deprivation initiates a dormant and resting cell state, referred to as quiescence, in the confluent cell sheets. Subsequently, serum re-stimulation of confluent quiescent cell sheets was shown to activate a highly coordinated collective cell migration response followed by cell division.

The experimental approach is based on the induction of quiescence, and preliminary results suggest that the efficient activation of collective cell migration observed origin from the buildup of a tension gradient in the cell layer during quiescence. Thus, the collective cell migration response is not activated by external stimuli or gradient in the cell culture, but an internal

gradient of tension. However, this is currently a hypothesis that need to be tested and confirmed by further experiments. Subsequent serum re-stimulation is essential to activate cell coordination and cell migration in this system. This experimental system was used to study how TGF-β regulates epithelial collective cell migration, and to examine the crosstalk between the TGF-β and EGF/EGFR signaling pathways.

1.4.2 ImageXpress Micro Confocal High-Content Imaging System

The ImageXpress Micro Confocal High-Content Imaging system is a high-content automated microscope that can change between a widefield and confocal imaging mode and image both fixed and live cells. The images acquired with the microscope are of high quality due to an AgileOptix™ spinning disk confocal technology. The microscope provides excellent contrast, high resolution, and bright light source, which makes it easier to monitor whole organisms, thick tissue slices, 2D and 3D models, and cellular or intracellular events (Molecular Devices, n.d.; Schindelin et al., 2012).

The MetaXpress High-Content Image Acquisition and Analysis Software is a high-content image analysis software developed for the ImageXpress Micro Confocal High-Content Imaging System. The software is featured with a time-lapse analyzing tool and can be used to accelerate the speed of the analysis in a high-throughput environment. The MetaXpress software can be used to acquire and analyze 2D and 3D images, streamline image analysis, and custom-made analysis are also possible (Molecular Devices, n.d.; Schindelin et al., 2012).

1.4.3 PIV analysis

PIV analysis is a quantitative technique used to study the flow distribution in a fluid to obtain instantaneous velocity measurements. The fluid field is measured by scattered light reflected from particles that are seeded into the fluid (Day et al., 2001; Kukura et al., 2003), and the measurements are used to calculate the displacement vector between two image frames (illustrated in figure 1.6) in a series of images (Cohen et al., 2014; Petitjean et al., 2010). The displacement vectors were used to calculate the magnitude of the velocity vectors to track how the particles are moving in the fluid (Taylor et al., 2010).

The series of images are captured by a high-speed digital camera using an illuminated pulsating laser, and the images are separated precisely with a known time interval, which makes it

possible to compare the particle displacement between two images within a frame. The velocity data gained from the experiments provide information about the flow and can also be used to validate computational simulations. This information allows measurements of the local velocity of the fluid at every region of the images (Day et al., 2001). Furthermore, the motion of the vectors can be used to calculate the speed and direction of the velocity field. By using this technique, it is possible to study biological processes like collective cell migration patterns (Lång et al., 2018) and morphogenetic movements (Supatto et al., 2005). In our experimental setup, PIV analysis was performed on acquired live cell imaging data to track individual cells in a confluent epithelial cell sheet over a long period of time and analyze migration patterns formed after treatment with different external stimuli.

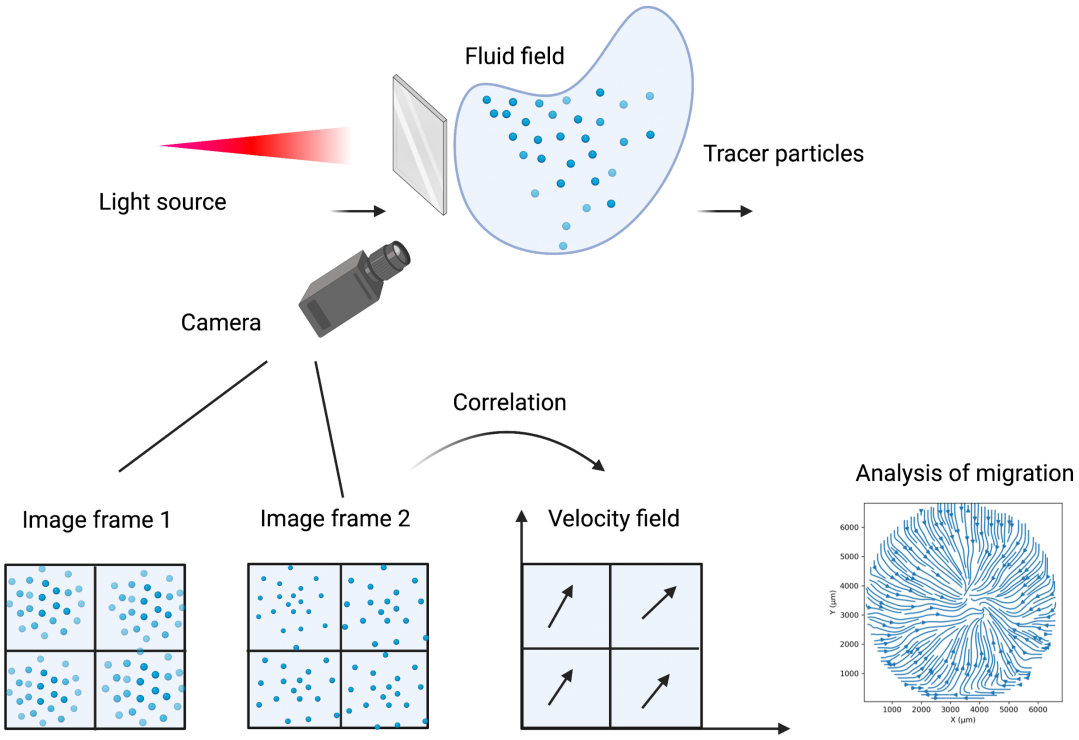

Figure 1.6. *Illustration of particle image velocimetry (PIV) analysis. The fluid field with tracer particles is measured by a high-speed digital camera using a laser to generate a series of images. The images are used to calculate the correlation between the particles in each frame pair to obtain a velocity field. The data can for instance be used to study cell migration patterns. Created with BioRender.com.*

1.5 Detection of proteins

Protein detection is a method used to study proteins by evaluating the concentration and amount of different proteins in a specific sample (Westermeier, 2016). Several approaches have been developed to identify proteins, including Bradford protein assay (Ernst & Zor, 2010), Lowry protein assay (Redmile-Gordon et al., 2013), the enzyme-linked immunosorbent assay (ELISA) (Hnasko et al., 2011), high-performance liquid chromatography (HPLC) (Mitulović & Mechtler, 2006), liquid chromatography-mass spectrometry (LC-MS) (van de Merbel, 2019), and western blotting analysis (Bass et al., 2017).

1.5.1 Western blotting

Western blotting, also known as immunoblotting, is a common technique used to separate and detect proteins by using polyacrylamide gel electrophoresis (PAGE). The detected protein is identified due to binding to specific antibodies and provided information about its molecular weight (Hnasko & Hnasko, 2015). The technique includes sample preparation of cell lysates, PAGE to separate protein sizes, transfer of proteins onto a membrane, blocking of non-specific proteins, primary and secondary antibody incubation, detection, and analysis, as illustrated in figure 1.7 (Bass et al., 2017).

The protein sample is acquired by lysis or disruption of the cell membranes using a mechanical, sonication, or chemical approach. Further, the extracted protein sample is homogenized with a buffer to ensure solubility and optimization of the proteins, and a reducing agent is used to unfold the proteins in the sample. The proteins are then coated with sodium dodecyl sulfate (SDS) detergents to obtain negative charges on the hydrophobic regions of the proteins. Negative charges allow the proteins to move in the electrical field and thereby be separated with PAGE. After the proteins are separated in the gel, the proteins are transferred to a nitrocellulose membrane to immobilize the proteins, and thereby allow for probing with primary and secondary antibodies. However, before the proteins are incubated with antibodies, the membrane is blocked to prevent binding of non-specific antibodies. Finally, the protein bands on the membrane are visualized with a fluorophore and detected with an imaging system, and the protein bands can then be analyzed with an imaging software (figure 1.7). Furthermore, the sizes of the protein bands are compared to a protein standard ladder in order to detect the protein of interest (Bass et al., 2017).

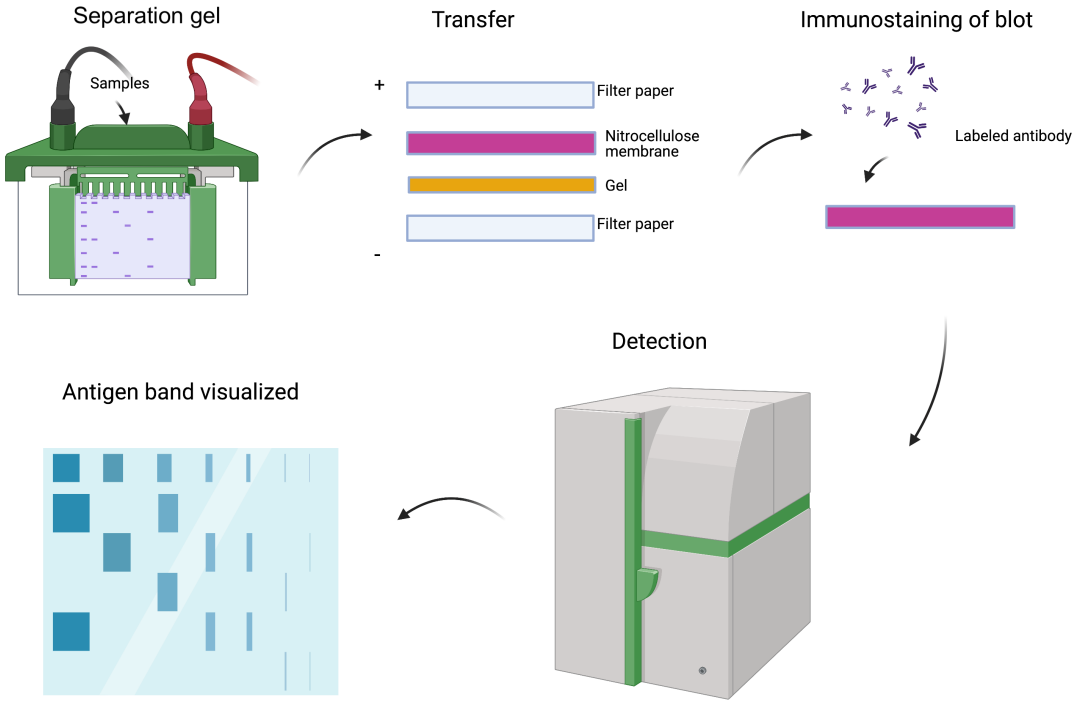

Figure 1.7. *Schematic overview of the western blotting technique. The samples are prepared and separated by electrophoresis before transferring to a nitrocellulose membrane. The membrane is incubated with primary and secondary antibodies. Finally, the protein bands are detected, and images acquired using an imaging system. Created with BioRender.com.*

2 Aim of the study

This master thesis was conducted within the research group "Experimental cancer therapy" led by Stig Ove Bøe. TGF-β is an interesting growth factor due to its diverse roles and functions in cell growth, cell differentiation, and apoptosis, as well as wound healing and metastasis. Several studies have shown that TGF-β signaling in cancer cells may lead to apoptosis or cell growth, depending on the cell state and the stages of the tumor. Recent studies have also shown that TGF-β regulates the spreading of cancer cells through transactivation of other cell signaling pathways, for instance, the EGF/EGFR signaling pathway. Further, both TGF-β and EGF are reported to be involved in wound healing by regulating epithelial cell migration. Preliminary results have shown that TGF-β and EGF can activate different patterns of cell migration. The intracellular connection between these signaling pathways may be important for the spreading of cancer cells and wound healing, which is associated with collective cell migration. However, the molecular mechanisms that regulate TGF-β induced cell migration are not yet known. A deeper understanding of the molecular mechanisms that drive TGF-β regulated cell migration is important for the development of new approaches to prevent the spreading of tumors and improve wound healing regimes.

The main purpose of this master thesis is to examine how TGF-β regulates collective cell migration, and which intracellular signaling pathways are activated during TGF-β-inducted keratinocyte migration. An understanding of the regulatory role of TGF-β in epithelial cell migration may give a deeper understanding of TGF-β signaling in metastatic cells and wound healing. Besides, the study aims to examine how the TGF-β signaling pathway is affected by other signaling pathways, for instance, the connection between the TGF-β and EGF/EGFR signaling pathways.

The main objectives of this master thesis are to:

I. Study the role of TGF-β signaling in collective cell migration using an *in vitro* human skin experimental approach.
II. Examine the inhibitory and stimulatory effects of TGF-β on collective cell migration in epithelial cell sheets.
III. Examine if the TGF-β and EGF/EGFR cell signaling pathways are collaborating in the regulation of collective cell migration in epithelial cell sheets.

3 Materials and Methods

Information about the materials, equipment, instruments, and computer software used in these experiments is provided in appendix A. All the materials and equipment used in cell culture work have to be sterile, and an aseptic technique was used under the working process unless specified otherwise. The cell work was conducted in a chemical fume hood, Safe 2020 Class II Biological Safety Cabinet (Thermo Fisher Scientific), at room temperature, and the solutions were removed with a vacuum aspiration tool (Integra Vacuboy) and added with a pipette unless specified otherwise. The experimental setup used in this study was based on a previously published article "Coordinated collective migration and asymmetric cell division in confluent human keratinocytes without wounding" (Lång et al., 2018).

3.1 Cell line and cultivation

3.1.1 Cell line

The cell line used in this project is called HaCaT, and it is a keratinocyte cell line derived from human skin. HaCaT cells are transformed to be an immortal cell line, yet nontumorigenic (Boukamp et al., 1988). Even though the cells are transformed, they still maintain a continuous and regulated cell cycle. The cell line undergoes normal cell cycle progression and is able to differentiate and reconstruct a well-structured epidermis (Schürer et al., 1993). Because of these features, the HaCaT cells are a good substitute for *in vitro* studies of epithelial collective cell migration mechanisms in human skin. HaCaT cells modified with mCherry-fluorescently tagged Histone H2B proteins were used to visualize the chromatin and cell nuclei in the live cell imaging experiments (Lång et al., 2012).

3.1.2 Culturing condition

The HaCaT cells (CLS) were cultured in Iscove's Modified Dulbecco's Medium (IMDM; Sigma-Aldrich) supplemented with 10% fetal bovine serum (FBS; Sigma-Aldrich) and 90 U/mL penicillin/streptomycin (PenStrep; Gibco). The cells were grown in a T75 cell culture flask (Thermo Fisher Scientific) and cultured at 37°C in a 5% CO_2 incubator (Thermo Fisher Scientific).

3.1.3 Cell culture maintenance

Daily observation and continuous cell culture maintenance are important in order to maintain an optimal growth rate and cell density in the cell culture. The cells are normally diluted in a ratio of 1:10 and maintained every other day. However, dilution ratios of 1:2 and up to 1:20 were also used, depending on if the cell were required for an experiment the next day or kept in culture during the weekend.

The HaCaT cells were passaged by removing the existing growth medium, IMDM supplemented with 10% FBS, and washed twice with 6 mL phosphate-buffered saline (PBS; Oslo University Hospital). Before the PBS was removed, the flask was tilted gently to ensure that all the cells were rinsed. After the cells were washed, PBS was substituted with 2 mL 0.25% Trypsin-EDTA (Gibco) to detach the cells from the surface of the flask. The cells were then incubated for 15 minutes at 37°C in a 5% CO_2 incubator. A lightly tapping on the flask could help the cells to detach easier as they are an adherent cell line. When the cells were completely detached, the cells were supplemented with 8 mL growth medium to deactivate the trypsin, and the cell suspension was mixed up and down a few times using a pipet to ensure that all the trypsin was neutralized. The cells were then resuspended with growth medium and diluted in a ratio of 1:10 in a total volume of 13 mL. The rest of the cell suspension was discarded, while the newly passaged cells were allowed to settle down overnight at 37°C and 5% CO_2.

3.1.4 Collagen coating

A 96-well Greiner Sensoplate with glass bottom (Greiner Bio-One) was used in live cell imaging experiments. Prior to an experiment, the 96-well plate was coated with collagen IV (Sigma-Aldrich) derived from the human placenta to ensure better cell attachment and a better environment for cell migration. A stock solution of collagen IV was premade by dissolving 50 mg collagen IV in sterile PBS to a final concentration of 1 mg/mL. The stock solution was aliquoted and stored at -20°C. Prior to coating, a working solution containing a collagen IV concentration of 20 µg/mL was prepared by an additional 1:50 dilution of the stock solution. Approximately 100 µL of the solution was added to each well of the 96-well plate, and the plate was sealed with parafilm to avoid evaporation of the collagen solution. The plate was stored in the refrigerator at 4°C overnight or during the weekend.

3.1.5 Cell counting

Before a live cell imaging experiment was performed, the cells were counted to calculate the amount of cell suspension and medium needed in the seeding protocol, described in section 3.1.6. Cell counting is important to ensure the right cell density, and that the right number of cells was seeded into each well. The cells were counted with the Countess™ 3 Automated Cell Counter (Invitrogen). This is an advanced machine that uses deep learning algorithms to analyze the cell sample to provide accurate cell counts and estimate cell viability (Thermo Fisher Scientific, n.d.).

Before counting, the cells were treated with 2 mL 0.25% Trypsin-EDTA and resuspended in 8 mL growth medium, as described in section 3.1.3. The cell suspension was mixed up and down a few times to ensure that all the cells were separated from each other, resulting in a cell suspension of single cells. Then, 15 µL of the cell suspension was added to 15 µL 0.4% Trypan Blue Stain Solution (Invitrogen) in an Eppendorf tube, and the solution was homogenized by pipetting up and down a few times. 10 µL of the solution was transferred into each chamber of a Countess™ Cell Counting Chamber Slide (Invitrogen), and the total cell count was then estimated with the cell counter.

3.1.6 Cell seeding in 96-well plates

After the total cell count was estimated, the cells were seeded in a 96-well plate coated with collagen IV to produce confluent epithelial cell sheets (figure 3.1.). A seeding suspension was prepared to achieve seeding of 75 000 cells in a total volume of 150 µL that was transferred to each well in the plate. In order to calculate the amount of cell suspension needed in the solution used for seeding, the following formula was used:

(1) $$The\ amount\ of\ cell\ suspension = \frac{Number\ of\ desired\ cells * Number\ of\ wells}{Total\ cell\ count}$$

To calculate the amount of growth medium needed in the seeding solution, the following formula was used:

(2) $$The\ amount\ of\ growth\ medium = (150\ \mu L * Number\ of\ wells) - The\ amount\ of\ cell\ suspension$$

The total number of wells in the plate was 96, but due to pipetting deviations or pipetting inconsistency, it is wise to make the calculation for 110 wells to ensure that we have enough solution for the whole plate. The calculated amount of cell suspension and growth medium were mixed in a plastic tray to make the seeding suspension. Before cell seeding, the wells in the 96-well plate were washed twice with PBS to remove excess collagen IV. Once the wells were washed, the cells were seeded in the 96-well plate using a multichannel pipette. The plate was then left standing on the bench at room temperature for 20 minutes to allow the cells to settle down in the wells. Finally, the cells were incubated in a 37°C incubator with 5% CO_2 overnight before starvation.

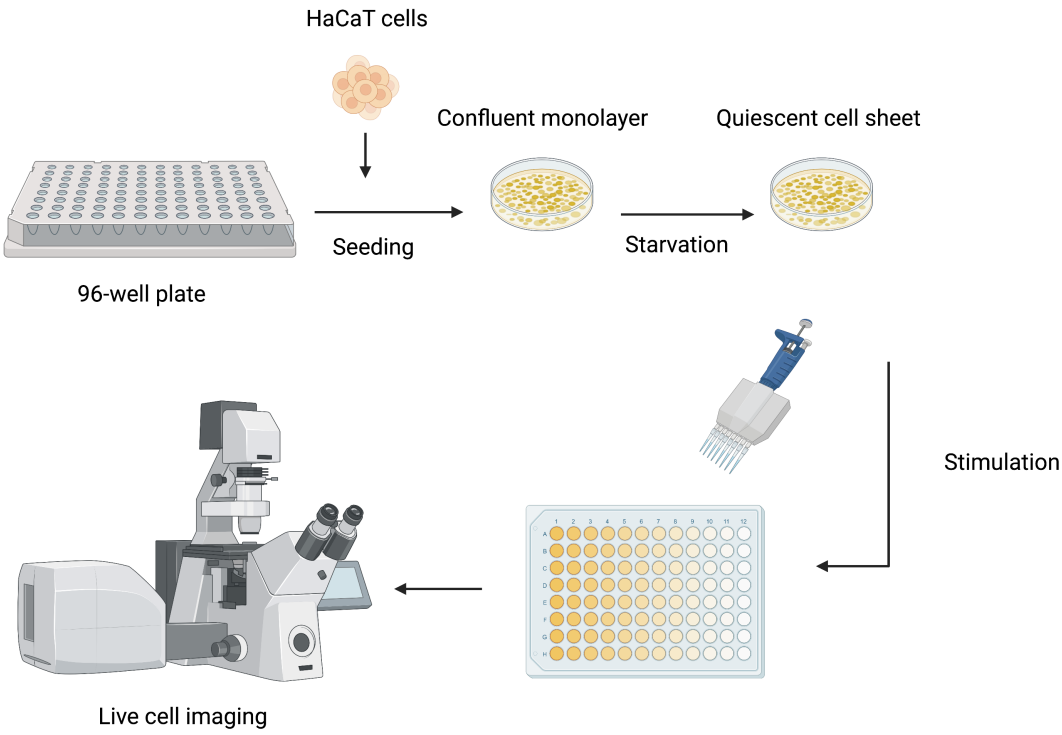

Figure 3.1. *Illustration of the experimental setup of live cell imaging experiments. The HaCaT cells were seeded into a 96-well plate and incubated overnight to produce a confluent monolayer of epithelial cells. Further, the cells were starved to form a quiescent cell sheet before stimulation. The different shades of yellow in the figure demonstrate each treatment used in the experimental setup. After stimulation, live cell imaging was performed to monitor cell movements. Created with BioRender.com.*

3.1.7 Cell starvation

Cell starvation was performed in order to form quiescent cell sheets before re-stimulation (figure 3.1). The cells were washed twice with serum-free IMDM medium, and the medium was removed and added with a multichannel pipette. The pipette tips were changed for every three rows. It is important to avoid touching the bottom of the wells, since this may cause holes or scratches in the cell sheet, which may affect the cell sheet migration during live cell imaging. After washing, the cell sheets were cultured in 150 µL serum-free IMDM medium at 37°C and 5% CO_2 for 48 to 72 hours.

3.2 Cell treatment with TGF-β, EGF, and inhibitors of their receptors

3.2.1 Preparing TGF-β and the TβR1 inhibitor SB431542

Preparation of a human TGF-β recombinant protein was done according to the protocol "Reconstituting and Aliquoting TGF-β1" (Farhat, 2012). Before TGF-β was dissolved, two solutions were prepared to make the reconstitution solution. A stock solution of 1.2 M HCl was prepared by diluting 12 M HCl (Sigma-Aldrich) in a ratio of 1:10. Further, a stock solution of bovine serum albumin (BSA; Saveen Werner AB) was prepared by dissolving BSA in Milli-Q (MQ) water to a concentration of 7.5% or 0.075 g/mL. The solutions were then sterile filtered by using a 0.20 µm non-pyrogenic filter.

Subsequently, a reconstitution solution of 160 µL BSA (7.5%), 40 µL HCl (1.2 M), and 11.8 mL MQ-water was made. To ensure that the solution was homogenized, the reconstitution solution was mixed up and down a few times using a pipet, and then sterile filtered using a 0.20 µm non-pyrogenic filter. Subsequently, 100 µL of the reconstitution solution was added to the vial containing 2 µg TGF-β1 recombinant protein (R&D Systems). The TGF-β1 protein was easily dissolved by pipetting up and down a few times. The TGF-β stock solution had a final concentration of 20 ng/µL, and to avoid unnecessary thawing of the protein solution, aliquots of 20 µL were made in Eppendorf tubes. The stock solution was stored at -80°C and the reconstitution solution was stored at -20°C (Farhat, 2012).

A stock solution of 10 mM SB431542 (Sigma-Aldrich), a TβR1 inhibitor, was made by dissolving 5 mg SB431542 in dimethyl sulfoxide (DMSO; Sigma-Aldrich) to a final concentration of 10 mM. Once the SB431542 was dissolved, aliquots were made and stored at -20°C.

3.2.2 Preparing EGF and the EGFR inhibitor Gefitinib

The stock solution of EGF was made by dissolving 1 mg EGF recombinant protein (R&D Systems) in sterile PBS to a final stock concentration of 20 µg/mL. The stock solution was aliquoted in Eppendorf tubes and stored at -20°C.

A stock solution of 50 mM Gefitinib, an EGFR inhibitor, was made by dissolving 110 mg of the crystalline solid Gefitinib (Sigma-Aldrich) in DMSO to a final stock concentration of 50 mM. The solution was vortexed to acquire a homogenized solution, and the solution was aliquoted and stored at -80°C.

3.2.3 Preparation of cell treatments

The cell sheets were treated with TGF-β, EGF, SB431542, or Gefitinib, and the reagents were diluted with serum-free IMDM or IMDM supplemented with 15% FBS (table 3.1). Each solution was prepared in a plastic tray with a total volume of 2 mL, and the volume of each reagent used in cell sheet stimulation was calculated using the following equation:

$$(3)\ Volume\ of\ stock\ solution = \frac{Total\ volume * Total\ concentration}{Concentration\ of\ stock\ solution}$$

The amount of medium used in the mixture was calculated with the following equation:

$$(4)\ Volume\ of\ medium = Total\ volume - Volume\ of\ stock\ solution$$

3.2.4 Cell stimulation and plate setup

Three different plate setups were used in the live cell imaging experiments performed (table 3.1), and two to three independent experiments were performed for each plate setup. Experiment 1 investigated the effects of different concentrations of TGF-β ± FBS and the effect of the TβR1 inhibitor, SB431542, on FBS stimulated cells. Experiment 2 investigated the effects of the combined treatment of TGF-β and EGF, and the regulatory effect of TGF-β on the EGF/EGFR signaling pathway by inhibiting the EGFR with Gefitinib. Further, Gefitinib was used on FBS stimulated cells in order to show the importance of the EGF/EGFR signaling pathway in epithelial cell migration. Similar to experiment 1, experiment 3 investigated the effects of different concentrations of TGF-β. In addition, the combined effect of TGF-β and EGF were tested for different TGF-β concentrations.

Table 3.1. An overview of the plate setup used in live cell imaging experiments. Three different live cell experiments were performed, and each experiment included twelve different treatments, corresponding to the number of columns in the 96-well plate as illustrated in figure 3.1.

	The plate setups in live cell experiments			
Treatments in each column of the plate		**Experiment 1**	**Experiment 2**	**Experiment 3**
	1	Starved	Starved	Starved
	2	15% FBS	15% FBS	15% FBS
	3	10 ng/mL EGF	10 ng/mL EGF	10 ng/mL EGF
	4	5 ng/mL TGF-β	5 ng/mL TGF-β	5 ng/mL TGF-β
	5	10 ng/mL TGF-β	15% FBS + 5 ng/mL TGF-β	10 ng/mL TGF-β
	6	20 ng/mL TGF-β	15% FBS + 20 ng/mL TGF-β	20 ng/mL TGF-β
	7	40 ng/mL TGF-β	10 ng/mL EGF + 5 ng/mL TGF-β	40 ng/mL TGF-β
	8	15% FBS + 5 ng/mL TGF-β	10 ng/mL EGF + 20 ng/mL TGF-β	10 ng/mL EGF + 5 ng/mL TGF-β
	9	15% FBS + 10 ng/mL TGF-β	5 μM Gefitinib + 5 ng/mL TGF-β	10 ng/mL EGF + 10 ng/mL TGF-β
	10	15% FBS + 20 ng/mL TGF-β	5 μM Gefitinib + 20 ng/mL TGF-β	10 ng/mL EGF + 20 ng/mL TGF-β
	11	15% FBS + 40 ng/mL TGF-β	15% FBS + 5 μM Gefitinib	10 ng/mL EGF + 40 ng/mL TGF-β
	12	15% FBS + 10 μM SB431542	15% FBS + 10 μM SB431542	15% FBS + 5 ng/mL TGF-β

The cell sheets were either starved with serum-free IMDM medium, or stimulated with IMDM medium supplemented with 15% FBS, EGF, TGF-β, Gefitinib, SB431542, or a combination of these. The treatment solutions were made as described in section 3.2.3, and the existing medium in the plate was substituted with 150 μL of the treatment. Each solution was added to the wells according to the plate setup, as specified in table 3.1. The plate was then placed in the ImageXpress Micro Confocal Microscope (Molecular Devices) to capture images of the cell sheet migration. Before running the microscope, the plate was incubated at 37°C and 5% CO_2 for 1 hour in a compartment of the microscope, to ensure a stable temperature in the whole system. A variation in temperature between the plate and the instrument will affect the automated focusing on the sample during image acquisition.

Additionally, vibrations and mechanical disturbances in the system can affect image acquisition. An example of this is observed in some of the cell sheet velocity plots, where the line plots displayed missing data points. This can be explained by irregular movements in the XY-stage of the instrument during image acquisition, leading to exclusion of these images during PIV analysis. A change in position will affect the computer's ability to analyze and track the cells between image frames, and a misalignment will therefore lead to exclusion of images. If all four images from a well, acquired at a specific time point, are excluded, no information on cell migration speed at that time point will be provided by the PIV analysis.

3.3 Monitoring migration patterns

3.3.1 Live cell imaging

Live cell imaging was performed using the ImageXpress Micro Confocal Microscope equipped with a 4x Plan Apo Lambda Nikon air objective lens with a camera binning of 2 and a pixel size of 3.367 µm x 3.367 µm. Using the 4x objective, the cell sheets in each well can be monitored by acquiring 4 images. These images can be either analyzed as single images by PIV analysis or combined into one image for each well and time point, producing time-lapse movies for further visualization and analysis of migration patterns.

The microscope consists of an incubation compartment with a built-in microscope stage, where the 96-well plate was placed. The images were obtained in widefield mode, and the time series were generated by time-lapse comprising of 114 timepoints at intervals of 16 minutes, resulting in a total acquisition period of 30 hours. Further, the MetaXpress High-Content Image Software was used to create time-lapse movies of the acquired images. The acquired images were tiled together with a custom-made analysis tool made in the MetaXpress High-Content Image Software to produce movies of the entire cell sheet in each well of the 96-well plate. These movies were analyzed with the Fiji ImageJ, Python, and PyCharm software to generate data of cell coordination and cell migration velocities.

3.3.2 Analysis of migration patterns with PIV

In order to describe the magnitude and directionality of collective motions, the cell sheets were monitored using an ImageXpress Micro Confocal Microscope, as described in section 1.4.1 in the introduction and section 3.3.1 above. The data obtained were analyzed with available *in-house* Python scripts using PyCharm (2019.2.3), which is an integrated development

environment (IDE) used in computer programming, specifically developed for the Python language. The scripts used for the analysis were file_sorting.py, 4xPIV_4.py, 4xPIV_5.py, plot_speed.py, plot_order.py, and stream_line.py, and all the scripts can be found in appendix B.

The separated images from each well, generated from the ImageXpress Micro Confocal Microscope, were organized in time points, and the script file_sorting.py was used to sort the images in order to get all time points from one well in the same folder. PIV-based cell motility analysis, described in section 1.4.2 in the introduction, was performed with the scripts 4xPIV_4.py and 4xPIV_5.py. The data from the script 4xPIV_4.py was further processed with the script plot_speed.py to generate the mean migration speed and the standard deviation of the cell sheets over time. The data from the script 4xPIV_5.py was further processed with the script plot_order.py to generate the mean cell coordination and the standard deviation. The cell coordination plot describes how coordinated the cell migration was over time. The degree of cell coordination was defined by the order parameter, φ, which is derived from the average of the cosine of the angle of each vector (equation 5) from PIV analysis for the direction of the field (Cohen et al., 2014).

$$(5)\ \varphi = \frac{1}{n} * \sum_i \cos(\theta_i)$$

By using this equation, the amount of cell coordination parallel to the direction of the field is captured during stimulation (Cohen et al., 2014). A φ-value of 1 describes perfectly uniform cell coordination over time, whereas 0 describes a randomly oriented cell migration with no coordination. Finally, the script stream_line.py was used to visualize the migration pattern of the cells. The migration pattern of the cells was illustrated as arrows to show the direction of the cell movements at a given time point after stimulation. This plot is also based on PIV analysis, where the vector components in the vector field are interpreted as cells in the cell sheet.

3.4 Western blot

3.4.1 Cell preparation

The HaCaT cells used in western blot analysis were wild-type cells, and before the cell lysate was prepared, the cells were seeded, subjected to starvation, and stimulation in a 12-well

Nunclon Delta Surface plate (Thermo Fisher Scientific). The plate was coated with collagen IV, as previously described in section 3.1.4, and the cells were counted as described in section 3.1.5. The number of cells required for this experiment was 600 000 cells per well, and the number of cells was calculated with the formulas from section 3.1.6. The cell suspension was diluted with growth medium to obtain the correct cell density. Subsequently, 1.5 mL of the solution was added into each well and the cells were incubated in a 37°C and 5% CO_2 incubator overnight. After incubation, the cells were starved with 2 mL serum-free IMDM medium in each well, as described in section 3.1.7.

After starvation, the cells were stimulated with 5 ng/mL TGF-β at different time points: 1 hour, 10 hours, and 25 hours, respectively. Additionally, a control of starved cells was left unstimulated, and a control stimulated with 10 ng/mL EGF for 1 hour was made (table 3.2). The volume of TGF-β and EGF stock solutions used in each well was calculated with equation (3), described in section 3.2.3, and the reagents were diluted with serum-free IMDM medium to a final volume of 2 mL.

Table 3.2. An overview of treatments and stimulation time used in the preparation of each cell lysate.

	Treatments	**Stimulation time**
1	Starved	0 h
2	10 ng/mL EGF	1 h
3	5 ng/mL TGF-β	1 h
4	5 ng/mL TGF-β	10 h
5	5 ng/mL TGF-β	25 h

3.4.2 Western blot cell lysate

A protein cracking buffer, premade by Bøe's research group, was used to lyse the cells. This buffer contained 6% SDS (Sigma-Aldrich), 30% glycerol (Sigma-Aldrich), 10 mM Tris-EDTA buffer solution pH 8 (Sigma-Aldrich), and bromophenol blue (Sigma-Aldrich). The stock solution of the protein cracking buffer was prepared by adding 150 µL of β-mercaptoethanol (βME; Sigma-Aldrich) to 1 mL of the buffer before use. The solution was mixed up and down with a pipet a few times, and 1 mL of the solution was further diluted with 2 mL MQ-water. Before the protein cracking buffer was added to the cells, the existing medium was removed, and the cells were washed twice with PBS. 200 µL of the cracking buffer was added to each

well, and the cells were scraped with a cell scraper until a viscous mixture was formed. The mixtures were then transferred to QIA-shredder columns with collection tubes (Qiagen). Finally, the columns were centrifuged with Biofuge Pico (Heraeus) for 1 minute at maximal speed, roughly 13000 rpm. The collection tubes, containing the cell lysates, were then stored at -20°C prior to western blot analysis.

3.4.3 Western blotting

The cell lysates were thawed on the bench at room temperature, and heated on an AccuBlock Digital Dry Bath (Labnet) for 10 minutes at 70°C. In the meantime, the SDS-PAGE gel electrophoresis was prepared by filling the mini gel tank (Invitrogen) halfway with MOPS SDS Running Buffer (Invitrogen), and the Bolt™ 10% Bis-Tris Plus gels with 10 wells (Invitrogen) were installed in the tank. The tank was then filled with MOPS SDS Running Buffer again until all the wells were filled with buffer.

The cell lysates and the protein standard marker, Precision Plus Protein™ Dual Color standards (Bio-Rad), were loaded into the wells of each gel. 5 µL of the protein standard marker and 15 µL of the cell lysates were used. The gels were then run at 200 V for 40-50 minutes, or until the three smallest bands in the protein ladder had passed through the gel. This was done to allow for good separation of the protein in the middle-sized range. The proteins were transferred from the gels to the nitrocellulose membranes, Trans-Blot Turbo Transfer pack (Bio-Rad), by using a western blotting transfer system, Trans-Blot Turbo Transfer System (Bio-Rad). The transfer pack contained a "bottom stack" with an anode and membrane, and a "top stack" with a cathode and moist buffer paper. The gels were placed in between the bottom stack and the top stack, and a rolling tool was used to remove air bubbles from the "sandwich". The blotting was carried out with the program "High MW Mini" at 25 V and 1.3 A for 10 minutes.

After the proteins were transferred to the membranes, the membranes were placed in separated containers and blocked in 10 mL 5% skimmed milk. The skimmed milk was made with 2.5 g skim milk powder (Sigma-Aldrich) and 50 mL PBS-Tween, which consisted of 4.5 L MQ-water, 0.5 L 10x PBS, and 5 mL 0.1% Tween-20 (Sigma-Aldrich). The membranes were blocked for 1 hour at room temperature and a tilt shaker was used to keep the membrane moist at all times. The blocking solution was then removed, and the membranes were incubated with primary antibody (table 3.3) diluted in 5% skimmed milk at 4°C overnight with agitation. The containers were sealed with parafilm to avoid evaporation of the primary antibody solution.

The next day, the primary antibody solution was removed, and the membranes were washed in PBS-Tween for 3x10 minutes with agitation. The membranes were then incubated with secondary antibody (table 3.3) diluted in PBS-Tween for 1 hour at room temperature with agitation. After 1 hour incubation, the secondary antibody solution was removed, and the membranes were washed 3x10 minutes with PBS-Tween with agitation. After washing, the membranes were developed using a SuperSignal™ West Pico PLUS Chemiluminescent Substrate Kit (Thermo Fisher Scientific), consisting of SuperSignal West Pico PLUS Luminol/Enhancer and SuperSignal West Pico PLUS Stable Peroxide. This is a horseradish peroxidase (HRP) substrate that binds to the secondary antibody, and an equal amount of each solution was mixed together before adding to the membranes. The membranes were transferred to a plastic pocket, and the HRP substrate was added drop by drop to each membrane. The membranes were then developed one by one in the ChemiDoc MP Imaging System (Bio-Rad) for protein detection, and the images were acquired with the Image Lab Software (Bio-Rad). The settings used to develop the western blot were "Chemi High Sensitivity (4x4 binning)" and "BioRad Ready Gel".

Table 3.3. Primary and secondary antibodies used in western blot analysis.

Target protein	**Primary antibody**	**Dilution**	**Secondary antibody (HRP-conjugated)**	**Dilution**	**The estimated protein size**
p-AKT	Phospho-AKT (Ser473) (193H12) Rabbit monoclonal antibody (4058S)	1:1000	Donkey Anti-Rabbit IgG H&L	1:5000	60 kDa
α-Tubulin	α-Tubulin DM1A Mouse monoclonal antibody (Sc-32293)	1:1000	Donkey Anti-Mouse IgG H&L	1:5000	55 kDa

4 Results

TGF-β is an interesting growth factor due to its diverse roles and functions in cell regulation. Notably, previous studies have reported that TGF-β can act as both a tumor suppressor and promoter, depending on the cell culture condition and cell state. TGF-β regulates the spreading of cancer cells through collective cell migration, however, the molecular mechanisms that mediates TGF-β regulated cell migration is not elucidated. Additionally, recent studies suggest that TGF-β is able to activate the EGF/EGFR cell signaling pathway through receptor transactivation. Therefore, we opted to examine the role of TGF-β in epithelial collective cell migration using a previously established *in vitro* human skin experimental approach (Lång et al., 2018). The human keratinocytes were treated with different concentrations of TGF-β to study how TGF-β regulates collective cell migration in epithelial cell sheets. Furthermore, the cells were stimulated with TGF-β, EGF, and inhibitors of their receptors, SB431542 and Gefitinib, to study the potential crosstalk between the TGF-β and EGF/EGFR signaling pathways.

4.1 The role of TGF-β in collective cell migration

In order to examine how TGF-β regulates cell migration and cell coordination in a confluent quiescent cell sheet, the cell sheets were treated with different concentrations of TGF-β ± FBS to find the optimal concentration of TGF-β for stimulation of HaCaT cells. FBS is essential for cell growth and migration, and contains a range of important components, such as hormones and growth factors (Fang et al., 2017; Jochems et al., 2002), including EGF (Kwon et al., 2016) and TGF-β (Oida & Weiner, 2010). Additionally, FBS was recently shown to activate collective cell migration in confluent quiescent epithelial cell sheets (Lång et al., 2018). The serum-associated growth factor, EGF, is known to activate cell movements, but does not contribute to the collective motions seen in FBS stimulated cells. Therefore, FBS and EGF were used as controls when examining the migration pattern formed by TGF-β stimulation. Moreover, FBS stimulated cell sheets were treated with the TβR1 inhibitor, SB431542, to examine if inhibition of the TGF-β signaling pathway affected the collective cell migration response. The cell sheets were treated with TGF-β, EGF, FBS, and SB431542 according to the plate setup (table 3.1) visualized in section 3.2.4.

4.1.1 TGF-β stimulated activation of cell sheet migration

PIV-based cell motility analysis was used to generate the mean and standard deviation of cell migration velocities. This was used to examine the impact of different TGF-β concentrations ± FBS on confluent quiescent cell sheets. In order to examine the regulatory role of TGF-β in epithelial collective cell migration, TGF-β was applied on starved cells to examine if TGF-β alone is able to activate cell sheet migration. Further, TGF-β in combination with FBS examined if TGF-β inhibits or amplify the effect of serum-activated collective cell migration. The cell sheets were treated with 5 ng/mL, 10 ng/mL, 20 ng/mL, and 40 ng/mL TGF-β.

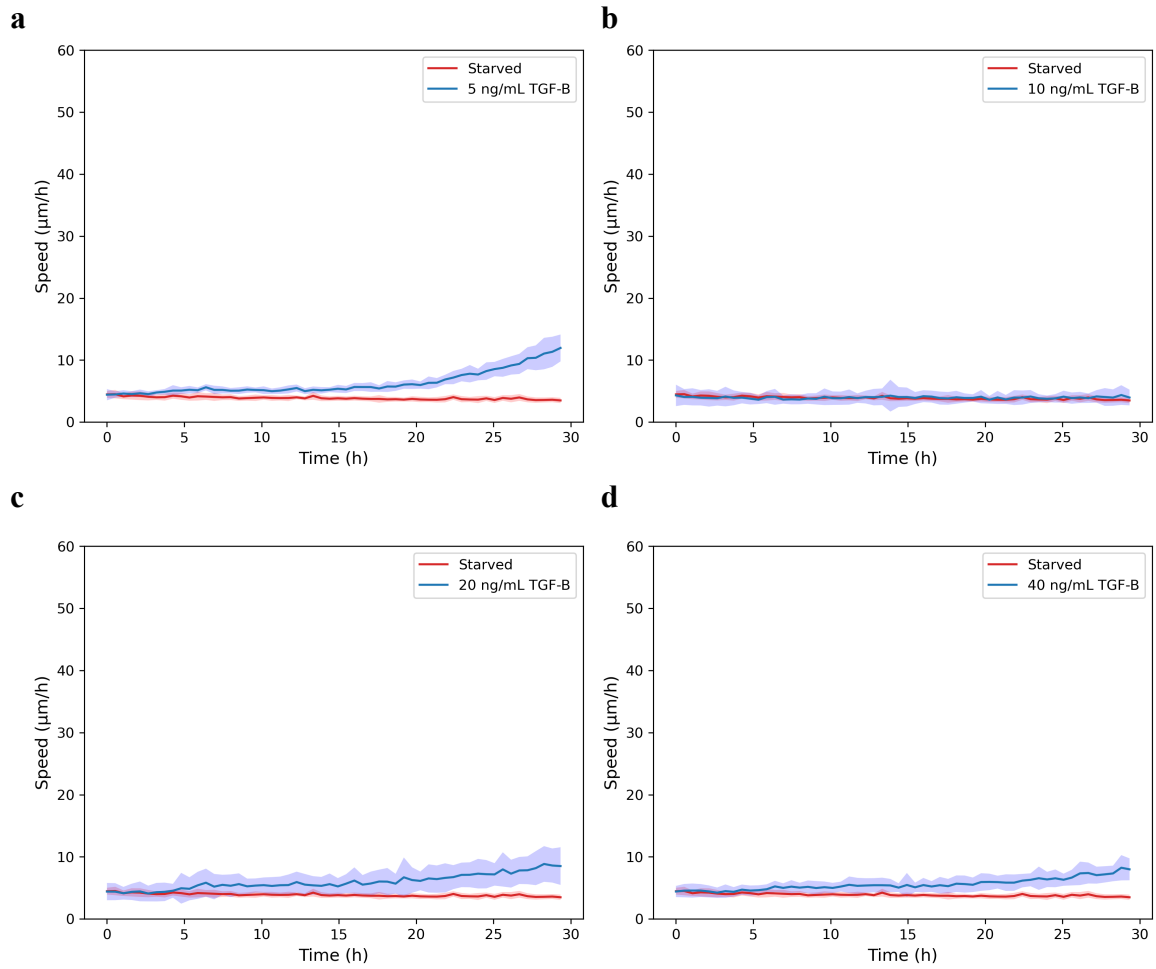

Figure 4.1. *TGF-β stimulated cell migration in quiescent cell sheets. The velocity of the cell sheet migration was extracted from the PIV data, and the TGF-β stimulated quiescent cell sheets were compared to the starved control. The darker blue and red lines represent the mean velocity, while the lighter colored area is the standard deviation. Quiescent cell sheets were stimulated with* ***a*** *5 ng/mL TGF-β,* ***b*** *10 ng/mL TGF-β,* ***c*** *20 ng/mL TGF-β, or* ***d*** *40 ng/mL TGF-β.*

Results presented in figure 4.1 indicate that TGF-β is able to activate cell sheet migration, however, the cell sheet migration was activated after a long stimulation time compared to FBS stimulated cell sheet (figure 4.3.a). None of the included concentrations of TGF-β showed the ability to activate motions during the first 15 hours of stimulation and looked like the starved controls. However, after approximately 15 hours of stimulation, the cell sheets began to migrate. The cell sheets stimulated with 5 ng/mL TGF-β (figure 4.1.a) showed the most rapid increase in speed and reached a maximal velocity of 10 μm/h after 30 hours of stimulation. In contrast, 10 ng/mL TGF-β (figure 4.1.b) did not activate cell sheet migration and looked like the starved control after 30 hours of stimulation. The cell sheets stimulated with 20 ng/mL TGF-β (figure 4.1.c) and 40 ng/mL TGF-β (figure 4.1.d) started to migrate after approximately 15 hours of stimulation, as observed with 5 ng/mL TGF-β. However, the higher concentrations of TGF-β did not generate as high maximal velocity as 5 ng/mL TGF-β. There were no significant differences between the cell sheets stimulated with 20 ng/mL TGF-β and 40 ng/mL TGF-β, and both concentrations produced a maximal cell sheet velocity of 8 μm/h after 30 hours of stimulation.

Stimulation with TGF-β in combination with FBS showed activation of cell sheet migration instantaneously. The FBS stimulated cell sheets with 5 ng/mL TGF-β (figure 4.2.a) showed generation of the highest maximum velocity, however, cell sheets treated with 10 ng/mL TGF-β (figure 4.2.b) and 20 ng/mL TGF-β (figure 4.2.c) showed a more rapid increase in cell sheet velocities at the early time points (10-15 hours post-stimulation). The FBS stimulated cell sheets with 40 ng/mL TGF-β (figure 4.2.d) showed the same initial acceleration as the cell sheets stimulated with 5 ng/mL TGF-β, but did not reach the same maximal velocity. These observations suggest that a lower concentration of TGF-β might be more efficient in stimulating confluent cell sheet migration. Therefore, a concentration of 5 ng/mL TGF-β was the preferred concentration to use in the next experiments to further examine the regulatory role of TGF-β in confluent cell sheet migration. Furthermore, the results might suggest that a higher concentration of TGF-β could reduce the initial cell sheet migration. Therefore, a concentration of 20 ng/mL TGF-β was also used to examine confluent cell sheet migration to study if a higher concentration of TGF-β actually produces an inhibitory effect.

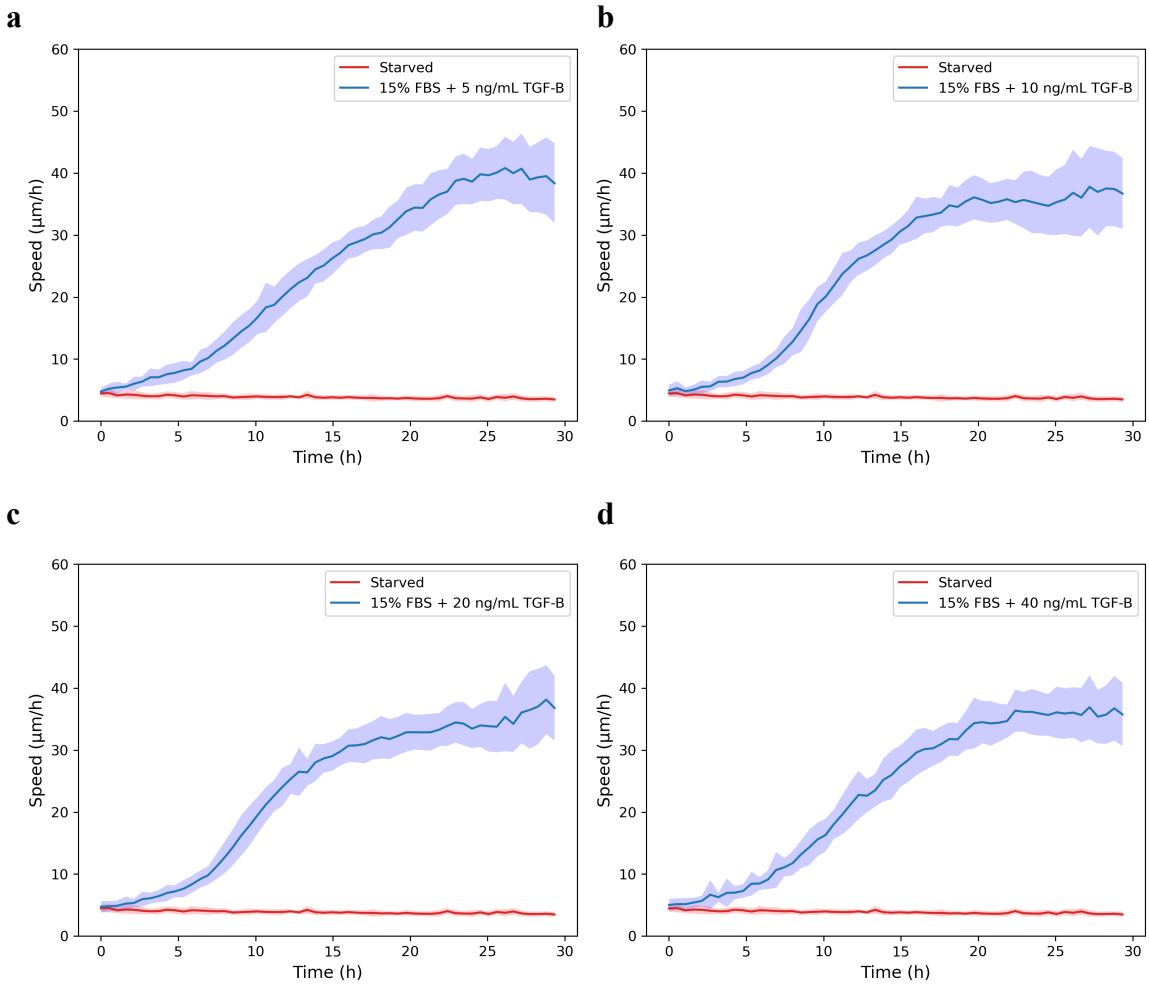

Figure 4.2. *Serum-stimulated collective cell migration with TGF-β in quiescent cell sheets. The velocity of the collective cell migration was extracted from the PIV data, and the serum-stimulated quiescent cell sheets were compared to the starved controls. The darker blue and red lines represent the mean velocity, while the lighter colored area is the standard deviation. Quiescent cell sheets were stimulated with* ***a*** *15% FBS + 5 ng/mL TGF-β,* ***b*** *15% FBS + 10 ng/mL TGF-β,* ***c*** *15% FBS + 20 ng/mL TGF-β, or* ***d*** *15% FBS + 40 ng/mL TGF-β.*

4.1.2 Stimulation and inhibition of the TGF-β receptor in serum-stimulated collective cell migration

An instantaneous activation of cell sheet migration was seen after stimulation with FBS (figure 4.3.a), FBS + TβR1 inhibitor; SB431542 (figure 4.3.b), FBS + TGF-β (figure 4.3.c), or EGF (figure 4.3.d). FBS stimulated cell sheets with SB431542 showed the same increase in speed during the first 10 hours after stimulation. However, FBS stimulated cell sheets (figure 4.3.a) reached a maximum velocity of 38 µm/h after 12 hours of stimulation, while in combination with the TβR1 inhibitor, SB431542 (figure 4.3.b), the cell sheets reached a maximum velocity

of 35 µm/hours. The cell sheet velocity also decreased faster in the presence of inhibitor compared to cell sheets stimulated with only FBS. In contrast, FBS stimulated cells in combination with TGF-β (figure 4.3.c) did not increase the velocity as fast as FBS ± SB431542 (5-12 hours post-stimulation). However, after approximately 15 hours of stimulation, TGF-β started to stimulate the cell sheet migration, which was also observed with TGF-β stimulation alone (figure 4.1). Notably, this is the time point where FBS ± SB431542 treated migrating cell sheets began to slow down.

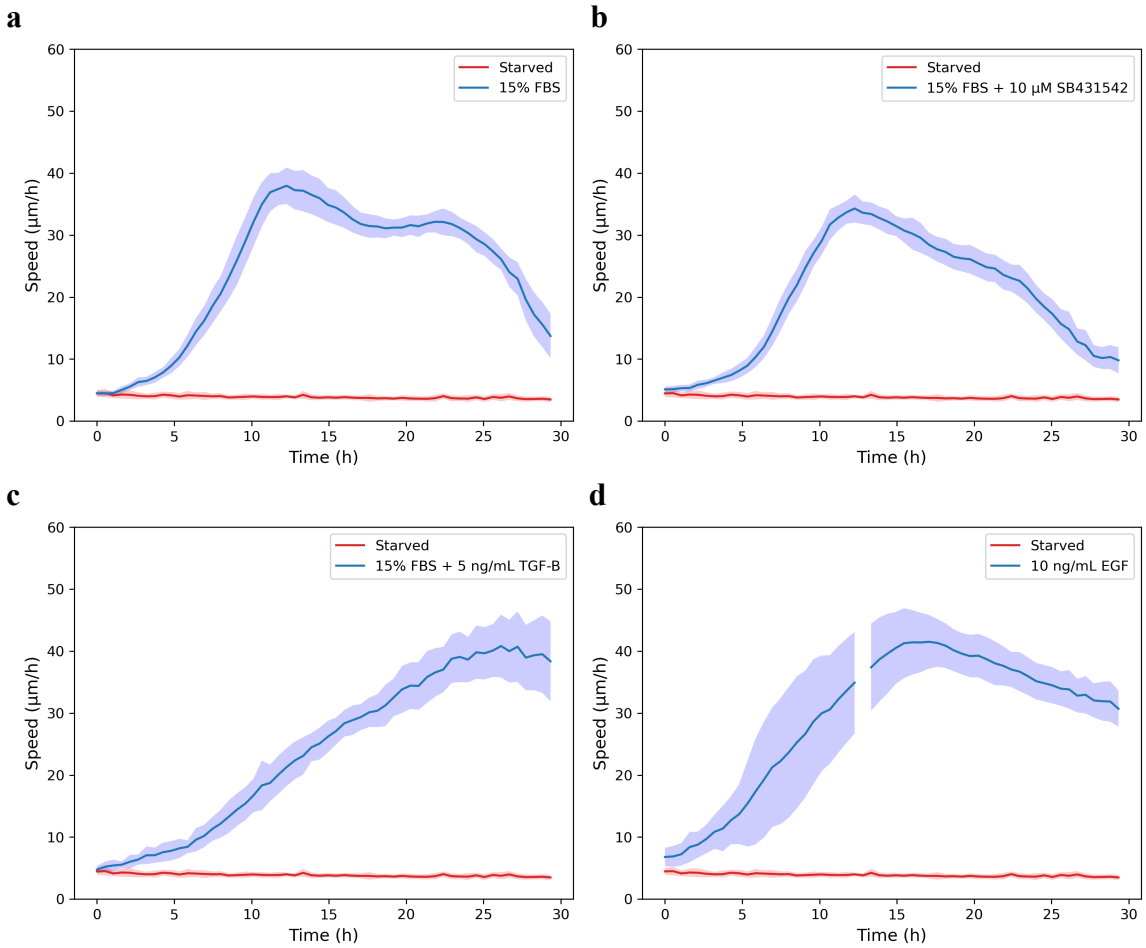

Figure 4.3. *Stimulated cell migration in quiescent cell sheets with FBS ± TGF-β or SB431542, or EGF. The velocity of the migrating cell sheet was extracted from the PIV data. Stimulated quiescent cell sheets were compared to starved controls. The darker blue and red lines represent the mean velocity, while the lighter colored area is the standard deviation. The missing data point are due to irregular movements in the XY-stage of the ImageXpress microscope. Quiescent cell sheets were stimulated with* ***a*** *15% FBS,* ***b*** *15% FBS + 10 µM SB431542,* ***c*** *15% FBS + 5 ng/mL TGF-β, or* ***d*** *10 ng/mL EGF.*

The FBS stimulated cell sheets in combination with TGF-β produced a slightly higher maximum speed of approximately 40 μm/h than the cells stimulated with FBS ± SB431542. The addition of extra TGF-β protein in FBS stimulated cells does not lead to a significant increase of the migration velocities produced. However, additional TGF-β does slow down the initial cell sheet acceleration while sustaining the migration velocities over time compared to FBS stimulation alone. Additionally, the cell sheets stimulated with EGF also showed a rapid increase in migration speed (figure 4.3.d) and reached higher maximum velocities than the cells stimulated with FBS. The cell sheets stimulated with EGF also decreased the migration speed after 15 hours of stimulation as seen in FBS stimulated cell sheets, however, the cell sheets did not decrease the migration speed as fast as observed with FBS. These observations might suggest that TGF-β could amplify the cell migration speed at a later time point compared to EGF and FBS, or that TGF-β might be important in order to sustain the ongoing cell migration response. However, inhibition of TβR1 in FBS stimulated cell sheets did not show a significant difference from FBS stimulated cell sheets and only led to a slight decrease in cell sheet migration.

4.1.3 TGF-β did not induce cell coordination

Further, we wanted to examine how the human TGF-β recombinant protein regulates coordination of cell sheet migration in comparison to FBS or EGF stimulation. Regulation of cell sheet coordination was examined with PIV analysis, as described in section 3.3.2, and the cell sheet migration patterns were visualized with the script stream_line.py.

The cell coordination plots generated from the script plot_oder.py illustrated that the cell sheets treated with 15% FBS (figure 4.4.a, left panel) displayed a high level of cell coordination over time with an order parameter, $\varphi = 0.9$. The cell migration motion of FBS stimulated cell sheets was well-coordinated in comparison to the starved controls, where there are no cell movements. This was also observed when visualizing the migration pattern using a streamline plot, which illustrated collective cell migration towards the center of the well and showed a high level of cell sheet coordination (figure 4.4.a, right panel). These observations are in agreement with a study by Lång and co-workers (2018), which reported that serum stimulation of quiescent cell sheets led to an activation of a highly coordinated collective cell migration response (Lång et al., 2018).

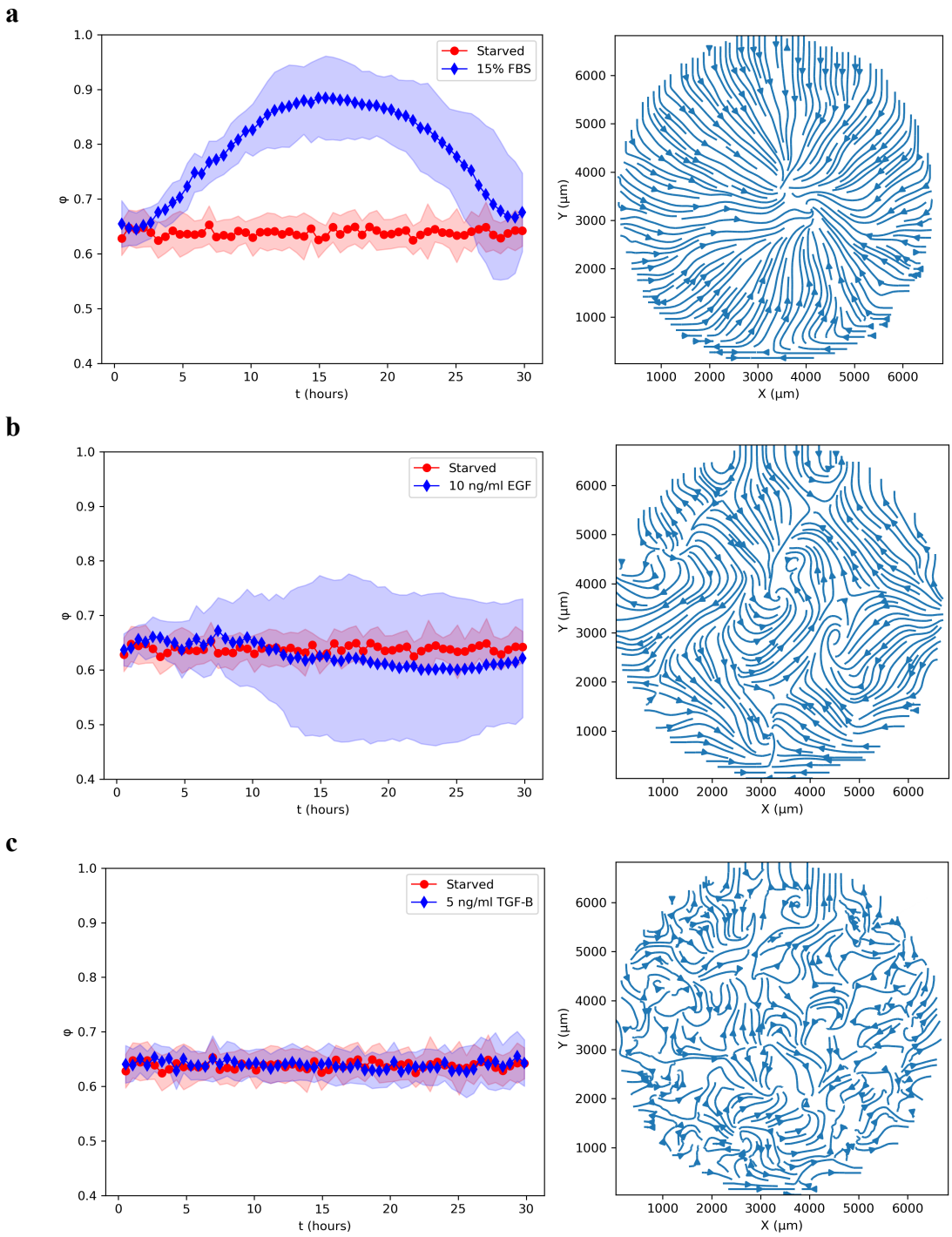

Figure 4.4. *Coordination (left) and visualization (right) of cell migration in stimulated quiescent cell sheets. The cell coordination was extracted from the PIV data, and the mean values are shown as dots and diamonds, while the lighter colored area is the standard deviation. Coordination of stimulated quiescent cell sheets were compared to starved controls. The migration pattern was derived from the time-lapse movies by the plot stream_line.py. The cell sheets were stimulated with* ***a*** *15% FBS,* ***b*** *10 ng/mL EGF, or* ***c*** *5 ng/mL TGF-β.*

In contrast, stimulation with EGF (figure 4.4.b, left panel) or TGF-β (figure 4.4.c, left panel) led to a lower level of coordination over time compared to FBS stimulated cell sheets. EGF and TGF-β stimulated cell sheets displayed a mean φ-value between 0.6 and 0.7 as the starved controls. However, the standard deviation of EGF stimulated cell sheets was significantly larger than with TGF-β stimulation. The EGF stimulated cell sheets produced a migration pattern consisting of local swirls (figure 4.4.b, right panel), which could explain why EGF stimulation showed a larger standard deviation of cell sheet coordination than TGF-β stimulation or the starved control.

Stimulation with EGF resulted in short time periods with collective cell migration in smaller regions of the cell sheets, where the cells move in the same direction with high cell coordination. However, other parts of the cell sheets were more disoriented, resulting in lower levels of cell sheet coordination. Thus, the cells showed a higher φ-value when they moved in the same direction, and a lower φ-value when they moved in different directions. These coordinated and disorientated movements cancel each other out, which explains why EGF stimulation displayed the same mean φ-value as the starved controls. The cells stimulated with TGF-β showed a disoriented migration pattern with no distinct cell sheet coordination (figure 4.4.c, right panel), which explains the low level of cell coordination compared to FBS stimulated cell sheets. The results acquired in these experiments indicate that stimulation with TGF-β can potentially activate some form of cell migration, but does not stimulate activation of a coordinated and collective cell migration response under these experimental conditions.

4.2 The crosstalk between the TGF-β and EGF/EGFR signaling pathways

A recent study reported that TGF-β could regulate the spreading of cancer cells through the transactivation of the EGF/EGFR cell signaling pathway (Zhao et al., 2018). To study the participation of TGF-β in the EGF/EGFR signaling pathway, a low and high TGF-β concentration was used to examine how TGF-β affects the EGF/EGFR signaling pathway. The cells were stimulated with both TGF-β and the EGFR inhibitor, Gefitinib, to examine if TGF-β could activate the EGFR signaling, and subsequently activate cell migration through the TGF-β receptor. Furthermore, the FBS stimulated cell sheets were stimulated with Gefitinib in order to show the importance of EGFR activation in cell sheet migration, as EGF alone is known to activate cell motions. The crosstalk between the TGF-β and EGF/EGFR signaling pathways was examined by stimulating the cell sheets with both TGF-β and EGF simultaneously. The

cell sheets stimulated with only EGF were used as controls to observe if TGF-β stimulates or inhibits the activation of cell migration in EGF stimulated cell sheets.

4.2.1 Activation of cell migration through EGFR

The EGFR inhibitor, Gefitinib, was used to block EGFR activation to study if TGF-β could activate the intracellular pathway of EGF/EGFR signaling through the TGF-β receptor. The cell sheets were stimulated with 5 μM Gefitinib in combination with 5 ng/mL TGF-β (figure 4.5.a) or 20 ng/mL TGF-β (figure 4.5.b) to examine if either concentration could activate cell sheet migration. Interestingly, no activation of migration was observed in cell sheets treated with Gefitinib in combination with TGF-β. These observations indicate that TGF-β did not transactivate the EGFR or activate cell migration through the intracellular EGF/EGFR signaling pathway in HaCaT cells under these experimental conditions.

The importance of the EGF/EGFR signaling pathway was examined by inhibiting the EGFR in FBS stimulated cell sheets. Figure 4.5.c showed that FBS activates collective cell migration as observed earlier, however, in combination with Gefitinib (figure 4.5.d), the cell sheet migration response was significantly inhibited. This result showed that activation of the EGF/EGFR signaling pathway is important in serum-induced activation of cell migration, as was previously shown by Lång and co-workers (2018). In contrast, the cell sheets stimulated with 15% FBS and 10 μM SB431542 (as shown earlier in figure 4.3.b) did not show a significant difference in cell sheet velocity, compared to FBS stimulated cell sheets. These results indicate that the EGF/EGFR signaling pathway plays a more important role in activation of cell sheet migration than the TGF-β signaling pathway.

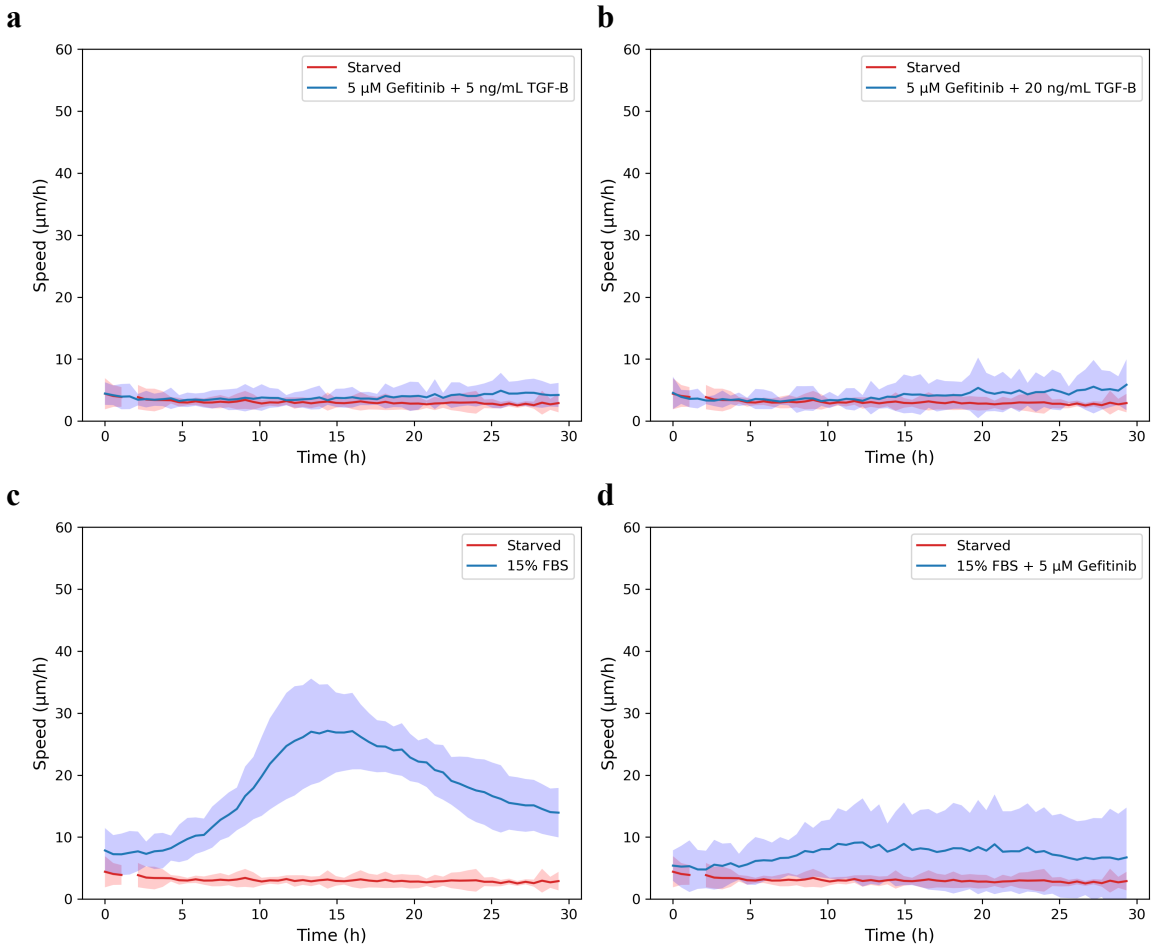

Figure 4.5. *Cell migration stimulated with FBS ± Gefitinib, or Gefitinib combined with TGF-β in quiescent cell sheets. The velocity of the cell migration was extracted from the PIV data, and the stimulated quiescent cell sheets were compared to the starved controls. The darker blue and red lines represent the mean velocity, while the lighter colored area is the standard deviation. The missing data point are due to irregular movements in the XY-stage of the ImageXpress microscope. Quiescent cell sheets were stimulated with* ***a*** *5 µM Gefitinib + 5 ng/mL TGF-β,* ***b*** *5 µM Gefitinib + 20 ng/mL TGF-β,* ***c*** *15% FBS, or* ***d*** *15% FBS + 5 µM Gefitinib.*

4.2.2 The effect of TGF-β and EGF on cell migration

Although TGF-β did not appear to stimulate transactivation of the EGF/EGFR signaling pathway in our experiments, we still wanted to examine if there were any form of collaboration between TGF-β and EGF signaling during activation of epithelial cell migration. Subsequently, the cells were stimulated with both TGF-β and EGF to examine the intracellular crosstalk between these signaling pathways. A low and high TGF-β concentration was combined with 10 ng/mL EGF to examine the inhibitory and/or stimulatory effects of TGF-β in the cell migration response activated by EGF.

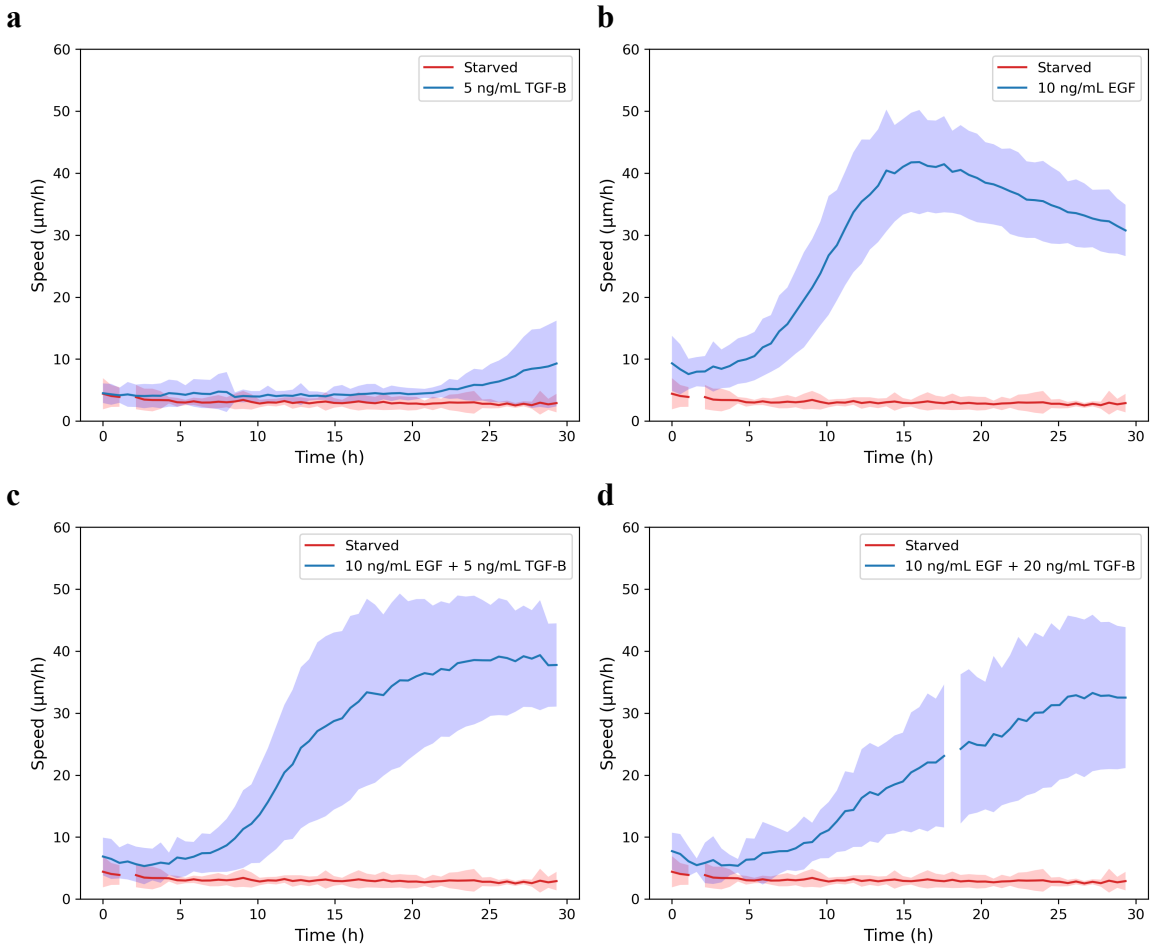

Figure 4.6. *Stimulated cell migration with EGF and/or TGF-β in quiescent cell sheets. The velocity of the cell migration was extracted from the PIV data, and the stimulated quiescent cell sheets were compared to the starved controls. The darker blue and red lines represent the mean velocity, while the lighter colored area is the standard deviation. The missing data point are due to irregular movements in the XY-stage of the ImageXpress microscope. Quiescent cell sheets were stimulated with* ***a*** *5 ng/mL TGF-β,* ***b*** *10 ng/mL EGF,* ***c*** *10 ng/mL EGF + 5 ng/mL TGF-β, or* ***d*** *10 ng/mL EGF + 20 ng/mL TGF-β.*

As observed in earlier experiments, stimulation with 5 ng/mL TGF-β (figure 4.6.a) activated cell sheet migration at much later time points, while stimulation with EGF (figure 4.6.b) led to an instantaneous activation of cell sheet migration. Moreover, stimulation with EGF in combination with 5 ng/mL TGF-β (figure 4.6.c) and 20 ng/mL TGF-β (figure 4.6.d) resulted in a lower acceleration of the migration speed generated, compared to EGF stimulated cell sheets. The EGF stimulated cell sheets combined with TGF-β did not increase the speed as fast as cell sheet stimulated with only EGF (5-15 hours post-stimulation), however, the migration velocities in these cell sheets were sustained over a longer time period (20-30 hours post-

stimulation) compared to EGF stimulated cell sheets. In addition, cell sheets stimulated with 5 ng/mL TGF-β (figure 4.6.c) produced higher migration velocities compared to the cell sheets stimulated with 20 ng/mL TGF-β (figure 4.6.d).

These observations showed the same trend as the cell sheets stimulated with FBS in combination with TGF-β, as shown in figure 4.2. Furthermore, these observations indicate that TGF-β does not activate cell migration at early time points (0-15 hours after stimulation). However, TGF-β signaling mediates activation of cell migration after a long time of stimulation (20-30 hours). Additionally, a higher concentration of TGF-β seemed to reduce the initial cell migration velocities compared to a lower concentration, but the mechanism behind this was not elucidated. To confirm these observations, EGF stimulated cell sheets were combined with different concentrations of TGF-β to further study the regulatory role of TGF-β in epithelial cell migration stimulated by EGF.

4.2.3 The effect of TGF-β in EGF stimulated cell sheet migration

Earlier observations showed that TGF-β is able to sustain cell migration velocities over a longer time period. However, at the earlier time points, higher concentrations of TGF-β seemed to produce a more inhibitory effect on cell migration velocities compared to lower concentrations. Therefore, we wanted to examine the effect of different concentrations of TGF-β in EGF stimulated cell sheets to investigate if higher TGF-β concentrations actually produced an inhibitory effect on the initial cell migration velocities. This experiment is similar to the experiment summarized in figure 4.2, investigating FBS stimulated cell sheets in combination with different concentrations of TGF-β. However, FBS was replaced with EGF to study the effect of different TGF-β concentrations on EGF stimulated cell migration.

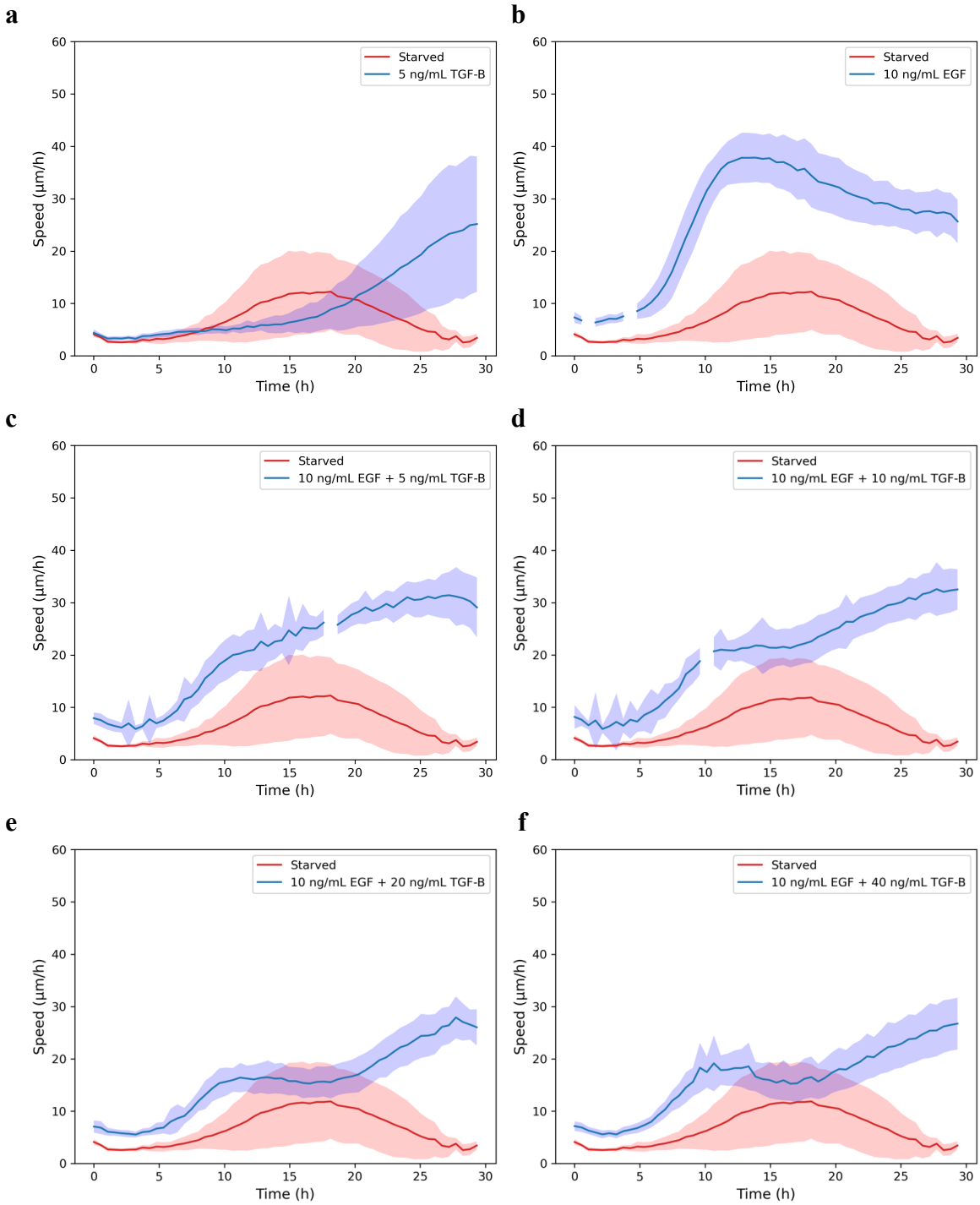

Figure 4.7. *Velocity of cell sheet migration stimulated with EGF and/or TGF-β in quiescent cell sheets. The velocity of the cell sheet migration was extracted from the PIV data, and the stimulated quiescent cell sheets were compared to the starved controls. The darker blue and red lines represent the mean velocity, while the lighter colored area is the standard deviation. The missing data point are due to irregular movements in the XY-stage of the ImageXpress microscope. Quiescent cell sheets were stimulated with* ***a*** *5 ng/mL TGF-β,* ***b*** *10 ng/mL EGF,* ***c*** *10 ng/mL EGF + 5 ng/mL TGF-β,* ***d*** *10 ng/mL EGF + 10 ng/mL TGF-β,* ***e*** *10 ng/mL EGF + 20 ng/mL TGF-β, or* ***f*** *10 ng/mL EGF + 40 ng/mL TGF-β.*

In this experiment, the starved controls started to migrate and reached a mean velocity up to 10 μm/h. Additionally, the cell sheets stimulated with TGF-β (figure 4.7.a) displayed a faster cell migration speed than earlier, with a mean velocity reaching up to 25 μm/h. An explanation could be that the results acquired from the TGF-β stimulated cell sheets were amplified, since the cell sheets were already moving before stimulation. This observation supports earlier claims about TGF-β signaling being dependent on the cell state in the cell culture (Roberts et al., 1985). In contrast, the cell migration response initiated by EGF (figure 4.7.b) did not seem to be affected by the activation of cell migration before stimulation. In the first 15 hours post-stimulation, the cell sheets stimulated with both growth factors showed lower acceleration compared to EGF stimulated cell sheets and higher acceleration compared to TGF-β stimulated cell sheets. However, after 15 hours of stimulation, the average velocities in these cell sheets did not decrease as observed in EGF stimulated cell sheets. EGF combined with TGF-β showed an ability to sustain the activated cell sheet migration at the same time point where TGF-β alone started to activate cell sheet migration.

The combination of EGF with 5 ng/mL TGF-β (figure 4.7.c) looked similar to the cell sheets stimulated with EGF combined with 10 ng/mL TGF-β (figure 4.7.d) during the first 10 hours of stimulation. However, cell sheets stimulated with 10 ng/mL TGF-β showed a reduction in cell sheet migration speed between 10 to 15 hours post-stimulation. The same trend was observed with cell sheets stimulated with EGF combined with 20 ng/mL TGF-β (figure 4.7.e) and 40 ng/mL TGF-β (figure 4.7.f), but these cell sheets showed a more significant decrease in migration velocities than cell sheets stimulated with the lower TGF-β concentrations. Notably, the migration velocities in these cell sheets started to increase again after about 17 hours of stimulation. Finally, all the TGF-β concentrations examined in EGF stimulated cell sheets reached a maximal migration velocity of 30 μm/h.

These observations showed that TGF-β could act as both an inhibitor and stimulator of cell migration in EGF stimulated cell sheets. These results also support the observations seen in FBS stimulated cell sheets in combination with TGF-β. The cell sheet migration seemed to be inhibited by TGF-β during the early time points after stimulation and subsequently activated at later time points. Furthermore, a lower concentration of TGF-β seemed to be more efficient to stimulate activation of cell sheet migration, while a higher concentration seemed to produce a more inhibitory effect. However, additional live cell experiments monitoring cell sheet migration over a longer time period are required in order to verify these observations.

4.3 TGF-β induced phosphorylation of AKT

Results acquired by live cell imaging showed that TGF-β could activate some form of cell migration response after a long stimulation time. In order to verify these observations, we opted to examine if TGF-β stimulated cells express p-AKT, since phosphorylation of AKT is known to promote cell migration (Ackah et al., 2005). Western blot analysis was performed to examine the protein expression of p-AKT in TGF-β stimulated cell sheets. Western blot analysis of cell lysate from EGF stimulated quiescent cell sheets was used as a control as AKT is known to be activated by phosphorylation downstream of EGFR activation (Garay et al., 2015; Nishimura et al., 2015). The control cell sheets were treated with 10 ng/mL EGF for 1 hour. Additionally, cell lysates were prepared from a starved cell sheet, and cell sheets treated with 5 ng/ml TGF-β for 1 hour, 10 hours, and 25 hours.

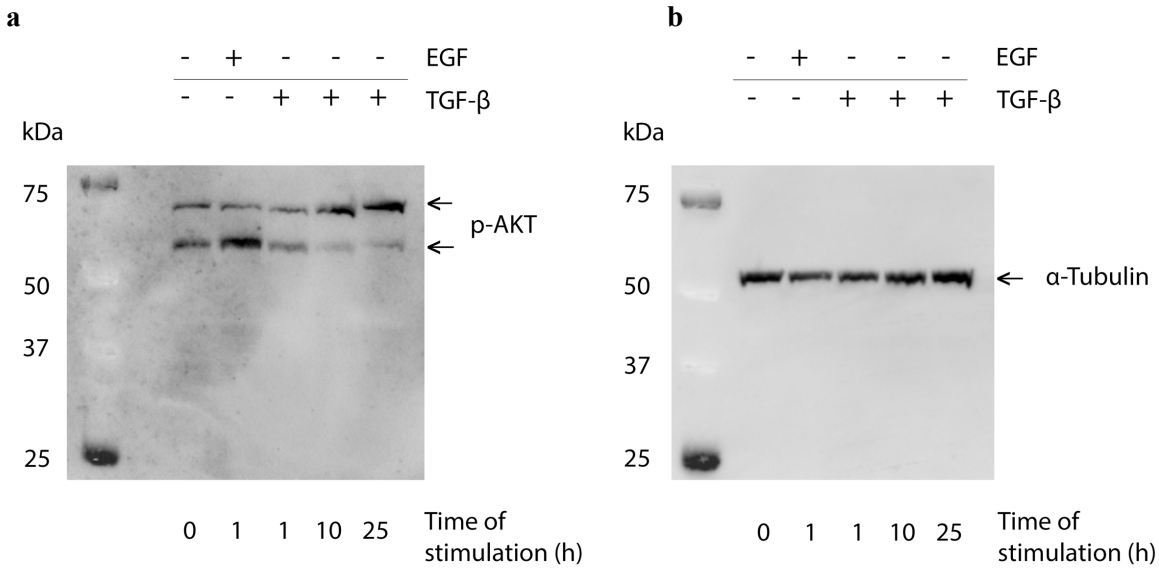

Figure 4.8. *Expression of p-AKT and α-Tubulin in HaCaT cells. Western blotting was performed with different stimulation time of 5 ng/mL TGF-β. Cells stimulated with 10 ng/mL EGF and starved cells were used as controls. The loading from left to right: Starved, 10 ng/mL EGF for 1 hour, 5 ng/mL TGF-β for 1 hour, 5 ng/mL TGF-β for 10 hours, and 5 ng/mL TGF-β for 25 hours.* ***a*** *Western blotting with phospho-AKT (Ser473) antibody showed two bands, an upper and a lower band. p-AKT has a molecular weight of 60 kDa, and the lower band was assumed to be p-AKT1.* ***b*** *Western blotting with α-Tubulin antibody was performed as a loading control. α-Tubulin has a molecular weight of 55 kDa.*

Western blotting with a p-AKT specific antibody detected two bands, an upper band with a molecular weight of ~70 kDa, and a lower band of ~60 kDa, as shown in figure 4.8.a. The phospho-AKT (Ser473) antibody is supposed to specifically detect AKT1 at serine 473. However, this antibody can also detect AKT2 and AKT3 when phosphorylated at the corresponding residues (Cell Signaling Technology, n.d.), suggesting that there are two isoforms of AKT present in the cell lysates. Additionally, a loading control with α-Tubulin (figure 4.8.b) was performed to ensure loading of the same amount of protein in each well. This is important to avoid a biased distribution in protein detection. All the bands in the western blot looked approximately the same, which demonstrated that all the samples were loaded in equal amounts.

The western blot with p-AKT showed a rapid increase in phosphorylation of AKT at serine 473 in the 60 kDa band of EGF stimulated cell sheets. In contrast, the TGF-β stimulated cell sheets showed the same amount of phosphorylation as the starved control or less. The intensity of phosphorylation in both bands seemed to be equal in the starved cell sheets, and the cell sheets stimulated with TGF-β for 1 hour. The intensity of phosphorylation in the 60 kDa band was stronger than the 70 kDa band after EGF stimulation, while the intensity of the 70 kDa band was stronger in cell sheets stimulated with TGF-β for 10 and 25 hours. The 70 kDa band detected in the TGF-β stimulated cell sheets became more pronounced with longer stimulation, which indicates an increase in phosphorylation of this AKT isoform with longer TGF-β stimulation. In contrast, the 60 kDa band became weaker, indicating a decrease in phosphorylation of this AKT isoform. Since EGF and TGF-β stimulation demonstrated different phosphorylation patterns of AKT, it is assumed that TGF-β signaling leads to activation of another isoform of AKT compared to EGF/EGFR signaling in order to initiate cell migration.

5 Discussion

This study aimed to examine the regulatory role of TGF-β in collective cell migration, and the interaction between the TGF-β and EGF/EGFR cell signaling pathways. Our results showed that TGF-β stimulation activated cell sheet migration in confluent quiescent cell sheets using an *in vitro* human skin experimental approach. However, TGF-β alone did not stimulate activation of cell sheet migration instantaneously, as observed in FBS and EGF stimulated cell sheet migration, but required a longer stimulation time to activate a cell migration response. In addition, the migrating cell sheets did not show activation of coordinated collective cell migration, indicating that TGF-β does not regulate coordinated and collective cell movements in epithelial cell sheets. Further, the cell sheets stimulated with either FBS or EGF in combination with TGF-β showed a reduction in cell migration during the first 15 hours compared to cell sheets stimulated with only FBS or EGF. However, the cell migration velocities became amplified 15 hours post-stimulation, indicating that TGF-β is able to stimulate cell sheet migration and amplify the migration speed after a long stimulation time. Together, these results showed that the TGF-β signaling pathway activates cell migration at a slower rate than the EGF/EGFR signaling pathway.

More insight into the mechanism of TGF-β activation and regulation of cell sheet migration is important as TGF-β is strongly associated with malignant cell spreading and wound healing. TGF-β might potentially be used as a stimulating drug to speed up the wound healing process and thus improve the recovery of epithelial tissue in chronic wounds. Importantly, a deeper understanding of the molecular mechanisms of TGF-β mediated activation of epithelial cell sheet migration, and its stimulatory and inhibitory effects may facilitate the development of improved wound healing agents or new medications used to treat cancers.

5.1 The experimental setup

Live cell imaging is a method used to study living cells, where the cells can be visualized and tracked during migration by using time-lapse movies. Live cell imaging can be combined with automated data processing to perform data analysis on large data sets. Subsequently, information on the migration velocities and cell coordination in collectively migrating cell sheets can be extracted. The experimental setup used in this study is a well-established method, that has been further optimized and quality assured by Bøe's research group. Consequently, this is a good method to use for cell migration studies to examine how different stimuli activate cell

motility in epithelial cell sheets. However, like every experimental method, there are also some weaknesses in our experimental setup. One of the disadvantages is that the outcome of the cell sheet migration responses observed depends on the cell state and cell culture condition.

The cells need to maintain optimal growth and cell density in the cell culture, enter a quiescent cell state and respond well to the cell stimulation in order to produce a successful result. However, the cell behavior cannot be determined in advance, which could make it difficult to analyze the cell sheet migration pattern. For example, if the cells are responding poorly to the treatment, the cells will require a longer time to activate cell sheet migration, and the cells will also migrate at a lower speed. Therefore, at least three independent experiments are required in order to compensate for these irregularities.

5.2 The role of TGF-β in cell migration

5.2.1 Inhibition of the TGF-β receptor does not affect cell migration

The importance of TGF-β signaling in collective cell migration was addressed by inhibition of TβR1 with SB431542 in FBS stimulated cells. FBS contains several growth factors and is known to stimulate the activation of collective cell migration (Lång et al., 2018). By blocking TβR1 activation in FBS stimulated cell sheets, we investigated the regulatory role of TGF-β in serum-activated collective cell migration. The cell sheets stimulated with FBS in combination with SB431542 did not show any difference in the cell migration response produced compared to cell sheets stimulated with only FBS (figure 4.3). However, inhibition of the TGF-β signaling pathway led to a slight reduction in cell sheet motility, but did not have a significant effect compared with inhibition of the EGF/EGFR signaling pathway in FBS stimulated cell sheets. Inhibition of EGFR signaling with the EGFR inhibitor, Gefitinib, showed a significant reduction in cell sheet migration (figure 4.5), which emphasizes the importance of EGF in the activation of cell sheet migration. Thus, our observations show that TGF-β signaling might not be directly involved in the activation of cell migration in confluent keratinocyte cell sheets. However, TGF-β could still play an important role in the regulation of cell sheet migration.

5.2.2 TGF-β activates and amplifies the cell migration

Several studies have shown that both TGF-β and EGF can induce EMT (Akhurst & Padgett, 2015; Schelch et al., 2021; Sundqvist et al., 2020), and that EGFR activation is essential to enhance TGF-β stimulated cell migration in breast cancer cells (Zhao et al., 2018). The same

observation was made in our experiments using keratinocyte cells, where stimulation with both growth factors led to enhanced cell sheet migration (figures 4.6 and 4.7). Cell sheet migration activated by FBS (figure 4.2) or EGF (figure 4.6. and figure 4.7) were amplified when combined with TGF-β, leading to a sustained migration speed rather than migration velocities that decreased over time. These results indicate that activation of the TGF-β signaling pathway might be important to sustain cell migration velocities over time. Furthermore, a lower TGF-β concentration was more efficient to enhance and sustain cell migration velocities, while higher concentrations showed a more inhibitory effect. Thus, regulation of cell motility by TGF-β signaling is affected by the TGF-β concentration used to stimulate cell sheet migration. These results suggest that the phenotypic outcome in response to TGF-β stimulation is concentration-dependent.

Further, TGF-β stimulated cell sheet migration was observed 15 hours post-stimulation (figure 4.1), showing that the cellular responses of TGF-β did not result in activation of cell sheet migration immediately, as observed with FBS or EGF stimulated cell sheets (figure 4.3). Additionally, the maximal migration velocities of TGF-β stimulated cell sheets were not as high as in cell sheets stimulated with FBS or EGF. An explanation could be that TGF-β stimulates the activation of cell motility at a lower rate than EGF-activated cell migration. Consequently, this could lead to a lower acceleration, which further leads to lower migration velocities. Thus, the cell sheets stimulated with TGF-β might not reached the potential maximal velocities after 30 hours of stimulation. In order to examine if TGF-β is able to stimulate higher maximal cell migration velocities over time, live cell imaging experiments with a longer image acquisition time is required.

Moreover, our results showed that TGF-β did not stimulate coordinated cell movements, but showed a disoriented cell migration (figure 4.4). The cell migration pattern acquired from the script stream_line.py showed the same, which further supports our results. As a control, FBS stimulated cell sheets were used to show how the cell sheets moved during serum-activated collective cell migration. The FBS stimulated cell sheets showed high cell sheet coordination and the migrating cells moved collectively towards the center of the well, which was not observed in TGF-β stimulated cell sheets. These observations indicate that TGF-β and activation of the TGF-β signaling pathway do not regulate coordinated and collective cell migration. Previously studies have reported that activation of TGF-β signaling led to a shift from collective cell migration to single cell motility in MTLn3E cells, 410.4 cells (Giampieri

et al., 2009), and mammary tumor epithelial cells (Matise et al., 2012). This is consistent with the observed results, showing that stimulation with TGF-β can activate cell migration, but do not generate coordinated collective cell migration. Therefore, we conclude that TGF-β might stimulate single cell migration in epithelial cell sheets and not collective cell migration due to the low cell coordination observed in figure 4.4.

5.2.3 The crosstalk between TGF-β and EGF

Several studies have reported that TGF-β is able to transactivate EGFR (Sundqvist et al., 2020; Zhao et al., 2018), and the crosstalk between the TGF-β and EGF/EGFR signaling pathways have been discussed in several studies. However, the interaction between TGF-β and EGFR signaling depends on the cell type, the experimental conditions, and the experimental approach used. Further, the crosstalk between TGF-β and EGFR has been reported to synergistically promote EMT (Richter et al., 2011; Schelch et al., 2021; Zhao et al., 2018), which might lead to enhanced cell migration. This is consistent with our results (figures 4.6 and 4.7), where EGF stimulation in combination with TGF-β showed an inhibitory effect in the early stages of cell sheet migration, and subsequent stimulation of cell sheet migration in the later stages. However, it is important to mention that the migration phenotype observed in the confluent cell sheet is not consistent with a mesenchymal cell state. These cell cultures do not go through a complete EMT, but stay as epithelial cells throughout the experiments.

Stimulation with both growth factors showed reduced migration velocities at the earlier time points compared to only EGF stimulation. A possible explanation could be that TGF-β acts as a competitive ligand and would compete with EGF to bind to EGFR. The binding of TGF-β to EGFR leads to inhibition of the EGF/EGFR signaling pathway, which further affects the stimulation of cell motilities. A reduced EGFR activation would lead to reduced cell migration velocities, as observed in figures 4.6 and 4.7. However, the binding of TGF-β to EGFR is a reversible interaction, subsequently, TGF-β would be outcompeted by EGF and the EGF/EGFR signaling would be activated. Therefore, a combination of TGF-β and EGF would lead to an inhibitory effect on cell migration at the earlier time points. Further, EGF would use a longer time to outcompete TGF-β when stimulated with a higher concentration compared to a lower concentration of TGF-β. In agreement with this, a higher concentration of TGF-β showed a higher inhibitory effect of the cell migration velocities observed. One possibility is that stimulation with TGF-β leads to blockage of EGFR, leading to an inhibitory effect and reduced cell motility.

TGF-β was also shown to stimulate cell motility in EGF stimulated cell sheets, leading to sustained and amplified migration velocities over time. A possibility can be found in the signaling pathways activated by TGF-β and EGF, respectively. Activation of the EGF/EGFR signaling pathway leads to direct phosphorylation of AKT, and initial activation of cell motility. The TGF-β signaling pathway includes more intracellular proteins that must be activated in order to stimulate the activation of cell sheet migration through AKT phosphorylation. Thus, although both growth factors stimulated cell sheet migration, they activated cell motilities at different time points due to differences in the intracellular signaling pathways (Schelch et al., 2021). EGF stimulates activation of cell motility at the earlier time points, whereas stimulation with TGF-β activates cell motility at the later time points. Together, these growth factors give rise to sustained and enhanced migration velocities over time compared to EGF stimulation alone. This may also explain the delayed activation of cell migration and the sustained migration phenotype observed at later time points.

Furthermore, the cell sheets were stimulated with both Gefitinib and TGF-β. Inhibition of EGFR by Gefitinib was used to suppress cell motility, while stimulation with TGF-β was performed in order to investigate if TGF-β stimulates transactivation of cell migration through the EGF/EGFR signaling pathway. However, treatment with Gefitinib in combination with TGF-β did not result in activation of cell sheet migration (figure 4.5). Thus, our observations indicate that TGF-β is not able to transactivate the EGF/EGFR signaling pathway to stimulate the activation of cell sheet migration in HaCaT cells under these experimental conditions. However, since our results showed that TGF-β had an impact on EGF stimulated cell sheet migration, we assumed that both signaling pathways need to be activated for TGF-β and EGF to work together synergistically. The activated cell signaling pathways are closely connected and are combined to produce a different migration response than observed with the two growth factors alone. We hypothesize that EGF activates cell motility first through the PI3K-AKT signaling pathway, and that the TGF-β signaling regulates the cell motility by phosphorylating more AKT, leading to a sustained and enhanced migration phenotype. Thus, both growth factors are interacting through PI3K-AKT signaling to stimulate activation of cell migration in epithelial cell sheets.

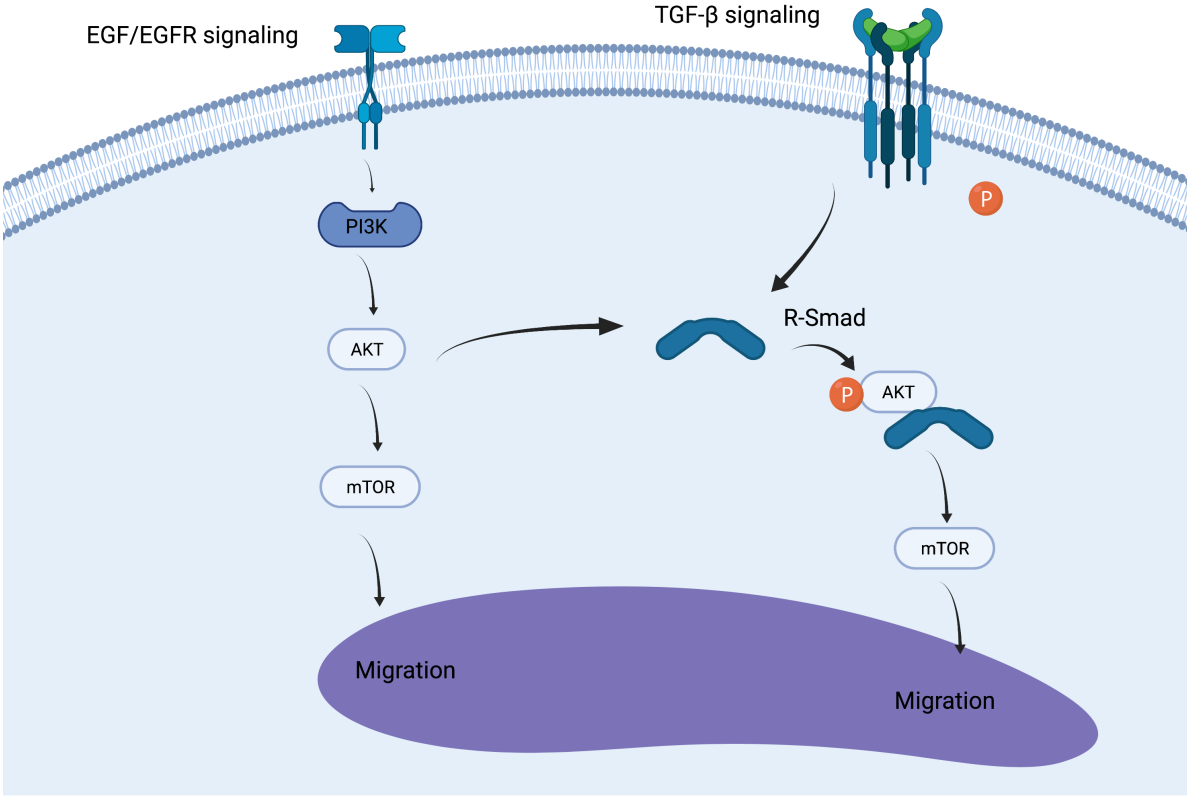

Figure 5.1. *A simplified illustration of the crosstalk between the TGF-β and EGF/EGFR signaling pathways. Activation of EGF/EGFR signaling leads to activation of PI3K and phosphorylation of AKT, which further activates mTOR and regulation of cell motility. In combination with TGF-β signaling, AKT interacts directly with unphosphorylated R-Smad, and inhibits R-Smad mediated transcription, leading to phosphorylation of AKT and activation of mTOR and cell motility. Created with BioRender.com.*

Figure 5.1 is a simplified illustration of our hypothesis, where activation of EGF/EGFR signaling leads to activation of cell motility through PI3K, AKT, and mTOR. TGF-β signaling, however, involves additional intracellular proteins, including Smads. Thus, TGF-β mediated cell motility includes several intracellular steps in the signaling pathway compared to EGF mediated cell motility. This could explain the delay in activation of cell sheet migration stimulated by TGF-β. Furthermore, we assumed that EGF is essential for the activation of AKT, which is necessary to stimulate cell migration. Activation of EGFR leads to upregulation and phosphorylation of AKT, which results in activation of cell migration as observed in our results. Further, unphosphorylated AKT can bind to Smad3, leading to phosphorylation of AKT and activation of cell motility through the TGF-β signaling pathway. Thus, a combination of TGF-β and EGF signaling would lead to an accumulation of p-AKT, and an amplified migration

velocity compared to activation of EGFR signaling alone. To further examine how different downstream regulators affect the cell migration response, we should design and perform additional experiments in which we inhibit or knock out specific intracellular proteins in the TGF-β and EGF/EGFR signaling pathways.

5.2.4 TGF-β mediates cell motility through another AKT isoform compared to EGF

In order to further investigate and verify TGF-β stimulated cell motility, we performed western blot analysis using a specific phospho-AKT (Ser473) antibody, as AKT is known to activate cell migration (Ackah et al., 2005). The western blot (figure 4.8) showed phosphorylation of AKT in TGF-β stimulated cell sheets, indicating that TGF-β mediates cell motility through AKT as in EGF mediated cell migration. However, TGF-β stimulation resulted in phosphorylation of AKT that displayed a large molecule weight compared to EGF stimulation, which is known to phosphorylate the AKT1 isoform (Li et al., 2015). Therefore, we assumed that TGF-β stimulates phosphorylation of another isoform of AKT, such as AKT2 or AKT3.

A previous study by Nakatani et al. (1999) implied that Ser473 is conserved in the human isoform AKT3 sequence, which indicates that the phospho-AKT (Ser473) antibody could recognize and bind to the AKT3 isoform (Okano et al., 2000). This might suggest that the phosphorylated AKT isoform detected in TGF-β stimulated cell sheets in our western blot analysis could be the AKT3 isoform. The lower band (~60 kDa) was assumed to be AKT1 based on the increased intensity of this band in the EGF stimulated cell sheet, and the fact that AKT1 is known to be phosphorylated through the EGFR pathway. Therefore, the upper band (~70 kDa) was assumed to be AKT3, and the western blot analysis showed an increase in the phosphorylation of AKT3 in cell sheets stimulated with TGF-β. This result indicates that TGF-β stimulation mainly phosphorylates AKT3 and not AKT1.

A study by Okano et al. (2000) reported that EGF induces phosphorylation of both AKT1 and AKT3 in some cell types, which could explain why EGF stimulated cell sheets displayed two bands in our western blot analysis. Further, the study reported that both AKT1 and AKT3 could be inhibited by a PI3K-inhibitor, indicating that activation of both isoforms is mediated through the PI3K pathway. This might suggest that TGF-β mediates activation of cell motility through the PI3K-AKT3 signaling pathway, since cell sheet stimulated with TGF-β led to an increase in phosphorylation of AKT3. Furthermore, longer stimulation of TGF-β led to an increase in AKT3 phosphorylation, and a subsequent decrease in the amount of phosphorylated AKT1.

The amount of p-AKT increased gradually with the stimulation time, which corresponds to our observations showing that TGF-β stimulates activation of cell migration after a long stimulation time. In contrast, stimulation with EGF showed a rapid increase in p-AKT after 1 hour, which corresponds to the rapid activation of cell migration in EGF stimulated cell sheets. In order to further explore this, we could perform a western blot analysis including an antibody that specifically targets AKT3 to confirm our assumptions.

In summary, the data analysis from the live cell imaging experiments and the western blot analysis indicates that TGF-β might stimulate the activation of cell migration through AKT phosphorylation, similar to EGF. However, TGF-β mediated cell migration does not phosphorylate AKT directly but includes several secondary signaling proteins, including Smads as described in section 1.3.4 in the introduction. Since TGF-β signaling includes several intracellular signaling proteins, activation of this signaling cascade might potentially require a longer time to activate cell migration compared to the EGF/EGFR signaling pathway. Further, we assume that TGF-β stimulated cell motility is mediated through another isoform of AKT compared to the EGFR signaling pathway, which also might affect the cell sheet response time to stimuli. However, the molecular mechanism behind this is not elucidated.

6 Conclusion

The purpose of this study was to examine TGF-β and its regulatory role in collective cell migration, as well as the crosstalk between the TGF-β and EGF/EGFR cell signaling pathways. Stimulation with TGF-β led to activation of cell motility, but the cell sheet did not produce a collective cell migration response. Inhibition of the TGF-β signaling pathway in serum-activated collective cell migration did not affect the cell motility response produced. In comparison, stimulation with TGF-β in FBS stimulated cell sheets led to a sustained and enhanced cell migration response. Thus, we conclude that TGF-β does not regulate cell sheet coordination or activate collective cell migration, but might be important to sustain the migration velocities produced in confluent epithelial cell sheets. This ability may be potentially useful during wound healing and in the development of improved wound healing agents.

Additionally, TGF-β showed inhibitory effects in FBS and EGF stimulated cell sheet migration at the earlier time points after stimulation. A possible explanation could be that TGF-β can interact with EGFR, without activation of the EGF/EGFR signaling pathway. We assumed that this interaction blocks EGFR, giving an inhibitory effect, however, the interactions are assumed to be reversible. Thus, EGF would outcompete TGF-β and stimulate the activation of cell sheet migration over time. Furthermore, TGF-β also showed activation of cell sheet migration and contributes to amplified cell migration velocities. TGF-β amplifies and sustains cell sheet migration activated by FBS and EGF at the later time points. Therefore, we conclude that TGF-β also has a stimulatory effect on epithelial cell migration. However, we assume that TGF-β might activate single cell migration due to a lack of cell coordination, as was previously reported by Matise et al. (2012).

Lastly, it is believed that stimulation of both TGF-β and EGF leads to amplified cell sheet migration due to enhanced activation of p-AKT. Both growth factors were shown to phosphorylate AKT, which in turn leads to activation of cell motility. Therefore, we conclude that there might be crosstalk between the TGF-β and EGFR signaling pathways through the PI3K-AKT signaling pathway, as TGF-β was shown to affect the cell sheet migration response observed after EGF stimulation.

7 Future perspectives

To further investigate and acquire a deeper understanding of the regulatory role of TGF-β in epithelial cell migration, we should perform live cell imaging experiments monitoring cell sheets over a longer period of time, for instance, 50-60 hours. A longer image acquisition could give us more information about how TGF-β stimulates the activation of cell sheet migration. By examining TGF-β mediated cellular responses over a longer time period, we could potentially observe further changes in the migration velocities, and thereby acquire more comprehensive details on how TGF-β regulates cellular movements. Additionally, the migration pattern of the cells could be investigated further in order to examine if TGF-β activates single cell migration after a longer period of stimulation. However, this was not performed due to lack of time.

In order to get a deeper understanding of the crosstalk between TGF-β and EGF, we should inhibit or knock out different signaling proteins in the TGF-β and EGF/EGFR signaling pathways. Inhibition of different signaling proteins is important to examine how different downstream regulators affect cell migration. For instance, a gene knockout of R-Smads could verify if TGF-β stimulated cell motility is mediated through Smads. Further, we could perform gene knock out of AKT in order to examine if TGF-β stimulates activation of cell migration through the PI3K-AKT pathway as EGF stimulated cell migration does. This could also verify our assumptions about TGF-β and EGF signaling being connected through the PI3K-AKT signaling pathway, or if TGF-β and EGF stimulate cell migration through separate signaling pathways. Moreover, a western blot analysis that specifically targets AKT2 and AKT3 isoform could be performed to examine which AKT isoform is activated and phosphorylated in the TGF-β signaling pathway.

Elucidation of the molecular mechanisms mediating TGF-β stimulated cell migration could be important for improved wound care of chronic wound patients. Further, it is important to gain a better understanding of how TGF-β regulates cell migration in relation to cancer cell spreading of malignant cells in order to develop new approaches to prevent tumor metastasis. However, a more detailed understanding of the cellular and molecular mechanism of TGF-β cell signaling is required.

References

Ackah, E., Yu, J., Zoellner, S., Iwakiri, Y., Skurk, C., Shibata, R., Ouchi, N., Easton, R. M., Galasso, G., Birnbaum, M. J., et al. (2005). Akt1/protein kinase Balpha is critical for ischemic and VEGF-mediated angiogenesis. *J Clin Invest*, 115 (8): 2119-27. doi: 10.1172/jci24726.

Akhurst, R. J. & Padgett, R. W. (2015). Matters of context guide future research in TGFβ superfamily signaling. *Science Signaling*, 8 (399): re10. doi: 10.1126/scisignal.aad0416.

Allavena, P., Sica, A., Garlanda, C. & Mantovani, A. (2008). The Yin-Yang of tumor-associated macrophages in neoplastic progression and immune surveillance. *Immunological reviews*, 222 (1): 155-161.

Assoian, R. K., Komoriya, A., Meyers, C. A., Miller, D. M. & Sporn, M. B. (1983). Transforming growth factor-beta in human platelets. Identification of a major storage site, purification, and characterization. *J Biol Chem*, 258 (11): 7155-60.

Bakin, A. V., Tomlinson, A. K., Bhowmick, N. A., Moses, H. L. & Arteaga, C. L. (2000). Phosphatidylinositol 3-Kinase Function Is Required for Transforming Growth Factor β-mediated Epithelial to Mesenchymal Transition and Cell Migration*. *Journal of Biological Chemistry*, 275 (47): 36803-36810. doi: https://doi.org/10.1074/jbc.M005912200.

Balkwill, F., Charles, K. A. & Mantovani, A. (2005). Smoldering and polarized inflammation in the initiation and promotion of malignant disease. *Cancer Cell*, 7 (3): 211-7. doi: 10.1016/j.ccr.2005.02.013.

Bass, J. J., Wilkinson, D. J., Rankin, D., Phillips, B. E., Szewczyk, N. J., Smith, K. & Atherton, P. J. (2017). An overview of technical considerations for Western blotting applications to physiological research. *Scandinavian journal of medicine & science in sports*, 27 (1): 4-25. doi: 10.1111/sms.12702.

Bodnar, R. J. (2013). Epidermal Growth Factor and Epidermal Growth Factor Receptor: The Yin and Yang in the Treatment of Cutaneous Wounds and Cancer. *Adv Wound Care (New Rochelle)*, 2 (1): 24-29. doi: 10.1089/wound.2011.0326.

Boukamp, P., Petrussevska, R. T., Breitkreutz, D., Hornung, J., Markham, A. & Fusenig, N. E. (1988). Normal keratinization in a spontaneously immortalized aneuploid human keratinocyte cell line. *The Journal of cell biology*, 106 (3): 761-771. doi: 10.1083/jcb.106.3.761.

Carpenter, G. (1987). Receptors for epidermal growth factor and other polypeptide mitogens. *Annual review of biochemistry*, 56 (1): 881-914.

Cell Signaling Technology. (n.d.). *Phospho-Akt (Ser473) Antibody #9271*. Cell Signaling Technology. Available at: https://www.cellsignal.com/products/primary-antibodies/phospho-akt-ser473-antibody/9271 (accessed: 27/04/2021).

Chen, R.-H., Su, Y.-H., Chuang, R. L. C. & Chang, T.-Y. (1998). Suppression of transforming growth factor-β-induced apoptosis through a phosphatidylinositol 3-kinase/Akt-dependent pathway. *Oncogene*, 17 (15): 1959-1968. doi: 10.1038/sj.onc.1202111.

Chen, W. S., Lazar, C. S., Poenie, M., Tsien, R. Y., Gill, G. N. & Rosenfeld, M. G. (1987). Requirement for intrinsic protein tyrosine kinase in the immediate and late actions of the EGF receptor. *Nature*, 328 (6133): 820-823. doi: 10.1038/328820a0.

Cohen, D. J., James Nelson, W. & Maharbiz, M. M. (2014). Galvanotactic control of collective cell migration in epithelial monolayers. *Nature Materials*, 13 (4): 409-417. doi: 10.1038/nmat3891.

Colak, S. & Ten Dijke, P. (2017). Targeting TGF-β Signaling in Cancer. *Trends Cancer*, 3 (1): 56-71. doi: 10.1016/j.trecan.2016.11.008.

Daopin, S., Piez, K. A., Ogawa, Y. & Davies, D. R. (1992). Crystal structure of transforming growth factor-beta 2: an unusual fold for the superfamily. *Science*, 257 (5068): 369-73. doi: 10.1126/science.1631557.

Dawson, J. P., Berger, M. B., Lin, C. C., Schlessinger, J., Lemmon, M. A. & Ferguson, K. M. (2005). Epidermal growth factor receptor dimerization and activation require ligand-induced conformational changes in the dimer interface. *Mol Cell Biol*, 25 (17): 7734-42. doi: 10.1128/mcb.25.17.7734-7742.2005.

Day, S. W., McDaniel, J. C., Wood, H. G., Allaire, P. E., Landrot, N. & Curtas, A. (2001). Particle image velocimetry measurements of blood velocity in a continuous flow ventricular assist device. *Asaio j*, 47 (4): 406-11. doi: 10.1097/00002480-200107000-00021.

de Visser, K. E., Eichten, A. & Coussens, L. M. (2006). Paradoxical roles of the immune system during cancer development. *Nature Reviews Cancer*, 6 (1): 24-37. doi: 10.1038/nrc1782.

Derynck, R., Akhurst, R. J. & Balmain, A. (2001). TGF-beta signaling in tumor suppression and cancer progression. *Nat Genet*, 29 (2): 117-29. doi: 10.1038/ng1001-117.

Derynck, R. & Zhang, Y. E. (2003). Smad-dependent and Smad-independent pathways in TGF-beta family signalling. *Nature*, 425 (6958): 577-84. doi: 10.1038/nature02006.

Desai, R. A., Gopal, S. B., Chen, S. & Chen, C. S. (2013). Contact inhibition of locomotion probabilities drive solitary versus collective cell migration. *Journal of The Royal Society Interface*, 10 (88): 20130717. doi: doi:10.1098/rsif.2013.0717.

Dunfield, L. D. & Nachtigal, M. W. (2003). Inhibition of the antiproliferative effect of TGFbeta by EGF in primary human ovarian cancer cells. *Oncogene*, 22 (30): 4745-51. doi: 10.1038/sj.onc.1206617.

Dunham, L. J. (1972). Cancer in Man at Site of Prior Benign Lesion of Skin or Mucous Membrane: A Review. *Cancer Research*, 32 (7): 1359.

Dvorak, H. F. (1986). Tumors: wounds that do not heal. Similarities between tumor stroma generation and wound healing. *N Engl J Med*, 315 (26): 1650-9. doi: 10.1056/nejm198612253152606.

Ehata, S., Johansson, E., Katayama, R., Koike, S., Watanabe, A., Hoshino, Y., Katsuno, Y., Komuro, A., Koinuma, D., Kano, M. R., et al. (2011). Transforming growth factor-β decreases the cancer-initiating cell population within diffuse-type gastric carcinoma cells. *Oncogene*, 30 (14): 1693-705. doi: 10.1038/onc.2010.546.

Ernst, O. & Zor, T. (2010). Linearization of the bradford protein assay. *Journal of visualized experiments : JoVE* (38): 1918. doi: 10.3791/1918.

Fang, C.-Y., Wu, C.-C., Fang, C.-L., Chen, W.-Y. & Chen, C.-L. (2017). Long-term growth comparison studies of FBS and FBS alternatives in six head and neck cell lines. *PLOS ONE*, 12 (6): e0178960. doi: 10.1371/journal.pone.0178960.

Farhat, Y. (2012). *Reconstituting and Aliquoting TGF-β1*. The Protocol Place. Available at: http://protocol-place.com/basic-lab-techniques/reagent-preparation/reconstituting-and-aliquoting-tgf-1/ (accessed: 18/01/2021).

Feng, X. H., Lin, X. & Derynck, R. (2000). Smad2, Smad3 and Smad4 cooperate with Sp1 to induce p15(Ink4B) transcription in response to TGF-beta. *The EMBO journal*, 19 (19): 5178-5193. doi: 10.1093/emboj/19.19.5178.

Feng, X. H. & Derynck, R. (2005). Specificity and versatility in tgf-beta signaling through Smads. *Annu Rev Cell Dev Biol*, 21: 659-93. doi: 10.1146/annurev.cellbio.21.022404.142018.

Friedl, P. (2004). Prespecification and plasticity: shifting mechanisms of cell migration. *Current Opinion in Cell Biology*, 16 (1): 14-23. doi: https://doi.org/10.1016/j.ceb.2003.11.001.

Friedl, P. & Gilmour, D. (2009). Collective cell migration in morphogenesis, regeneration and cancer. *Nature Reviews Molecular Cell Biology*, 10 (7): 445-457. doi: 10.1038/nrm2720.

Frigault, M. M., Lacoste, J., Swift, J. L. & Brown, C. M. (2009). Live-cell microscopy – tips and tools. *Journal of Cell Science*, 122 (6): 753-767. doi: 10.1242/jcs.033837.

Garay, C., Judge, G., Lucarelli, S., Bautista, S., Pandey, R., Singh, T. & Antonescu, C. N. (2015). Epidermal growth factor-stimulated Akt phosphorylation requires clathrin or ErbB2 but not receptor endocytosis. *Molecular biology of the cell*, 26 (19): 3504-3519. doi: 10.1091/mbc.E14-09-1412.

Giampieri, S., Manning, C., Hooper, S., Jones, L., Hill, C. S. & Sahai, E. (2009). Localized and reversible TGFbeta signalling switches breast cancer cells from cohesive to single cell motility. *Nature cell biology*, 11 (11): 1287-1296. doi: 10.1038/ncb1973.

Goumans, M.-J., Valdimarsdottir, G., Itoh, S., Rosendahl, A., Sideras, P. & ten Dijke, P. (2002). Balancing the activation state of the endothelium via two distinct TGF-beta type I receptors. *The EMBO journal*, 21 (7): 1743-1753. doi: 10.1093/emboj/21.7.1743.

Gu, S. & Feng, X. H. (2018). TGF-beta signaling in cancer. *Acta Biochim Biophys Sin (Shanghai)*, 50 (10): 941-949. doi: 10.1093/abbs/gmy092.

Guo, S. & Dipietro, L. A. (2010). Factors affecting wound healing. *J Dent Res*, 89 (3): 219-29. doi: 10.1177/0022034509359125.

Gurtner, G. C., Werner, S., Barrandon, Y. & Longaker, M. T. (2008). Wound repair and regeneration. *Nature*, 453 (7193): 314-21. doi: 10.1038/nature07039.

H.M. Berman, J. Westbrook, Z. Feng, G. Gilliland, T.N. Bhat, H. Weissig, I.N. Shindyalov & Bourne, P. E. (2000). The Protein Data Bank Nucleic Acids Research 28:235-242.

Hahn, S. A., Schutte, M., Shamsul Hoque, A. T. M., Moskaluk, C. A., da Costa, L. T., Rozenblum, E., Weinstein, C. L., Fischer, A., Yeo, C. J., Hruban, R. H., et al. (1996). DPC4, A Candidate Tumor Suppressor Gene at Human Chromosome 18q21.1. *Science*, 271 (5247): 350. doi: 10.1126/science.271.5247.350.

Hamidi, A., Song, J., Thakur, N., Itoh, S., Marcusson, A., Bergh, A., Heldin, C.-H. & Landström, M. (2017). TGF-β promotes PI3K-AKT signaling and prostate cancer cell migration through the TRAF6-mediated ubiquitylation of p85α. *Science Signaling*, 10 (486): eaal4186. doi: 10.1126/scisignal.aal4186.

Hamm, M. J., Kirchmaier, B. C. & Herzog, W. (2016). Sema3d controls collective endothelial cell migration by distinct mechanisms via Nrp1 and PlxnD1. *The Journal of cell biology*, 215 (3): 415-430. doi: 10.1083/jcb.201603100.

Hanahan, D. & Weinberg, Robert A. (2011). Hallmarks of Cancer: The Next Generation. *Cell*, 144 (5): 646-674. doi: https://doi.org/10.1016/j.cell.2011.02.013.

Hanson, S. E., Kleinbeck, K. R., Cantu, D., Kim, J., Bentz, M. L., Faucher, L. D., Kao, W. J. & Hematti, P. (2016). Local delivery of allogeneic bone marrow and adipose tissue-derived mesenchymal stromal cells for cutaneous wound healing in a porcine model. *J Tissue Eng Regen Med*, 10 (2): E90-e100. doi: 10.1002/term.1700.

Haraguchi, T. (2002). Live Cell Imaging: Approaches for Studying Protein Dynamics in Living Cells. *Cell Structure and Function*, 27 (5): 333-334. doi: 10.1247/csf.27.333.

Hnasko, R., Lin, A., McGarvey, J. A. & Stanker, L. H. (2011). A rapid method to improve protein detection by indirect ELISA. *Biochem Biophys Res Commun*, 410 (4): 726-31. doi: 10.1016/j.bbrc.2011.06.005.

Hnasko, T. S. & Hnasko, R. M. (2015). The Western Blot. In Hnasko, R. (ed.) *ELISA: Methods and Protocols*, pp. 87-96. New York, NY: Springer New York.

Hoshino, Y., Nishida, J., Katsuno, Y., Koinuma, D., Aoki, T., Kokudo, N., Miyazono, K. & Ehata, S. (2015). Smad4 Decreases the Population of Pancreatic Cancer-Initiating Cells

through Transcriptional Repression of ALDH1A1. *Am J Pathol*, 185 (5): 1457-70. doi: 10.1016/j.ajpath.2015.01.011.
Hussain, S. P., Hofseth, L. J. & Harris, C. C. (2003). Radical causes of cancer. *Nature Reviews Cancer*, 3 (4): 276-285.
Ignotz, R. A. & Massagué, J. (1985). Type beta transforming growth factor controls the adipogenic differentiation of 3T3 fibroblasts. *Proc Natl Acad Sci U S A*, 82 (24): 8530-4. doi: 10.1073/pnas.82.24.8530.
Ikushima, H., Todo, T., Ino, Y., Takahashi, M., Miyazawa, K. & Miyazono, K. (2009). Autocrine TGF-beta signaling maintains tumorigenicity of glioma-initiating cells through Sry-related HMG-box factors. *Cell Stem Cell*, 5 (5): 504-14. doi: 10.1016/j.stem.2009.08.018.
Jian, H., Shen, X., Liu, I., Semenov, M., He, X. & Wang, X.-F. (2006). Smad3-dependent nuclear translocation of beta-catenin is required for TGF-beta1-induced proliferation of bone marrow-derived adult human mesenchymal stem cells. *Genes & development*, 20 (6): 666-674. doi: 10.1101/gad.1388806.
Jochems, C. E., van der Valk, J. B., Stafleu, F. R. & Baumans, V. (2002). The use of fetal bovine serum: ethical or scientific problem? *Altern Lab Anim*, 30 (2): 219-27. doi: 10.1177/026119290203000208.
Kalluri, R. & Neilson, E. G. (2003). Epithelial-mesenchymal transition and its implications for fibrosis. *The Journal of clinical investigation*, 112 (12): 1776-1784. doi: 10.1172/JCI20530.
Kalluri, R. & Weinberg, R. A. (2009). The basics of epithelial-mesenchymal transition. *J Clin Invest*, 119 (6): 1420-8. doi: 10.1172/jci39104.
Kretzschmar, M., Doody, J., Timokhina, I. & Massagué, J. (1999). A mechanism of repression of TGFbeta/ Smad signaling by oncogenic Ras. *Genes Dev*, 13 (7): 804-16. doi: 10.1101/gad.13.7.804.
Kukura, J., Arratia, P. E., Szalai, E. S. & Muzzio, F. J. (2003). Engineering Tools for Understanding the Hydrodynamics of Dissolution Tests. *Drug Development and Industrial Pharmacy*, 29 (2): 231-239. doi: 10.1081/DDC-120016731.
Kwon, D., Kim, J. S., Cha, B. H., Park, K. S., Han, I., Park, K. S., Bae, H., Han, M. K., Kim, K. S. & Lee, S. H. (2016). The Effect of Fetal Bovine Serum (FBS) on Efficacy of Cellular Reprogramming for Induced Pluripotent Stem Cell (iPSC) Generation. *Cell Transplant*, 25 (6): 1025-42. doi: 10.3727/096368915x689703.
Lafyatis, R. (2014). Transforming growth factor β—at the centre of systemic sclerosis. *Nature Reviews Rheumatology*, 10 (12): 706-719. doi: 10.1038/nrrheum.2014.137.
Lamouille, S. & Derynck, R. (2007). Cell size and invasion in TGF-β–induced epithelial to mesenchymal transition is regulated by activation of the mTOR pathway. *Journal of Cell Biology*, 178 (3): 437-451. doi: 10.1083/jcb.200611146.
Le Bras, G. F., Taylor, C., Koumangoye, R. B., Revetta, F., Loomans, H. A. & Andl, C. D. (2015). TGFβ loss activates ADAMTS-1-mediated EGF-dependent invasion in a model of esophageal cell invasion. *Experimental cell research*, 330 (1): 29-42. doi: 10.1016/j.yexcr.2014.07.021.
Lee, Y. H. & Schiemann, W. P. (2014). Chemotherapeutic Targeting of the Transforming Growth Factor-β Pathway in Breast Cancers. *Breast Cancer Manag*, 3 (1): 73-85. doi: 10.2217/bmt.13.74.
Li, J., Su, W., Zhang, S., Hu, Y., Liu, J., Zhang, X., Bai, J., Yuan, W., Hu, L., Cheng, T., et al. (2015). Epidermal growth factor receptor and AKT1 gene copy numbers by multi-gene fluorescence in situ hybridization impact on prognosis in breast cancer. *Cancer science*, 106 (5): 642-649. doi: 10.1111/cas.12637.

Liarte, S., Bernabe-Garcia, A. & Nicolas, F. J. (2020). Role of TGF-beta in Skin Chronic Wounds: A Keratinocyte Perspective. *Cells*, 9 (2). doi: 10.3390/cells9020306.

Lin, T.-H., Yeh, T.-H., Wang, T.-W. & Yu, J.-Y. (2014). The Hippo pathway controls border cell migration through distinct mechanisms in outer border cells and polar cells of the Drosophila ovary. *Genetics*, 198 (3): 1087-1099. doi: 10.1534/genetics.114.167346.

Liu, Z., Yi, L., Du, M., Gong, G. & Zhu, Y. (2019). Overexpression of TGF-β enhances the migration and invasive ability of ectopic endometrial cells via ERK/MAPK signaling pathway. *Exp Ther Med*, 17 (6): 4457-4464. doi: 10.3892/etm.2019.7522.

Lonardo, E., Hermann, P. C., Mueller, M. T., Huber, S., Balic, A., Miranda-Lorenzo, I., Zagorac, S., Alcala, S., Rodriguez-Arabaolaza, I., Ramirez, J. C., et al. (2011). Nodal/Activin signaling drives self-renewal and tumorigenicity of pancreatic cancer stem cells and provides a target for combined drug therapy. *Cell Stem Cell*, 9 (5): 433-46. doi: 10.1016/j.stem.2011.10.001.

Loosdregt, I. T. (2020). *Modes of Cell Migration*. CytoSMART. Available at: https://cytosmart.com/resources/modes-of-cell-migration (accessed: 22/4/21).

Lång, E., Grudic, A., Pankiv, S., Bruserud, O., Simonsen, A., Bjerkvig, R., Bjørås, M. & Bøe, S. O. (2012). The arsenic-based cure of acute promyelocytic leukemia promotes cytoplasmic sequestration of PML and PML/RARA through inhibition of PML body recycling. *Blood*, 120 (4): 847-57. doi: 10.1182/blood-2011-10-388496.

Lång, E., Polec, A., Lång, A., Valk, M., Blicher, P., Rowe, A. D., Tonseth, K. A., Jackson, C. J., Utheim, T. P., Janssen, L. M. C., et al. (2018). Coordinated collective migration and asymmetric cell division in confluent human keratinocytes without wounding. *Nat Commun*, 9 (1): 3665. doi: 10.1038/s41467-018-05578-7.

Mahdavian Delavary, B., van der Veer, W. M., van Egmond, M., Niessen, F. B. & Beelen, R. H. (2011). Macrophages in skin injury and repair. *Immunobiology*, 216 (7): 753-62. doi: 10.1016/j.imbio.2011.01.001.

Mak, M., Spill, F., Kamm, R. D. & Zaman, M. H. (2016). Single-Cell Migration in Complex Microenvironments: Mechanics and Signaling Dynamics. *Journal of biomechanical engineering*, 138 (2): 021004-021004. doi: 10.1115/1.4032188.

Mani, S. A., Guo, W., Liao, M. J., Eaton, E. N., Ayyanan, A., Zhou, A. Y., Brooks, M., Reinhard, F., Zhang, C. C., Shipitsin, M., et al. (2008). The epithelial-mesenchymal transition generates cells with properties of stem cells. *Cell*, 133 (4): 704-15. doi: 10.1016/j.cell.2008.03.027.

Massagué, J. (2012). TGFβ signalling in context. *Nat Rev Mol Cell Biol*, 13 (10): 616-30. doi: 10.1038/nrm3434.

Massagué, J. (2012). TGFβ signalling in context. *Nature reviews. Molecular cell biology*, 13 (10): 616-630. doi: 10.1038/nrm3434.

Mast, B. A. & Schultz, G. S. (1996). Interactions of cytokines, growth factors, and proteases in acute and chronic wounds. *Wound Repair Regen*, 4 (4): 411-20. doi: 10.1046/j.1524-475X.1996.40404.x.

Matise, L. A., Palmer, T. D., Ashby, W. J., Nashabi, A., Chytil, A., Aakre, M., Pickup, M. W., Gorska, A. E., Zijlstra, A. & Moses, H. L. (2012). Lack of transforming growth factor-β signaling promotes collective cancer cell invasion through tumor-stromal crosstalk. *Breast cancer research : BCR*, 14 (4): R98-R98. doi: 10.1186/bcr3217.

Mayor, R. & Etienne-Manneville, S. (2016). The front and rear of collective cell migration. *Nat Rev Mol Cell Biol*, 17 (2): 97-109. doi: 10.1038/nrm.2015.14.

Mendelsohn, J. & Baselga, J. (2000). The EGF receptor family as targets for cancer therapy. *Oncogene*, 19 (56): 6550-6565. doi: 10.1038/sj.onc.1204082.

Mitulović, G. & Mechtler, K. (2006). HPLC techniques for proteomics analysis—a short overview of latest developments. *Briefings in Functional Genomics*, 5 (4): 249-260. doi: 10.1093/bfgp/ell034.

Molecular Devices. (n.d.). *High-content confocal imaging solution with water objective options*. Available at: https://www.moleculardevices.com/products/cellular-imaging-systems/high-content-imaging/imagexpress-micro-confocal (accessed: 14/01/2021).

Morikawa, M., Derynck, R. & Miyazono, K. (2016). TGF-beta and the TGF-beta Family: Context-Dependent Roles in Cell and Tissue Physiology. *Cold Spring Harb Perspect Biol*, 8 (5). doi: 10.1101/cshperspect.a021873.

Nakatani, K., Sakaue, H., Thompson, D. A., Weigel, R. J. & Roth, R. A. (1999). Identification of a Human Akt3 (Protein Kinase B γ) Which Contains the Regulatory Serine Phosphorylation Site. *Biochemical and Biophysical Research Communications*, 257 (3): 906-910. doi: https://doi.org/10.1006/bbrc.1999.0559.

Nishimura, Y., Takiguchi, S., Ito, S. & Itoh, K. (2015). EGF-stimulated AKT activation is mediated by EGFR recycling via an early endocytic pathway in a gefitinib-resistant human lung cancer cell line. *Int J Oncol*, 46 (4): 1721-9. doi: 10.3892/ijo.2015.2871.

Ohta, M., Greenberger, J. S., Anklesaria, P., Bassols, A. & Massagué, J. (1987). Two forms of transforming growth factor-beta distinguished by multipotential haematopoietic progenitor cells. *Nature*, 329 (6139): 539-41. doi: 10.1038/329539a0.

Oida, T. & Weiner, H. L. (2010). Depletion of TGF-β from fetal bovine serum. *Journal of immunological methods*, 362 (1-2): 195-198. doi: 10.1016/j.jim.2010.09.008.

Okano, J., Gaslightwala, I., Birnbaum, M. J., Rustgi, A. K. & Nakagawa, H. (2000). Akt/protein kinase B isoforms are differentially regulated by epidermal growth factor stimulation. *J Biol Chem*, 275 (40): 30934-42. doi: 10.1074/jbc.M004112200.

Otten, J., Bokemeyer, C. & Fiedler, W. (2010). TGF-β Superfamily Receptors—Targets for Antiangiogenic Therapy? *Journal of Oncology*, 2010: 317068. doi: 10.1155/2010/317068.

Pardali, K., Kurisaki, A., Morén, A., ten Dijke, P., Kardassis, D. & Moustakas, A. (2000). Role of Smad proteins and transcription factor Sp1 in p21(Waf1/Cip1) regulation by transforming growth factor-beta. *J Biol Chem*, 275 (38): 29244-56. doi: 10.1074/jbc.M909467199.

Park, B. S., Jang, K. A., Sung, J. H., Park, J. S., Kwon, Y. H., Kim, K. J. & Kim, W. S. (2008). Adipose-derived stem cells and their secretory factors as a promising therapy for skin aging. *Dermatol Surg*, 34 (10): 1323-6. doi: 10.1111/j.1524-4725.2008.34283.x.

Parvani, J. G., Taylor, M. A. & Schiemann, W. P. (2011). Noncanonical TGF-β signaling during mammary tumorigenesis. *J Mammary Gland Biol Neoplasia*, 16 (2): 127-46. doi: 10.1007/s10911-011-9207-3.

Pastar, I., Stojadinovic, O., Krzyzanowska, A., Barrientos, S., Stuelten, C., Zimmerman, K., Blumenberg, M., Brem, H. & Tomic-Canic, M. (2010). Attenuation of the transforming growth factor beta-signaling pathway in chronic venous ulcers. *Mol Med*, 16 (3-4): 92-101. doi: 10.2119/molmed.2009.00149.

Penn, J. W., Grobbelaar, A. O. & Rolfe, K. J. (2012). The role of the TGF-β family in wound healing, burns and scarring: a review. *International journal of burns and trauma*, 2 (1): 18-28.

Petitjean, L., Reffay, M., Grasland-Mongrain, E., Poujade, M., Ladoux, B., Buguin, A. & Silberzan, P. (2010). Velocity fields in a collectively migrating epithelium. *Biophysical journal*, 98 (9): 1790-1800. doi: 10.1016/j.bpj.2010.01.030.

Postlethwaite, A. E., Keski-Oja, J., Moses, H. L. & Kang, A. H. (1987). Stimulation of the chemotactic migration of human fibroblasts by transforming growth factor beta. *The Journal of experimental medicine*, 165 (1): 251-256. doi: 10.1084/jem.165.1.251.

Redmile-Gordon, M. A., Armenise, E., White, R. P., Hirsch, P. R. & Goulding, K. W. T. (2013). A comparison of two colorimetric assays, based upon Lowry and Bradford techniques, to estimate total protein in soil extracts. *Soil biology & biochemistry*, 67 (100): 166-173. doi: 10.1016/j.soilbio.2013.08.017.

Reibman, J., Meixler, S., Lee, T. C., Gold, L. I., Cronstein, B. N., Haines, K. A., Kolasinski, S. L. & Weissmann, G. (1991). Transforming growth factor beta 1, a potent chemoattractant for human neutrophils, bypasses classic signal-transduction pathways. *Proceedings of the National Academy of Sciences of the United States of America*, 88 (15): 6805-6809. doi: 10.1073/pnas.88.15.6805.

Remy, I., Montmarquette, A. & Michnick, S. W. (2004). PKB/Akt modulates TGF-β signalling through a direct interaction with Smad3. *Nature Cell Biology*, 6 (4): 358-365. doi: 10.1038/ncb1113.

Revenu, C. & Gilmour, D. (2009). EMT 2.0: shaping epithelia through collective migration. *Current Opinion in Genetics & Development*, 19 (4): 338-342. doi: https://doi.org/10.1016/j.gde.2009.04.007.

Richter, P., Umbreit, C., Franz, M., Berndt, A., Grimm, S., Uecker, A., Böhmer, F. D., Kosmehl, H. & Berndt, A. (2011). EGF/TGFβ1 co-stimulation of oral squamous cell carcinoma cells causes an epithelial-mesenchymal transition cell phenotype expressing laminin 332. *J Oral Pathol Med*, 40 (1): 46-54. doi: 10.1111/j.1600-0714.2010.00936.x.

Ridley, A. J., Schwartz, M. A., Burridge, K., Firtel, R. A., Ginsberg, M. H., Borisy, G., Parsons, J. T. & Horwitz, A. R. (2003). Cell Migration: Integrating Signals from Front to Back. *Science*, 302 (5651): 1704. doi: 10.1126/science.1092053.

Roberts, A. B., Anzano, M. A., Lamb, L. C., Smith, J. M. & Sporn, M. B. (1981). New class of transforming growth factors potentiated by epidermal growth factor: isolation from non-neoplastic tissues. *Proceedings of the National Academy of Sciences of the United States of America*, 78 (9): 5339-5343. doi: 10.1073/pnas.78.9.5339.

Roberts, A. B., Anzano, M. A., Wakefield, L. M., Roche, N. S., Stern, D. F. & Sporn, M. B. (1985). Type beta transforming growth factor: a bifunctional regulator of cellular growth. *Proceedings of the National Academy of Sciences of the United States of America*, 82 (1): 119-123. doi: 10.1073/pnas.82.1.119.

Rørth, P. (2009). Collective cell migration. *Annu Rev Cell Dev Biol*, 25: 407-29. doi: 10.1146/annurev.cellbio.042308.113231.

Scarpa, E. & Mayor, R. (2016). Collective cell migration in development. *The Journal of cell biology*, 212 (2): 143-155. doi: 10.1083/jcb.201508047.

Schelch, K., Vogel, L., Schneller, A., Brankovic, J., Mohr, T., Mayer, R. L., Slany, A., Gerner, C. & Grusch, M. (2021). EGF Induces Migration Independent of EMT or Invasion in A549 Lung Adenocarcinoma Cells. *Frontiers in Cell and Developmental Biology*, 9 (484). doi: 10.3389/fcell.2021.634371.

Schindelin, J., Arganda-Carreras, I., Frise, E., Kaynig, V., Longair, M., Pietzsch, T., Preibisch, S., Rueden, C., Saalfeld, S., Schmid, B., et al. (2012). Fiji: an open-source platform for biological-image analysis. *Nat Methods*, 9 (7): 676-82. doi: 10.1038/nmeth.2019.

Schürer, N., Köhne, A., Schliep, V., Barlag, K. & Goerz, G. (1993). Lipid composition and synthesis of HaCaT cells, an immortalized human keratinocyte line, in comparison with normal human adult keratinocytes. *Experimental Dermatology*, 2 (4): 179-185. doi: https://doi.org/10.1111/j.1600-0625.1993.tb00030.x.

Schäfer, M. & Werner, S. (2008). Cancer as an overhealing wound: an old hypothesis revisited. *Nature Reviews Molecular Cell Biology*, 9 (8): 628-638. doi: 10.1038/nrm2455.

Seyedin, S. M., Thomas, T. C., Thompson, A. Y., Rosen, D. M. & Piez, K. A. (1985). Purification and characterization of two cartilage-inducing factors from bovine

demineralized bone. *Proc Natl Acad Sci U S A*, 82 (8): 2267-71. doi: 10.1073/pnas.82.8.2267.

Shin, I., Bakin, A. V., Rodeck, U., Brunet, A. & Arteaga, C. L. (2001). Transforming growth factor beta enhances epithelial cell survival via Akt-dependent regulation of FKHRL1. *Mol Biol Cell*, 12 (11): 3328-39. doi: 10.1091/mbc.12.11.3328.

Shu, D. Y., Hutcheon, A. E. K., Zieske, J. D. & Guo, X. (2019). Epidermal Growth Factor Stimulates Transforming Growth Factor-Beta Receptor Type II Expression In Corneal Epithelial Cells. *Scientific reports*, 9 (1): 8079-8079. doi: 10.1038/s41598-019-42969-2.

Singla, S., Singla, S., Kumar, A. & Singla, M. (2012). Role of epidermal growth factor in healing of diabetic foot ulcers. *Indian J Surg*, 74 (6): 451-5. doi: 10.1007/s12262-012-0447-2.

Smith, J. T., Elkin, J. T. & Reichert, W. M. (2006). Directed cell migration on fibronectin gradients: effect of gradient slope. *Exp Cell Res*, 312 (13): 2424-32. doi: 10.1016/j.yexcr.2006.04.005.

Song, K., Cornelius, S. C., Reiss, M. & Danielpour, D. (2003). Insulin-like growth factor-I inhibits transcriptional responses of transforming growth factor-beta by phosphatidylinositol 3-kinase/Akt-dependent suppression of the activation of Smad3 but not Smad2. *J Biol Chem*, 278 (40): 38342-51. doi: 10.1074/jbc.M304583200.

Spear, M. (2013). Acute or chronic? What's the difference? *Plast Surg Nurs*, 33 (2): 98-100. doi: 10.1097/PSN.0b013e3182965e94.

Sporn, M. B., Roberts, A. B., Shull, J. H., Smith, J. M., Ward, J. M. & Sodek, J. (1983). Polypeptide transforming growth factors isolated from bovine sources and used for wound healing in vivo. *Science*, 219 (4590): 1329-31. doi: 10.1126/science.6572416.

Stramer, B. & Mayor, R. (2017). Mechanisms and in vivo functions of contact inhibition of locomotion. *Nat Rev Mol Cell Biol*, 18 (1): 43-55. doi: 10.1038/nrm.2016.118.

Sundqvist, A., Vasilaki, E., Voytyuk, O., Bai, Y., Morikawa, M., Moustakas, A., Miyazono, K., Heldin, C.-H., ten Dijke, P. & van Dam, H. (2020). TGFβ and EGF signaling orchestrates the AP-1- and p63 transcriptional regulation of breast cancer invasiveness. *Oncogene*, 39 (22): 4436-4449. doi: 10.1038/s41388-020-1299-z.

Supatto, W., Débarre, D., Moulia, B., Brouzés, E., Martin, J.-L., Farge, E. & Beaurepaire, E. (2005). In vivo modulation of morphogenetic movements in Drosophila embryos with femtosecond laser pulses. *Proceedings of the National Academy of Sciences of the United States of America*, 102 (4): 1047-1052. doi: 10.1073/pnas.0405316102.

Suriyamurthy, S., Baker, D., Ten Dijke, P. & Iyengar, P. V. (2019). Epigenetic Reprogramming of TGF-beta Signaling in Breast Cancer. *Cancers (Basel)*, 11 (5). doi: 10.3390/cancers11050726.

Suwanabol, P. A., Seedial, S. M., Zhang, F., Shi, X., Si, Y., Liu, B. & Kent, K. C. (2012). TGF-β and Smad3 modulate PI3K/Akt signaling pathway in vascular smooth muscle cells. *American journal of physiology. Heart and circulatory physiology*, 302 (11): H2211-H2219. doi: 10.1152/ajpheart.00966.2011.

Swaney, K. F., Huang, C.-H. & Devreotes, P. N. (2010). Eukaryotic chemotaxis: a network of signaling pathways controls motility, directional sensing, and polarity. *Annual review of biophysics*, 39: 265-289. doi: 10.1146/annurev.biophys.093008.131228.

Tai, G., Tai, M. & Zhao, M. (2018). Electrically stimulated cell migration and its contribution to wound healing. *Burns & trauma*, 6: 20-20. doi: 10.1186/s41038-018-0123-2.

Tang, B., Yoo, N., Vu, M., Mamura, M., Nam, J. S., Ooshima, A., Du, Z., Desprez, P. Y., Anver, M. R., Michalowska, A. M., et al. (2007). Transforming growth factor-beta can suppress tumorigenesis through effects on the putative cancer stem or early progenitor

cell and committed progeny in a breast cancer xenograft model. *Cancer Res*, 67 (18): 8643-52. doi: 10.1158/0008-5472.Can-07-0982.

Tarnuzzer, R. W. & Schultz, G. S. (1996). Biochemical analysis of acute and chronic wound environments. *Wound Repair Regen*, 4 (3): 321-5. doi: 10.1046/j.1524-475X.1996.40307.x.

Taylor, Z. J., Gurka, R., Kopp, G. A. & Liberzon, A. (2010). Long-Duration Time-Resolved PIV to Study Unsteady Aerodynamics. *IEEE Transactions on Instrumentation and Measurement*, 59 (12): 3262-3269. doi: 10.1109/TIM.2010.2047149.

te Boekhorst, V., Preziosi, L. & Friedl, P. (2016). Plasticity of Cell Migration In Vivo and In Silico. *Annual Review of Cell and Developmental Biology*, 32 (1): 491-526. doi: 10.1146/annurev-cellbio-111315-125201.

Thermo Fisher Scientific. (n.d.). *Countess 3 Automated Cell Counter*. Available at: https://www.thermofisher.com/no/en/home/life-science/cell-analysis/cell-analysis-instruments/automated-cell-counters/countess-3-automated-cell-counter.html (accessed: 20/01/2021).

Theveneau, E. & Mayor, R. (2013). Collective cell migration of epithelial and mesenchymal cells. *Cell Mol Life Sci*, 70 (19): 3481-92. doi: 10.1007/s00018-012-1251-7.

Ulloa, L., Doody, J. & Massagué, J. (1999). Inhibition of transforming growth factor-β/SMAD signalling by the interferon-γ/STAT pathway. *Nature*, 397 (6721): 710-713. doi: 10.1038/17826.

van de Merbel, N. C. (2019). Protein quantification by LC–MS: a decade of progress through the pages of Bioanalysis. *Bioanalysis*, 11 (7): 629-644. doi: 10.4155/bio-2019-0032.

Vincent, L. G., Choi, Y. S., Alonso-Latorre, B., del Álamo, J. C. & Engler, A. J. (2013). Mesenchymal stem cell durotaxis depends on substrate stiffness gradient strength. *Biotechnology journal*, 8 (4): 472-484. doi: 10.1002/biot.201200205.

Vitiello, P. P., Cardone, C., Martini, G., Ciardiello, D., Belli, V., Matrone, N., Barra, G., Napolitano, S., Della Corte, C., Turano, M., et al. (2019). Receptor tyrosine kinase-dependent PI3K activation is an escape mechanism to vertical suppression of the EGFR/RAS/MAPK pathway in KRAS-mutated human colorectal cancer cell lines. *J Exp Clin Cancer Res*, 38 (1): 41. doi: 10.1186/s13046-019-1035-0.

Wahl, S. M., Hunt, D. A., Wakefield, L. M., McCartney-Francis, N., Wahl, L. M., Roberts, A. B. & Sporn, M. B. (1987). Transforming growth factor type beta induces monocyte chemotaxis and growth factor production. *Proc Natl Acad Sci U S A*, 84 (16): 5788-92. doi: 10.1073/pnas.84.16.5788.

Wakefield, L. M. & Hill, C. S. (2013). Beyond TGFβ: roles of other TGFβ superfamily members in cancer. *Nature reviews. Cancer*, 13 (5): 328-341. doi: 10.1038/nrc3500.

Wang, W., Kansakar, U., Markovic, V., Wang, B. & Sossey-Alaoui, K. (2020). WAVE3 phosphorylation regulates the interplay between PI3K, TGF-beta, and EGF signaling pathways in breast cancer. *Oncogenesis*, 9 (10): 87. doi: 10.1038/s41389-020-00272-0.

Weijer, C. J. (2009). Collective cell migration in development. *Journal of Cell Science*, 122 (18): 3215. doi: 10.1242/jcs.036517.

Westermeier, R. (2016). Protein Detection - Electrophoresis in Practice. *Electrophoresis in Practice*: 131-164. doi: 10.1002/9783527695188.ch6.

Yan, X., Liu, Z. & Chen, Y. (2009). Regulation of TGF-beta signaling by Smad7. *Acta Biochim Biophys Sin (Shanghai)*, 41 (4): 263-72. doi: 10.1093/abbs/gmp018.

Zallen, J. A. & Blankenship, J. T. (2008). Multicellular dynamics during epithelial elongation. *Semin Cell Dev Biol*, 19 (3): 263-70. doi: 10.1016/j.semcdb.2008.01.005.

Zhao, Y., Ma, J., Fan, Y., Wang, Z., Tian, R., Ji, W., Zhang, F. & Niu, R. (2018). TGF-β transactivates EGFR and facilitates breast cancer migration and invasion through

canonical Smad3 and ERK/Sp1 signaling pathways. *Molecular oncology*, 12 (3): 305-321. doi: 10.1002/1878-0261.12162.

Appendix A

Materials

Table A.1: Reagents used in the live cell imaging experiments and western blot analysis

Product name	Product number	Supplier
Bovine Serum Albumin	B2000-500	Saveen Werner AB
Bromophenol blue	B-6896	Sigma-Aldrich
Collagen IV	C7521	Sigma-Aldrich
Dimethyl Sulfoxide	D8418	Sigma-Aldrich
Donkey Anti-Mouse IgG H&L	Ab6820	Abcam
Donkey Anti-Rabbit IgG H&L	Ab6802	Abcam
EGF	236-EG	R&D Systems
Fetal Bovine Serum	F7524	Sigma-Aldrich
Gefitinib	Y0001813	Sigma-Aldrich
Glycerol	49767	Sigma-Aldrich
HaCaT mCherry Histone H2B	N/A	Produced by Bøe's research group
HaCaT cells (WT)	300493	CLS
HCl 37%	258148	Sigma-Aldrich
Iscove's Modified Dulbecco's Medium	16529	Sigma-Aldrich
MOPS SDS Running Buffer (20x)	B000102	Invitrogen
Penicillin Streptomycin	15140-122	Gibco
Phosphate-buffered Saline	2012513	Oslo University Hospital
Phospho-AKT (Ser473) (193H12) Rabbit monoclonal antibody	4058S	Cell Signaling Technology
Precision Plus Protein™ Dual Color Standards	L001648A	Bio-Rad
Recombinant Human TGF-β1	240-B-002	R&D Systems
SB431542	S4317	Sigma-Aldrich
Skim milk powder	BCCB5939	Sigma-Aldrich
Sodium dodecyl sulfate	05030	Sigma-Aldrich
SuperSignal™ West Pico PLUS Chemiluminescent Substrate Kit	34580	Thermo Fisher Scientific
Tris-EDTA buffer solution pH 8	93283	Sigma-Aldrich
Trypan Blue Stain Solution 0.4%	T10282	Invitrogen
Trypsin-EDTA	25200-056	Gibco
Tween-20	P1379	Sigma-Aldrich
α-Tubulin DM1A Mouse monoclonal antibody	Sc-32293	Santa Cruz Technologies
β-mercaptoethanol	M6250	Sigma-Aldrich

Equipment

Table A.2: Equipment used in the live cell imaging experiments and western blot analysis

Equipment	Product number	Supplier
12-well Nunclon Delta Surface Plate	150628	Thermo Fisher Scientific
96-well Greiner Sensoplate Microplate Plate with glass bottom	655892	Greiner Bio-One
Bolt™ 10% Bis-Tris Plus gels with 10 wells	NW00100BOX	Invitrogen
Countess™ Cell Counting Chamber Slides	C10228	Invitrogen
AccuBlock Digital Dry Bath	N/A	Labnet
Mini gel tank	N/A	Invitrogen
Vacuum aspiration tool	N/A	Integra Vacuboy
Tilt shaker WS 10	N/A	Edmund Bühler
T75 Cell Culture Flasks	156499	Thermo Fisher Scientific
Trans-Blot Turbo Transfer Pack	1704158	Bio-Rad
QIA-shredder column with collection tubes	79654	Qiagen

Instruments

Table A.3: Instruments used in the live cell imaging experiments and western blot analysis

Instrument	Version	Supplier
Biofuge Pico	N/A	Heraeus
ChemiDoc MP Imaging System	5.0	Bio-Rad
Countess™ 3 Automated Cell Counter	C10227	Invitrogen
Forma Steri-Cycle CO_2 Incubator	314567-4357	Thermo Fisher Scientific
ImageXpress Micro Confocal High-Content Imaging System	5150066	Molecular Devices
Olympus CJX53 Microscope	N/A	Olympus Life Science
Safe 2020 Class II Biological Safety Cabinet	42430546	Thermo Fisher Scientific
Trans-Blot Turbo System	N/A	Bio-Rad

Software

Table A.4: Software used in the live cell imaging experiments and western blot analysis

Software	Version	Supplier
Fiji ImageJ	2.1.0/1.53C	ImageJ
Image Lab Software	5.1	Bio-Rad
MetaXpress High-Content Image Acquisition and Analysis Software	6.5.3.427	Molecular Devices
PyCharm	2019.2.3	JetBrains
Python	3.6.4	Python Software Foundation

Appendix B

Script 1 – File_sorting.py

```
import os
import shutil
import sys

'''
This program sorts files from ImageXpress 96-well time-lapse experiments intoto folders where
each folder represents all timepoints from one well. To use the program, place all TimePoint
folders into the folder called "test". The "Wells"-folder containing all of the 96-well
subfolders will be generated automatically.

'''


Wells = "D:\\Jenny\\220321 MigrationAssay Jenny Exp4_Plate_6047\\Wells\\" #Dont change \\Wells\\
os.makedirs(Wells)

#make new folder names
folder_name = ["A01", "A02", "A03", "A04", "A05", "A06", "A07", "A08", "A09", "A10", "A11",
"A12", "B01", "B02", "B03", "B04", "B05", "B06", "B07", "B08", "B09", "B10", "B11", "B12",
"C01", "C02", "C03", "C04", "C05", "C06", "C07", "C08", "C09", "C10", "C11", "C12", "D01",
"D02", "D03", "D04", "D05", "D06", "D07", "D08", "D09", "D10", "D11", "D12", "E01", "E02",
"E03", "E04", "E05", "E06", "E07", "E08", "E09", "E10", "E11", "E12", "F01", "F02", "F03",
"F04", "F05", "F06", "F07", "F08", "F09", "F10", "F11", "F12", "G01", "G02", "G03", "G04",
"G05", "G06", "G07", "G08", "G09", "G10", "G11", "G12", "H01", "H02", "H03", "H04", "H05",
"H06", "H07", "H08", "H09", "H10", "H11", "H12"]

#Iterate through the files in your directory
for x in range(0,len(folder_name)):
    if not os.path.exists(Wells+folder_name[x]):
        os.makedirs(Wells+folder_name[x])

for Timepoints in range(0, 114): #number of timepoints (must be exact)
    path = "D:\\Jenny\\220321 MigrationAssay Jenny
Exp4_Plate_6047\\TimePoint_"+str(Timepoints+1)+"\\" #Dont change
\\TimePoint_"+str(Timepoints+1)+"\\
    time = "Timepoint_"+"%.3d" % (Timepoints + 1)


#make a list of all the flies in a directory and stors it in the variable names
#Note that the command os.listdi dose not work since the items wil not be iterable
    names = []
    for subdir, dirs, files in os.walk(path):
        for file in files:
           names.append(os.path.join(file))


    for files in names:
        if "A01" in files and not os.path.exists(Wells + "A01/" + time + "_" + files):
            shutil.move(path + files, Wells + "A01/" + time + "_" + files)
        if "A02" in files and not os.path.exists(Wells + "A02/" + time + "_" + files):
            shutil.move(path + files, Wells + "A02/" + time + "_" + files)
        if "A03" in files and not os.path.exists(Wells + "A03/" + time + "_" + files):
            shutil.move(path + files, Wells + "A03/" + time + "_" + files)
        if "A04" in files and not os.path.exists(Wells + "A04/" + time + "_" + files):
            shutil.move(path + files, Wells + "A04/" + time + "_" + files)
        if "A05" in files and not os.path.exists(Wells + "A05/" + time + "_" + files):
            shutil.move(path + files, Wells+"A05/"+time+"_"+files)
        if "A06" in files and not os.path.exists(Wells + "A06/" + time + "_" + files):
            shutil.move(path + files, Wells + "A06/" + time + "_" + files)
        if "A07" in files and not os.path.exists(Wells + "A07/" + time + "_" + files):
            shutil.move(path + files, Wells + "A07/" + time + "_" + files)
        if "A08" in files and not os.path.exists(Wells + "A08/" + time + "_" + files):
            shutil.move(path + files, Wells + "A08/" + time + "_" + files)
        if "A09" in files and not os.path.exists(Wells + "A09/" + time + "_" + files):
            shutil.move(path + files, Wells + "A09/" + time + "_" + files)
        if "A10" in files and not os.path.exists(Wells + "A10/" + time + "_" + files):
            shutil.move(path + files, Wells + "A10/" + time + "_" + files)
        if "A11" in files and not os.path.exists(Wells + "A11/" + time + "_" + files):
            shutil.move(path + files, Wells + "A11/" + time + "_" + files)
```

```
if "A12" in files and not os.path.exists(Wells + "A12/" + time + "_" + files):
    shutil.move(path + files, Wells + "A12/" + time + "_" + files)


if "B01" in files and not os.path.exists(Wells + "B01/" + time + "_" + files):
    shutil.move(path + files, Wells + "B01/" + time + "_" + files)
if "B02" in files and not os.path.exists(Wells + "B02/" + time + "_" + files):
    shutil.move(path + files, Wells + "B02/" + time + "_" + files)
if "B03" in files and not os.path.exists(Wells + "B03/" + time + "_" + files):
    shutil.move(path + files, Wells + "B03/" + time + "_" + files)
if "B04" in files and not os.path.exists(Wells + "B04/" + time + "_" + files):
    shutil.move(path + files, Wells + "B04/" + time + "_" + files)
if "B05" in files and not os.path.exists(Wells + "B05/" + time + "_" + files):
    shutil.move(path + files, Wells + "B05/" + time + "_" + files)
if "B06" in files and not os.path.exists(Wells + "B06/" + time + "_" + files):
    shutil.move(path + files, Wells + "B06/" + time + "_" + files)
if "B07" in files and not os.path.exists(Wells + "B07/" + time + "_" + files):
    shutil.move(path + files, Wells + "B07/" + time + "_" + files)
if "B08" in files and not os.path.exists(Wells + "B08/" + time + "_" + files):
    shutil.move(path + files, Wells + "B08/" + time + "_" + files)
if "B09" in files and not os.path.exists(Wells + "B09/" + time + "_" + files):
    shutil.move(path + files, Wells + "B09/" + time + "_" + files)
if "B10" in files and not os.path.exists(Wells + "B10/" + time + "_" + files):
    shutil.move(path + files, Wells + "B10/" + time + "_" + files)
if "B11" in files and not os.path.exists(Wells + "B11/" + time + "_" + files):
    shutil.move(path + files, Wells + "B11/" + time + "_" + files)
if "B12" in files and not os.path.exists(Wells + "B12/" + time + "_" + files):
    shutil.move(path + files, Wells + "B12/" + time + "_" + files)


if "C01" in files and not os.path.exists(Wells + "C01/" + time + "_" + files):
    shutil.move(path + files, Wells + "C01/" + time + "_" + files)
if "C02" in files and not os.path.exists(Wells + "C02/" + time + "_" + files):
    shutil.move(path + files, Wells + "C02/" + time + "_" + files)
if "C03" in files and not os.path.exists(Wells + "C03/" + time + "_" + files):
    shutil.move(path + files, Wells + "C03/" + time + "_" + files)
if "C04" in files and not os.path.exists(Wells + "C04/" + time + "_" + files):
    shutil.move(path + files, Wells + "C04/" + time + "_" + files)
if "C05" in files and not os.path.exists(Wells + "C05/" + time + "_" + files):
    shutil.move(path + files, Wells + "C05/" + time + "_" + files)
if "C06" in files and not os.path.exists(Wells + "C06/" + time + "_" + files):
    shutil.move(path + files, Wells + "C06/" + time + "_" + files)
if "C07" in files and not os.path.exists(Wells + "C07/" + time + "_" + files):
    shutil.move(path + files, Wells + "C07/" + time + "_" + files)
if "C08" in files and not os.path.exists(Wells + "C08/" + time + "_" + files):
    shutil.move(path + files, Wells + "C08/" + time + "_" + files)
if "C09" in files and not os.path.exists(Wells + "C09/" + time + "_" + files):
    shutil.move(path + files, Wells + "C09/" + time + "_" + files)
if "C10" in files and not os.path.exists(Wells + "C10/" + time + "_" + files):
    shutil.move(path + files, Wells + "C10/" + time + "_" + files)
if "C11" in files and not os.path.exists(Wells + "C11/" + time + "_" + files):
    shutil.move(path + files, Wells + "C11/" + time + "_" + files)
if "C12" in files and not os.path.exists(Wells + "C12/" + time + "_" + files):
    shutil.move(path + files, Wells + "C12/" + time + "_" + files)


if "D01" in files and not os.path.exists(Wells + "D01/" + time + "_" + files):
    shutil.move(path + files, Wells + "D01/" + time + "_" + files)
if "D02" in files and not os.path.exists(Wells + "D02/" + time + "_" + files):
    shutil.move(path + files, Wells + "D02/" + time + "_" + files)
if "D03" in files and not os.path.exists(Wells + "D03/" + time + "_" + files):
    shutil.move(path + files, Wells + "D03/" + time + "_" + files)
if "D04" in files and not os.path.exists(Wells + "D04/" + time + "_" + files):
    shutil.move(path + files, Wells + "D04/" + time + "_" + files)
if "D05" in files and not os.path.exists(Wells + "D05/" + time + "_" + files):
    shutil.move(path + files, Wells + "D05/" + time + "_" + files)
if "D06" in files and not os.path.exists(Wells + "D06/" + time + "_" + files):
    shutil.move(path + files, Wells + "D06/" + time + "_" + files)
if "D07" in files and not os.path.exists(Wells + "D07/" + time + "_" + files):
    shutil.move(path + files, Wells + "D07/" + time + "_" + files)
if "D08" in files and not os.path.exists(Wells + "D08/" + time + "_" + files):
    shutil.move(path + files, Wells + "D08/" + time + "_" + files)
if "D09" in files and not os.path.exists(Wells + "D09/" + time + "_" + files):
    shutil.move(path + files, Wells + "D09/" + time + "_" + files)
if "D10" in files and not os.path.exists(Wells + "D10/" + time + "_" + files):
    shutil.move(path + files, Wells + "D10/" + time + "_" + files)
if "D11" in files and not os.path.exists(Wells + "D11/" + time + "_" + files):
```

```
    shutil.move(path + files, Wells + "D11/" + time + "_" + files)
if "D12" in files and not os.path.exists(Wells + "D12/" + time + "_" + files):
    shutil.move(path + files, Wells + "D12/" + time + "_" + files)


if "E01" in files and not os.path.exists(Wells + "E01/" + time + "_" + files):
    shutil.move(path + files, Wells + "E01/" + time + "_" + files)
if "E02" in files and not os.path.exists(Wells + "E02/" + time + "_" + files):
    shutil.move(path + files, Wells + "E02/" + time + "_" + files)
if "E03" in files and not os.path.exists(Wells + "E03/" + time + "_" + files):
    shutil.move(path + files, Wells + "E03/" + time + "_" + files)
if "E04" in files and not os.path.exists(Wells + "E04/" + time + "_" + files):
    shutil.move(path + files, Wells + "E04/" + time + "_" + files)
if "E05" in files and not os.path.exists(Wells + "E05/" + time + "_" + files):
    shutil.move(path + files, Wells + "E05/" + time + "_" + files)
if "E06" in files and not os.path.exists(Wells + "E06/" + time + "_" + files):
    shutil.move(path + files, Wells + "E06/" + time + "_" + files)
if "E07" in files and not os.path.exists(Wells + "E07/" + time + "_" + files):
    shutil.move(path + files, Wells + "E07/" + time + "_" + files)
if "E08" in files and not os.path.exists(Wells + "E08/" + time + "_" + files):
    shutil.move(path + files, Wells + "E08/" + time + "_" + files)
if "E09" in files and not os.path.exists(Wells + "E09/" + time + "_" + files):
    shutil.move(path + files, Wells + "E09/" + time + "_" + files)
if "E10" in files and not os.path.exists(Wells + "E10/" + time + "_" + files):
    shutil.move(path + files, Wells + "E10/" + time + "_" + files)
if "E11" in files and not os.path.exists(Wells + "E11/" + time + "_" + files):
    shutil.move(path + files, Wells + "E11/" + time + "_" + files)
if "E12" in files and not os.path.exists(Wells + "E12/" + time + "_" + files):
    shutil.move(path + files, Wells + "E12/" + time + "_" + files)


if "F01" in files and not os.path.exists(Wells + "F01/" + time + "_" + files):
    shutil.move(path + files, Wells + "F01/" + time + "_" + files)
if "F02" in files and not os.path.exists(Wells + "F02/" + time + "_" + files):
    shutil.move(path + files, Wells + "F02/" + time + "_" + files)
if "F03" in files and not os.path.exists(Wells + "F03/" + time + "_" + files):
    shutil.move(path + files, Wells + "F03/" + time + "_" + files)
if "F04" in files and not os.path.exists(Wells + "F04/" + time + "_" + files):
    shutil.move(path + files, Wells + "F04/" + time + "_" + files)
if "F05" in files and not os.path.exists(Wells + "F05/" + time + "_" + files):
    shutil.move(path + files, Wells + "F05/" + time + "_" + files)
if "F06" in files and not os.path.exists(Wells + "F06/" + time + "_" + files):
    shutil.move(path + files, Wells + "F06/" + time + "_" + files)
if "F07" in files and not os.path.exists(Wells + "F07/" + time + "_" + files):
    shutil.move(path + files, Wells + "F07/" + time + "_" + files)
if "F08" in files and not os.path.exists(Wells + "F08/" + time + "_" + files):
    shutil.move(path + files, Wells + "F08/" + time + "_" + files)
if "F09" in files and not os.path.exists(Wells + "F09/" + time + "_" + files):
    shutil.move(path + files, Wells + "F09/" + time + "_" + files)
if "F10" in files and not os.path.exists(Wells + "F10/" + time + "_" + files):
    shutil.move(path + files, Wells + "F10/" + time + "_" + files)
if "F11" in files and not os.path.exists(Wells + "F11/" + time + "_" + files):
    shutil.move(path + files, Wells + "F11/" + time + "_" + files)
if "F12" in files and not os.path.exists(Wells + "F12/" + time + "_" + files):
    shutil.move(path + files, Wells + "F12/" + time + "_" + files)

if "G01" in files and not os.path.exists(Wells + "G01/" + time + "_" + files):
    shutil.move(path + files, Wells + "G01/" + time + "_" + files)
if "G02" in files and not os.path.exists(Wells + "G02/" + time + "_" + files):
    shutil.move(path + files, Wells + "G02/" + time + "_" + files)
if "G03" in files and not os.path.exists(Wells + "G03/" + time + "_" + files):
    shutil.move(path + files, Wells + "G03/" + time + "_" + files)
if "G04" in files and not os.path.exists(Wells + "G04/" + time + "_" + files):
    shutil.move(path + files, Wells + "G04/" + time + "_" + files)
if "G05" in files and not os.path.exists(Wells + "G05/" + time + "_" + files):
    shutil.move(path + files, Wells + "G05/" + time + "_" + files)
if "G06" in files and not os.path.exists(Wells + "G06/" + time + "_" + files):
    shutil.move(path + files, Wells + "G06/" + time + "_" + files)
if "G07" in files and not os.path.exists(Wells + "G07/" + time + "_" + files):
    shutil.move(path + files, Wells + "G07/" + time + "_" + files)
if "G08" in files and not os.path.exists(Wells + "G08/" + time + "_" + files):
    shutil.move(path + files, Wells + "G08/" + time + "_" + files)
if "G09" in files and not os.path.exists(Wells + "G09/" + time + "_" + files):
    shutil.move(path + files, Wells + "G09/" + time + "_" + files)
if "G10" in files and not os.path.exists(Wells + "G10/" + time + "_" + files):
    shutil.move(path + files, Wells + "G10/" + time + "_" + files)
if "G11" in files and not os.path.exists(Wells + "G11/" + time + "_" + files):
```

```
            shutil.move(path + files, Wells + "G11/" + time + "_" + files)
        if "G12" in files and not os.path.exists(Wells + "G12/" + time + "_" + files):
            shutil.move(path + files, Wells + "G12/" + time + "_" + files)

        if "H01" in files and not os.path.exists(Wells + "H01/" + time + "_" + files):
            shutil.move(path + files, Wells + "H01/" + time + "_" + files)
        if "H02" in files and not os.path.exists(Wells + "H02/" + time + "_" + files):
            shutil.move(path + files, Wells + "H02/" + time + "_" + files)
        if "H03" in files and not os.path.exists(Wells + "H03/" + time + "_" + files):
            shutil.move(path + files, Wells + "H03/" + time + "_" + files)
        if "H04" in files and not os.path.exists(Wells + "H04/" + time + "_" + files):
            shutil.move(path + files, Wells + "H04/" + time + "_" + files)
        if "H05" in files and not os.path.exists(Wells + "H05/" + time + "_" + files):
            shutil.move(path + files, Wells + "H05/" + time + "_" + files)
        if "H06" in files and not os.path.exists(Wells + "H06/" + time + "_" + files):
            shutil.move(path + files, Wells + "H06/" + time + "_" + files)
        if "H07" in files and not os.path.exists(Wells + "H07/" + time + "_" + files):
            shutil.move(path + files, Wells + "H07/" + time + "_" + files)
        if "H08" in files and not os.path.exists(Wells + "H08/" + time + "_" + files):
            shutil.move(path + files, Wells + "H08/" + time + "_" + files)
        if "H09" in files and not os.path.exists(Wells + "H09/" + time + "_" + files):
            shutil.move(path + files, Wells + "H09/" + time + "_" + files)
        if "H10" in files and not os.path.exists(Wells + "H10/" + time + "_" + files):
            shutil.move(path + files, Wells + "H10/" + time + "_" + files)
        if "H11" in files and not os.path.exists(Wells + "H11/" + time + "_" + files):
            shutil.move(path + files, Wells + "H11/" + time + "_" + files)
        if "H12" in files and not os.path.exists(Wells + "H12/" + time + "_" + files):
            shutil.move(path + files, Wells + "H12/" + time + "_" + files)

        print("...done with " + files)

    #os.rmdir(path)
```

Script 2 – 4xPIV_4.py

```
import numpy as np
from openpiv import tools, validation, process, filters, scaling, pyprocess
from scipy.ndimage import rotate
import os
import openpyxl
import time
import matplotlib.pyplot as plt

"""
This Program perform PIV on data from ImageXpress using 4x objective. If binning 2 is used pixel
size is 3.367 µm. Correct scaling in µm/h is obtained by multiplying the displacement (in pixels)
by the pixel size (in µm) and then divide by the time (in hours). This is what the function
"scale" does.
"""

def Vector_Magnitude(u, v):
    "Calculates vector magnitude from component vectors u and v"
    return np.sqrt((u**2) + (v**2))

#scaling_factor: µm/px

def scale(u, v, scaling_factor):
    scaled_u = np.multiply(u, scaling_factor)
    scaled_u = np.divide(scaled_u, 0.26)
    scaled_v = np.multiply(v, scaling_factor)
    scaled_v = np.divide(scaled_v, 0.26)
    return scaled_u, scaled_v

def frame_rotation(frame_1, rotation):
    frame_1 = tools.imread(frame_1)
    rotate_1 = rotate(frame_1, rotation)  # rotate image 45 degrees counter clockwise
    middel_Y = rotate_1.shape[0] / 2  # finds th middle of the image y-axis
    average_1 = np.average(rotate_1[int(middel_Y)][0:200])
    low_1 = average_1 / 3
    high_points_1 = []
    low_points_1 = []
    for i in rotate_1[int(middel_Y)]:
        if i > low_1:
            high_points_1.append(i)
        else:
            low_points_1.append(i)
            if len(low_points_1) > 10:
                break
    x_length = len(high_points_1)
    return middel_Y, x_length


def find_rectangle(frame_1):
    if "s1" in frame_1:
        return frame_rotation(frame_1=frame_1, rotation=225)
    elif "s2" in frame_1:
        return frame_rotation(frame_1=frame_1, rotation=315)
    elif "s3" in frame_1:
        return frame_rotation(frame_1=frame_1, rotation=135)
    elif "s4" in frame_1:
        return frame_rotation(frame_1=frame_1, rotation=45)
    else: pass


def reject_outliers(data, m):
    "algorithm for removal of outliers from a list"
    return data[abs(data - np.mean(data)) < m * np.std(data)]


def remove_outliers(array, k):
    "takes in an array, flips the array 90 degrees, removes outlier values from each row"
    # Returns a 1-dimensional list of cleaned averaged values

    array_90 = np.rot90(array, k=3)
    clean_list = []
    for dirt in array_90:
        clean = reject_outliers(dirt, m=k)
        clean_nr = np.average(clean)
        clean_list.append(clean_nr)
```

```
    return clean_list


def pick_angle(tag):
    if "s1" in tag:
        return 225
    elif "s2" in tag:
        return 315
    elif "s3" in tag:
        return 135
    elif "s4" in tag:
        return 45
    else:
        print("wrong tag")


def PIV(frame_a, frame_b, middel_Y, x_length, tag):
    angle = pick_angle(tag=tag)

    frame_a = tools.imread(frame_a)
    rotate_a = rotate(frame_a, angle)  # rotate image 45 degrees counter clockwise
    cropped_a = rotate_a[int(middel_Y - 100):int(middel_Y + 100), x_length - 900:x_length - 5]

    frame_b = tools.imread(frame_b)
    rotate_b = rotate(frame_b, angle)  # rotate image 45 degrees counter clockwise
    cropped_b = rotate_b[int(middel_Y - 100):int(middel_Y + 100), x_length - 900:x_length - 5]

    u,    v,    sig2noise    =    process.extended_search_area_piv(cropped_a.astype(np.int32),
cropped_b.astype(np.int32),
        window_size=24, overlap=12, search_area_size=48, sig2noise_method='peak2peak' )
    x, y = process.get_coordinates( image_size=frame_a.shape, window_size=24, overlap=12)
    u, v, mask = validation.sig2noise_val( u, v, sig2noise, threshold = 2)
    u, v, mask = validation.global_val( u, v, (-1000, 2000), (-1000, 1000) )
    u, v = filters.replace_outliers( u, v, method='localmean', max_iter=10, kernel_size=2)
    u, v = scale(u, v, scaling_factor = 1.68) #scaling factor 1.68 (binning 1); scaling factor
3.367 (binning 2)
    #tools.save(x, y, u, v, mask, 'test1.vec')
    #tools.display_vector_field('test1.vec', scale=75, width=0.0035)
    #plt.quiver(u,v)
    #plt.show()
    return u, v


def single_well(path, path_out):

    list_of_lists = [names_s1, names_s2, names_s3, names_s4] = [[], [], [], []]

    for subdir, dirs, files in os.walk(path):
        for file in files:
            if "s1" in file:
                names_s1.append(os.path.join(file))
            elif "s2" in file:
                names_s2.append(os.path.join(file))
            elif "s3" in file:
                names_s3.append(os.path.join(file))
            elif "s4" in file:
                names_s4.append(os.path.join(file))
            else:
                pass

    for list, tag in zip(list_of_lists, ["s1", "s2", "s3", "s4"]):
        list_u_mean = []
        list_V_mean = []
        middel_Y, x_length = find_rectangle(path + list[0])
        print(x_length)
        if x_length < 900:
            print("rectangle smaller than 1000 pixels")
            pass
        elif x_length is None:
            pass
        else:
            for frame_a, frame_b in zip(*[iter(list)]*2):
                u, v = PIV(frame_a=path + frame_a, frame_b=path + frame_b, middel_Y=middel_Y,
x_length=x_length, tag = tag)
                V = Vector_Magnitude(u, v)
                direction = remove_outliers(array=u, k=2)
                speed = remove_outliers(array=V, k=2)
```

```
            list_u_mean.append(direction)
            list_V_mean.append(speed)

        book = openpyxl.Workbook()
        sheet = book.active

        c = 1
        for list in list_u_mean:
            sheet.cell(row=1, column=c).value = "u"
            for i in range(0, len(list)):
                sheet.cell(row = i + 2, column = c).value = list[i]
            c = c + 2

        c2 = 2
        for list2 in list_V_mean:
            sheet.cell(row=1, column=c2).value = "V"
            for i in range(0, len(list2)):
                sheet.cell(row = i + 2, column = c2).value = list2[i]
            c2 = c2 + 2

        book.save(path_out + path[-4:-1] + tag + ".xlsx")
        print(tag + " done")


all_wells = ["A01", "A02", "A03", "A04", "A05", "A06", "A07", "A08", "A09", "A10", "A11", "A12",
"B01", "B02", "B03", "B04", "B05", "B06", "B07", "B08", "B09", "B10", "B11", "B12", "C01",
"C02", "C03", "C04", "C05", "C06", "C07", "C08", "C09", "C10", "C11", "C12", "D01", "D02",
"D03", "D04", "D05", "D06", "D07", "D08", "D09", "D10", "D11", "D12", "E01", "E02", "E03",
"E04", "E05", "E06", "E07", "E08", "E09", "E10", "E11", "E12", "F01", "F02", "F03", "F04",
"F05", "F06", "F07", "F08", "F09", "F10", "F11", "F12", "G01", "G02", "G03", "G04", "G05",
"G06", "G07", "G08", "G09", "G10", "G11", "G12", "H01", "H02", "H03", "H04", "H05", "H06",
"H07", "H08", "H09", "H10", "H11", "H12"]


list_of_wells = ["A01", "A02", "A03", "A04", "A05", "A06", "A07", "A08", "A09", "A10", "A11",
"A12", "B01", "B02", "B03", "B04", "B05", "B06", "B07", "B08", "B09", "B10", "B11", "B12",
"C01", "C02", "C03", "C04", "C05", "C06", "C07", "C08", "C09", "C10", "C11", "C12", "D01",
"D02", "D03", "D04", "D05", "D06", "D07", "D08", "D09", "D10", "D11", "D12", "E01", "E02",
"E03", "E04", "E05", "E06", "E07", "E08", "E09", "E10", "E11", "E12", "F01", "F02", "F03",
"F04", "F05", "F06", "F07", "F08", "F09", "F10", "F11", "F12", "G01", "G02", "G03", "G04",
"G05", "G06", "G07", "G08", "G09", "G10", "G11", "G12", "H01", "H02", "H03", "H04", "H05",
"H06", "H07", "H08", "H09", "H10", "H11", "H12"]


#Folder_in = "D:\\IXMC sorted files 2020\\220620 Inhibitor test_Plate_4196\\Wells\\"

Folder_in = "D:\\IXMC data\\210121 MigrationAssay Jenny 1_Plate_5672\\Wells\\"
Folder_out = "D:\\Jenny\\Pycharm_projects\\project1\\4xPIV_4_260121\\"

start = time.time()


um_per_pixel = 3.367
hours = 0.53
scaling_factor = um_per_pixel/hours

for well in list_of_wells:
    print("working on " + well)
    single_well(path = Folder_in + well + "\\", path_out = Folder_out)

end = time.time()
print("The entire analysis took " + str(end - start) + " seconds")
```

Script 3 – 4xPIV_5.py

```
import numpy as np
from openpiv import tools, validation, process, filters, scaling, pyprocess
from scipy.ndimage import rotate
import os
import openpyxl
import time
import math
import matplotlib.pyplot as plt

"""
This Program perform PIV on data from ImageXpress using 4x objective. If binning 2 is used pixel
size is 3.367 µm. Correct scaling in µm/h is obtained by multiplying the displacement (in pixels)
by the pixel size (in µm) and then divide by the time (in hours). This is what the function
"scale" does.
"""

def Vector_Magnitude(u, v):
    "Calculates vector magnitude from component vectors u and v"
    return np.sqrt((u**2) + (v**2))

#scaling_factor: µm/px

def scale(u, v, scaling_factor):
    scaled_u = np.multiply(u, scaling_factor)
    scaled_u = np.divide(scaled_u, 0.26)
    scaled_v = np.multiply(v, scaling_factor)
    scaled_v = np.divide(scaled_v, 0.26)
    return scaled_u, scaled_v

# Use the order parameter described by David Cohen et al. in Nature Material Paper
def order(u, v):
    angle = math.atan(v/u)
    number = math.cos(angle)
    return number

def frame_rotation(frame_1, rotation):
    frame_1 = tools.imread(frame_1)
    rotate_1 = rotate(frame_1, rotation)  # rotate image 45 degrees counter clockwise
    middel_Y = rotate_1.shape[0] / 2  # finds th middle of the image y-axis
    average_1 = np.average(rotate_1[int(middel_Y)][0:200])
    low_1 = average_1 / 3
    high_points_1 = []
    low_points_1 = []
    for i in rotate_1[int(middel_Y)]:
        if i > low_1:
            high_points_1.append(i)
        else:
            low_points_1.append(i)
            if len(low_points_1) > 10:
                break
    x_length = len(high_points_1)
    return middel_Y, x_length


def find_rectangle(frame_1):
    if "s1" in frame_1:
        return frame_rotation(frame_1=frame_1, rotation=225)
    elif "s2" in frame_1:
        return frame_rotation(frame_1=frame_1, rotation=315)
    elif "s3" in frame_1:
        return frame_rotation(frame_1=frame_1, rotation=135)
    elif "s4" in frame_1:
        return frame_rotation(frame_1=frame_1, rotation=45)
    else: pass


def reject_outliers(data, m):
    "algorithm for removal of outliers from a list"
    return data[abs(data - np.mean(data)) < m * np.std(data)]


def remove_outliers(array, k):
    "takes in an array, flips the array 90 degrees, removes outlier values from each row"
    # Returns a 1-dimensional list of cleaned averaged values
```

```
    array_90 = np.rot90(array, k=3)
    clean_list = []
    for dirt in array_90:
        clean = reject_outliers(dirt, m=k)
        clean_nr = np.average(clean)
        clean_list.append(clean_nr)
    return clean_list


def pick_angle(tag):
    if "s1" in tag:
        return 225
    elif "s2" in tag:
        return 315
    elif "s3" in tag:
        return 135
    elif "s4" in tag:
        return 45
    else:
        print("wrong tag")


def PIV(frame_a, frame_b, middel_Y, x_length, tag):
    angle = pick_angle(tag=tag)

    frame_a = tools.imread(frame_a)
    rotate_a = rotate(frame_a, angle)  # rotate image 45 degrees counter clockwise
    cropped_a = rotate_a[int(middel_Y - 100):int(middel_Y + 100), x_length - 900:x_length - 5]

    frame_b = tools.imread(frame_b)
    rotate_b = rotate(frame_b, angle)  # rotate image 45 degrees counter clockwise
    cropped_b = rotate_b[int(middel_Y - 100):int(middel_Y + 100), x_length - 900:x_length - 5]

    u,    v,    sig2noise    =    process.extended_search_area_piv(cropped_a.astype(np.int32),
cropped_b.astype(np.int32),
        window_size=24, overlap=12, search_area_size=48, sig2noise_method='peak2peak' )
    x, y = process.get_coordinates( image_size=cropped_a.shape, window_size=24, overlap=12)
    u, v, mask = validation.sig2noise_val( u, v, sig2noise, threshold = 2)
    u, v, mask = validation.global_val( u, v, (-50, 50), (-50, 50) )
    u, v = filters.replace_outliers( u, v, method='localmean', max_iter=10, kernel_size=2)
    #u, v = scale(u, v, scaling_factor = 1.68) #scaling factor 1.68 (binning 1); scaling factor
3.367 (binning 2)
    #tools.save(x, y, u, v, mask, 'test1.vec')
    #tools.display_vector_field('test1.vec', scale=75, width=0.0035)
    #plt.quiver(u,v)
    #plt.show()
    return u, v


def single_well(path, path_out):

    list_of_lists = [names_s1, names_s2, names_s3, names_s4] = [[], [], [], []]

    for subdir, dirs, files in os.walk(path):
        for file in files:
            if "s1" in file:
                names_s1.append(os.path.join(file))
            elif "s2" in file:
                names_s2.append(os.path.join(file))
            elif "s3" in file:
                names_s3.append(os.path.join(file))
            elif "s4" in file:
                names_s4.append(os.path.join(file))
            else:
                pass

    for list, tag in zip(list_of_lists, ["s1", "s2", "s3", "s4"]):
        list_u_mean = []
        list_V_mean = []
        list_order = []
        middel_Y, x_length = find_rectangle(path + list[0])
        print(x_length)
        if x_length < 900:
            print("rectangle smaller than 1000 pixels")
            pass
        elif x_length is None:
```

```
            pass
        else:
            for frame_a, frame_b in zip(*[iter(list)]*2):
                u, v = PIV(frame_a=path + frame_a, frame_b=path + frame_b, middel_Y=middel_Y,
x_length=x_length, tag = tag)
                flat_u = u.flatten()
                flat_v = v.flatten()
                box = []
                for cu, cv in zip(flat_u, flat_v):
                    number = order(cu, cv)
                    box.append(number)
                list_order.append(box)

            book = openpyxl.Workbook()
            sheet = book.active

            c = 1
            for list in list_order:
                sheet.cell(row=1, column=c).value = "order"
                for i in range(0, len(list)):
                    sheet.cell(row = i + 2, column = c).value = list[i]
                c = c + 1

            book.save(path_out + path[-4:-1] + tag + ".xlsx")
            print(tag + " done")


all_wells = ["A01", "A02", "A03", "A04", "A05", "A06", "A07", "A08", "A09", "A10", "A11", "A12",
"B01", "B02", "B03", "B04", "B05", "B06", "B07", "B08", "B09", "B10", "B11", "B12", "C01",
"C02", "C03", "C04", "C05", "C06", "C07", "C08", "C09", "C10", "C11", "C12", "D01", "D02",
"D03", "D04", "D05", "D06", "D07", "D08", "D09", "D10", "D11", "D12", "E01", "E02", "E03",
"E04", "E05", "E06", "E07", "E08", "E09", "E10", "E11", "E12", "F01", "F02", "F03", "F04",
"F05", "F06", "F07", "F08", "F09", "F10", "F11", "F12", "G01", "G02", "G03", "G04", "G05",
"G06", "G07", "G08", "G09", "G10", "G11", "G12", "H01", "H02", "H03", "H04", "H05", "H06",
"H07", "H08", "H09", "H10", "H11", "H12"]

list_of_wells = ["A01", "A02", "A03", "A04", "A05", "A06", "A07", "A08", "A09", "A10", "A11",
"A12", "B01", "B02", "B03", "B04", "B05", "B06", "B07", "B08", "B09", "B10", "B11", "B12",
"C01", "C02", "C03", "C04", "C05", "C06", "C07", "C08", "C09", "C10", "C11", "C12", "D01",
"D02", "D03", "D04", "D05", "D06", "D07", "D08", "D09", "D10", "D11", "D12", "E01", "E02",
"E03", "E04", "E05", "E06", "E07", "E08", "E09", "E10", "E11", "E12", "F01", "F02", "F03",
"F04", "F05", "F06", "F07", "F08", "F09", "F10", "F11", "F12", "G01", "G02", "G03", "G04",
"G05", "G06", "G07", "G08", "G09", "G10", "G11", "G12", "H01", "H02", "H03", "H04", "H05",
"H06", "H07", "H08", "H09", "H10", "H11", "H12"]


Folder_in = "D:\\IXMC data\\210121 MigrationAssay Jenny 1_Plate_5672\\Wells\\"
Folder_out = "D:\\Jenny\\Pycharm_projects\\project1\\Plot_order_260121\\"

for well in list_of_wells:
    print("working on " + well)
    single_well(path = Folder_in + well + "\\", path_out = Folder_out)
```

Script 4 – Plot_speed.py

```
import pandas as pd
import numpy as np
import matplotlib.pyplot as plt


def single_site(path, file):
    df = pd.read_excel (path + file)
    print(df)
    line = []
    for i in range(1, len(df.columns), 2):
        t = df.iloc[:, i]
        t = np.average(t)
        line.append(t)
    return(line)


def group_average_std(group):
    list_of_lists = []
    for file in group:
        t = single_site(path, file)
        list_of_lists.append(t)
    average = np.average(list_of_lists, axis=0)
    std = np.std(list_of_lists, axis=0)
    return average[1:], std[1:]

# Extracting data from  xlsx-files
path = "D:\\Jenny\\Pycharm_projects\\project1\\4xPIV_5_250121\\"


group1 = ["A01s1.xlsx", "A01s2.xlsx", "A01s3.xlsx", "B01s1.xlsx", "B01s2.xlsx", "C01s1.xlsx",
"C01s2.xlsx",   "C01s3.xlsx",   "D01s1.xlsx",   "D01s2.xlsx",   "D01s3.xlsx",   "E01s1.xlsx",
"E01s2.xlsx",   "E01s3.xlsx",   "F01s1.xlsx",   "F01s2.xlsx",   "F01s3.xlsx",   "G01s1.xlsx",
"G01s2.xlsx", "G01s3.xlsx", "H01s1.xlsx", "H01s2.xlsx", "H01s3.xlsx"]

group2 = ["A02s1.xlsx", "A02s2.xlsx", "A02s3.xlsx", "B02s1.xlsx", "B02s2.xlsx", "B02s3.xlsx",
"C02s1.xlsx",   "C02s2.xlsx",   "C02s3.xlsx",   "D02s1.xlsx",   "D02s2.xlsx",   "D02s3.xlsx",
"E02s1.xlsx",   "E02s2.xlsx",   "E02s3.xlsx",   "F02s1.xlsx",   "F02s2.xlsx",   "F02s3.xlsx",
"G02s1.xlsx", "G02s2.xlsx", "G02s3.xlsx", "H02s1.xlsx", "H02s2.xlsx", "H02s3.xlsx"]


average1, std1 = group_average_std(group1)
average2, std2 = group_average_std(group2)

print(average1)


# creating values along the x_axis
x = range(0, len(average1))
x = (np.multiply(x,32))/60

# plotting the data
fig, ax = plt.subplots(1,1)

ax.plot(x, average1, label="Starved", c="C3")
ax.fill_between(x, average1 + std1, average1 - std1, facecolor='red', alpha=0.2)

ax.plot(x, average2, label="15% FBS", c="C0")
ax.fill_between(x, average2 + std2, average2 - std2, facecolor='blue', alpha = 0.2)

ax.set_ylabel("Speed (µm/h)", fontsize=12)
ax.set_xlabel("Time (h)", fontsize=12)

plt.legend()
plt.show()

fig.savefig("D:\\Jenny\\Pycharm_projects\\project1\\Speed_plot_260121\\Fig   Starved_and_FBS",
dpi=300, bbox_inches='tight')



#nf = df.to_numpy()
#print(len(nf[0]))
```

Script 5 – Plot_order.py

```
import pandas as pd
import numpy as np
import matplotlib.pyplot as plt
import os

#plt.style.use('ggplot')

def extract_file_names_from_directory(directory):
    """This function takes in a directory and extract the file_names contained in it"""
    file_names = []
    for subdir, dirs, files in os.walk(directory):
        for file in files:
            file_names.append(os.path.join(file))
    return file_names


def one_sample(file_list):
    list_of_list = []
    for file in file_list:
        if file[0:5] in file_list:
            df_data = pd.read_excel(path + file + ".xlsx")
            data = df_data.to_numpy()
            data = np.rot90(data)
            data = np.flipud(data)
            #print(data[33])
            data[np.isnan(data)] = 0
            numbers = []
            for i in data:
                average = np.average(i)
                numbers.append(average)
            list_of_list.append(numbers)
        else:
            print(file)
    return list_of_list


def plot_one_sample(sample):
    sample_array = np.array(sample)
    sample_average = np.average(sample_array, 0)
    sample_std = np.std(sample_array, 0)
    return sample_average, sample_std


path = "D:\\Jenny\\Pycharm_projects\\project1\\4xPIV_5_250121\\"

Dataset1 = ["A03s1", "A03s2", "A03s3", "A03s4", "B03s1", "B03s2", "B03s3", "C03s1", "C03s2",
"C03s3", "C03s4", "D03s1", "D03s2", "D03s3", "D03s4", "E03s1", "E03s2", "E03s3", "E03s4",
"F03s1", "F03s2", "F03s3", "F03s4", "G03s1", "G03s2", "G03s3", "G03s4", "H03s1", "H03s2",
"H03s3", "H03s4"]

Dataset2 = ["A11s1", "A11s2", "A11s3", "B11s1", "B11s2", "B11s3", "C11s1", "C11s2", "C11s3",
"C11s4", "D11s1", "D11s2", "D11s3", "E11s1", "E11s2", "E11s3", "E11s4", "F11s1", "F11s2",
"F11s3", "F11s4", "G11s1", "G11s2", "G11s3", "G11s4", "H11s1", "H11s2", "H11s3", "H11s4"]


file_names = extract_file_names_from_directory(directory = path)
print(file_names)

sample1 = one_sample(Dataset1)
sample2 = one_sample(Dataset2)

# Generate average and standard deviation
sample1_a, sample1_s = plot_one_sample(sample1)
sample2_a, sample2_s = plot_one_sample(sample2)

# Generate X-axis
x = np.arange(len(sample1_a))
x = np.multiply(x, 32)
x = np.divide(x, 60)

fig, ax = plt.subplots()


ax.plot(x[1:], sample1_a[1:], linewidth = 1, color="red", marker='o')
```

```
ax.fill_between(x[1:], sample1_a[1:] - sample1_s[1:], sample1_a[1:] + sample1_s[1:], alpha=0.2,
color="red")
ax.plot(x[1:], sample2_a[1:], linewidth = 1, color="blue", marker='d')
ax.fill_between(x[1:], sample2_a[1:] - sample2_s[1:], sample2_a[1:] + sample2_s[1:], alpha=0.2,
color="blue")

labels = ["EGF", "5 ng/ml TGF-B"]
plt.legend(labels, fontsize=10)

ax.set_ylim(0.4 ,1)
ax.set_xlabel("t (hours)")
ax.set_ylabel("φ")
plt.savefig("Order_plot_EGF_and_5TGF-B", dpi = 300)

#plt.show()
```

Script 6 – Stream_line.py

```
import numpy as np
from openpiv import tools, validation, process, filters, scaling, pyprocess
from scipy.ndimage import rotate
import os
import openpyxl
import time
import matplotlib.pyplot as plt
import scipy.ndimage


def extract_file_names_from_directory(directory):
    """This function takes in a directory and extract the file_names contained in it"""
    file_names = []
    for subdir, dirs, files in os.walk(directory):
        for file in files:
            file_names.append(os.path.join(file))
    return file_names

def scale2(u, v, M, factor):
    u2 = np.multiply(u, factor)
    v2 = np.multiply(v, factor)
    M2 = np.multiply(M, factor)
    return u2, v2, M2

def PIV(frame_a, frame_b, window_size, overlap, search_area_size):
    frame_a = tools.imread(frame_a)
    frame_b = tools.imread(frame_b)
    u,     v,     sig2noise     =     process.extended_search_area_piv(frame_a.astype(np.int32),
frame_b.astype(np.int32),
        window_size=window_size,      overlap=overlap,      search_area_size=search_area_size,
sig2noise_method='peak2peak' )
    x,   y   =   process.get_coordinates(   image_size=frame_a.shape,   window_size=window_size,
overlap=overlap)
    u, v, mask = validation.sig2noise_val( u, v, sig2noise, threshold = 3)
    u, v, mask = validation.global_val( u, v, (-10, 10), (-10, 10) )
    u, v = filters.replace_outliers( u, v, method='localmean', max_iter=10, kernel_size=4)
    # tools.save(x, y, u, v, mask, 'exp1_001.txt')
    # display_vector_field('exp1_001.txt', scale=1000, width=0.0025)
    M = np.hypot(u, v)
    print(M.min(), M.max())
    return x, y, u, v, M

path = "E:\\040221 MigrationAssay Jenny Exp2_5985\\Treshold_RAW_data\\D11_del2\\"
path_out = "E:\\040221 MigrationAssay Jenny Exp2_5985\\Stream_line_out\\D11_del2\\"

names = extract_file_names_from_directory(path)
print(names)

k= 0
for frame_a, frame_b in zip(names, names[1:]):
    x, y, u, v, M = PIV(path + frame_a, path + frame_b,
                        window_size=24,
                        overlap=12,
                        search_area_size=48)
    # Scaling:
    # By default, all values are given in pixels/dt
    # if pixel size is 3.367 and time interval (dt) is 16 min per frame,
    # then factor = 3.367 x (60/16) = 3.367 x 3.75 = 12.63
    u, v, M =  scale2(u = u, v = v, M = M, factor = 12.63)
    x = np.multiply(x, 3.367)
    y = np.multiply(y, 3.367)

    # Flipping v-components 180 degrees is required to obtain the correct vector orientation:
    v = np.flipud(v)

    # These operations reduce the number of arrows in the plot through averaging:
    resized_x = scipy.ndimage.zoom(x, 24. / 169)
    resized_y = scipy.ndimage.zoom(y, 24. / 169)
    resized_u = scipy.ndimage.zoom(u, 24. / 169)
    resized_v = scipy.ndimage.zoom(v, 24. / 169)
    resized_M = scipy.ndimage.zoom(M, 24. / 169)

    # Make the quiver plot:
    fig, ax = plt.subplots(ncols=1, nrows=1)
```

```
im = ax.streamplot(x, y, u, v, density=2)
ax.set_xlabel("X (µm)")
ax.set_ylabel("Y (µm)")
plt.gca().set_aspect('equal', adjustable='box')
plt.savefig(path_out + "image" + str(k), dpi = 300)
print("Done with Image " + str(k))
k = k + 1
```

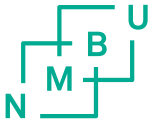

Norges miljø- og biovitenskapelige universitet
Noregs miljø- og biovitskapelege universitet
Norwegian University of Life Sciences

Postboks 5003
NO-1432 Ås
Norway